COLLECTING LYMPHATIC VESSEL PERMEABILITY TO ALBUMIN AND ITS MODIFICATION BY NATRIURETIC PEPTIDES

A Dissertation presented to
the Faculty of the Graduate School
at the University of Missouri-Columbia

In Partial Fulfillment
of the Requirements for the Degree

Doctor of Philosophy

---

by
JOSHUA SCALLAN

Dr. Virginia Huxley, Dissertation Supervisor

MAY 2010

The undersigned, appointed by the Dean of the Graduate School, have examined the dissertation entitled

COLLECTING LYMPHATIC VESSEL PERMEABILITY TO ALBUMIN AND ITS MODIFICATION BY NATRIURETIC PEPTIDES

presented by Joshua Scallan,

a candidate for the degree of Doctor of Philosophy

and hereby certify that, in their opinion, it is worthy of acceptance.

Professor Virginia H. Huxley

Professor Ronald J. Korthuis

Professor Michael J. Davis

Professor Steven S. Segal

Professor Douglas K. Bowles

DEDICATION

The following work is dedicated to…

My parents, for raising me in an environment supporting an academic career and for encouraging me to perform my best at school and in life. I hope both of you can look upon this achievement proudly.

My wife, Megan, for always supporting me emotionally, financially, and academically in my scientific endeavors. You always are there to give me strength or encouragement when I need it.

Two of my best friends, Baker and Brynn; by virtue of your continuous and contagious happiness you were always there to wash away a day of hard work in the laboratory.

"Problems worthy of attack prove their worth by hitting back."

- Piet Hein

ACKNOWLEDGMENTS

The work within this dissertation, as with many, was built upon novel ideas and data obtained throughout my graduate training; a process during which I was influenced and inspired by many individuals that deserve recognition.

The most credit should be given to my mentor, Virginia Huxley, for training me to be a good scientist. However, she was much more than a great mentor during the past 5 years – to quote Vicky Tucker (a former student), she was a "best friend, confidant, loyal fan, editor, surrogate mother, word processor, devil's advocate, whatever was most appropriate at the time." I believe that such a compliment cannot be restated any better and I would like to thank you for teaching and preparing me for my future in just about anything, but especially research. I will owe you indefinitely for all that you have taught me and hope that in the future we become collaborators.

I am indebted to my first mentor, Ron Korthuis, for letting me join his lab at LSU-HSC and for providing me with a fascinating introduction to research and physiology. Without this experience I wonder whether I would have even pursued a doctoral degree. Furthermore, I am grateful that you took the time and interest to recruit me to the University of Missouri to perform research in a very supportive and stimulating environment, one that will be difficult to match anywhere else.

Many thanks to Norman Harris, who also provided me with a great introduction to independence in research and thinking. It was a pleasure to work with you and to attempt to answer your question of whether lymphatic vessels are permeable to proteins, even

though it required a dissertation to do so. The lymphatic field is certainly a very intriguing one that has captured my interest ever since working in your lab.

In addition, I could not have explored the ideas and concepts I encountered during my training without discussions with others working on similar projects. I am grateful that Michael Davis worked right beside our lab, and always kept his door open to students. Our conversations were always a great way for me to organize my thoughts, to explore new ideas, or to even vent frustrations. I hope they were as helpful and enjoyable to you, and a reason I considered you a co-mentor and friend. Another person that influenced me with regard to my research on the lymphatic vasculature was David Zawieja who provided guidance from afar regarding both lymphatic concepts and proofreading several documents. I look forward to one day working alongside both of you.

Besides the other graduate students and postdocs in both the MPP program and the Huxley lab, I must thank Susan Bingaman and Steve Sieveking who provided excellent assistance with these projects. Thank you, Sue, for taking great pains in labeling protein meticulously and for teaching me molecular techniques. Steve, thank you for showing me that woodwork in the hospital is not only feasible but fun, too. I hope each of you remember that these projects would not be possible without your help.

Finally, this dissertation work would not have been able to take its present form without the guidance of my committee. Thanks to my committee members, as well as Michael Rovetto, for keeping my research projects and my writing focused and practicable. Each of you served as distinct role models and enhanced my training through your own unique scientific interests.

TABLE OF CONTENTS

LIST OF TABLES

Table Page

Appendix II Tables

LIST OF FIGURES

Figure Page

COLLECTING LYMPHATIC VESSEL PERMEABILITY TO ALBUMIN AND ITS MODIFICATION BY NATRIURETIC PEPTIDES

Joshua Paul Scallan

Dr. Virginia Huxley, Dissertation Supervisor

ABSTRACT

Macromolecules and water leave the blood microcirculation and bathe the tissues of the body, and cannot be constitutively reabsorbed by the blood vessels, necessitating an outflow pathway that is comprised by the lymphatic vasculature. The mechanisms underlying the transport of macromolecules and water *to* or *from* the lymphatic vessels have not been elucidated fully until now, due to the difficulty in manipulating these structures. Here we demonstrated that the microfluorometric technique designed to assess blood capillary solute permeability (P_s) could be modified to determine the P_s of single collecting lymphatic vessels. Lymphatic endothelium has recently been shown to be derived from the cardinal vein, suggesting that these endothelial types share many genes, thus functions; we hypothesized that collecting lymphatic and venular P_s, as well as its response to natriuretic peptides, do not differ. In accordance, we demonstrated that the median lymphatic and venular P_s to albumin did not differ, nor did their diffusive permeabilities (P_d) or estimated hydraulic conductivities (L_p). Follow-up studies were then performed to determine whether protein was absorbed or expelled by collecting lymphatics, and revealed that collecting lymphatic vessels possessed concentration

gradients of total protein and albumin favoring their loss into the tissue, contrary to our expectations.

During perfusion with atrial or brain natriuretic peptides (ANP and BNP; hormones released during fluid shifts such as congestive heart failure), the P_s responses to both peptides mirrored that of the venules. However, a differential sensitivity to these two peptides existed such that collecting lymphatics possessed greater P_s responses to BNP (2.7-fold) than ANP (2.0-fold). Further, lymphatic contraction amplitude and frequency could be monitored while these peptides were infused; ANP abolished contractions in a nitric oxide-dependent manner, while BNP increased contraction amplitude and frequency by ~2-fold.

In summary, the data presented in this dissertation show that collecting lymphatic vessels are permeable to albumin, protein diffuses into the tissue under basal conditions, and natriuretic peptides double this permeability. From these data we conclude that the lymphatic vasculature likely plays a prominent, previously unrecognized role in tissue exchange with several of the implications examined in this dissertation.

CHAPTER 1: INTRODUCTION

Microvessels carrying whole blood transport sugars, proteins, lipids and gases to and from the tissues to support life on a cellular and organismal level. To allow this exchange, vessels must be porous – or permeable – to both solute and water. As we will discuss, microvessels of most organs are unable to sustain reabsorption of their extravasated water and macromolecules from the tissues, necessitating an outflow pathway to prevent edema formation, a state ultimately incompatible with life. The lymphatic vasculature alone comprises the pathway required to maintain the steady return of this capillary filtrate to the blood circulatory system. Consequently, the lymphatic vasculature is associated intimately with the control of fluid and macromolecule movement as well as establishment of their homeostasis.

Until now the mechanisms governing solute and water transport across the walls of lymphatic vessels remained undefined despite acknowledgment of their importance to the understanding fluid homeostasis and edema formation. Therefore, the goal of this thesis was to develop a method to measure the permeability of the lymphatic vasculature to solutes, to put those measures into a meaningful context, and to determine definitively whether lymphatic vessel permeability is static or dynamic – i.e., whether permeability is a constant, or is regulated during conditions encountered in health and/or disease. Consequences of lymphatic vessel permeability will be discussed in terms of the ease with which solute (permeability, P_s) and water (hydraulic conductivity, L_p) traverse the lymphatic endothelial barrier.

Unfortunately for the lymphatic circulatory system, there exists a dearth of knowledge giving rise to many assumptions. A relevant summary of lymphatic vessel function, as well as the introduction of a consistent nomenclature for the elements of the lymphatic vasculature, is required before proceeding.

Lymphatic Anatomy and Nomenclature

While study of the blood vascular system dates back to the sixth century BC, the lymphatic vasculature was not "discovered" until 1622 by Asellius (6). In stark contrast to the blood vasculature, the lymphatic circulatory system has been far less extensively studied. The reason for this is not its late discovery, *per se*, but rather pertains to the prevailing misperception that the lymphatics represent a largely passive system for return of extravasated fluid and proteins to the systemic circulation, to the difficulty of visualizing lymphatic vessels in the tissue, and to the lack of specific molecular markers to distinguish cells from this circulatory system from that of the blood vasculature until recently (26). As such, no common nomenclature for the lymphatic vasculature has been agreed upon, so one previously used for rat mesenteric lymphatics will be introduced (110).

Interstitial fluid, formed from solute and fluid extravasated from the capillaries, enters blind-ended sacs composed only of an endothelial layer tethered to the interstitial matrix. These bulbous sacs (10-60 μm diameter) are called initial, or terminal, lymphatics. Initial lymphatics possess overlapping endothelial cells that behave collectively like a valve, only permitting entry of fluid, solute, and cells into the lumen of

these vessels. The fluid, thereafter referred to as lymph, next moves into lymphatic vessels of a similar diameter, termed microlymphatics here. Microlymphatics consist of an endothelial layer and basement membrane (126). Since the phrase 'lymphatic capillary' is sometimes applied to initial and microlymphatics collectively, and 'lymphatic capillaries' may be much larger than traditional capillaries carrying whole blood, this ambiguous phrase will be avoided hereafter. Microlymphatic vessels then carry lymph towards the larger collecting lymphatic vessels. Collecting lymphatics (50-200 μm diam.) are composed of endothelial cells, a basement membrane, lymphatic muscle cells, pericytes, and endothelial valves that prevent retrograde lymph flow (96, 133). Pericytes do not envelope the smaller initial and microlymphatics (96). Valves are present in collecting lymphatics and differ from the initial lymphatic 'valve' in that they consist of two modified endothelial cell leaflets that meet in the vessel lumen, not unlike valves of the larger mammalian veins. The lymphatic muscle layer is unique in that it possesses both tonic and phasic contractile activity (113, 133). Phasic contractions, referred to as spontaneous contractions, aid in propelling lymph along the intervalvular segments of the lymphatic vessel, called lymphangions. After passing through lymph nodes and then larger collecting lymphatic ducts, lymph is finally propelled to the thoracic duct, which empties into the left subclavian vein (see Figure 1).

The anatomy of collecting lymphatic vessels appears similar to that of comparable veins in that they both are low-pressure vessels vested with a muscle layer and intraluminal valves. In support of the theory of lymphatic development originally proposed by Sabin (106), one group has shown that lymphatic endothelial cells are

derived directly from the cardinal vein (114). Akin to the venules numerous cytoplasmic vesicles have been reported in initial lymphatic endothelium (1, 21, 69-71, 88). To date, a role for these vesicles in solute uptake has not been elucidated fully. Further, whether lymphatic vessels possess other features similar to the vessels carrying whole blood – such as a glycocalyx or caveoli – has not been demonstrated. Nor is it known whether lymphatic vessels possess the same receptors to physiological agonists and antagonists as displayed by the blood vasculature.

Although the preceding description is accurate for the rat mesenteric lymphatic vasculature, it is important to recognize that lymphatic vessel morphology varies greatly between organs. Since it is beyond the scope of this dissertation to thoroughly summarize these varying anatomical features, the reader is directed to several excellent detailed reviews for this information (8, 91, 113). Two of these reviews (8, 113) summarize classical views on several aspects of the lymphatic vasculature: the present chapter will provide the reader with the relevant, current perspectives on lymphatic vessel function.

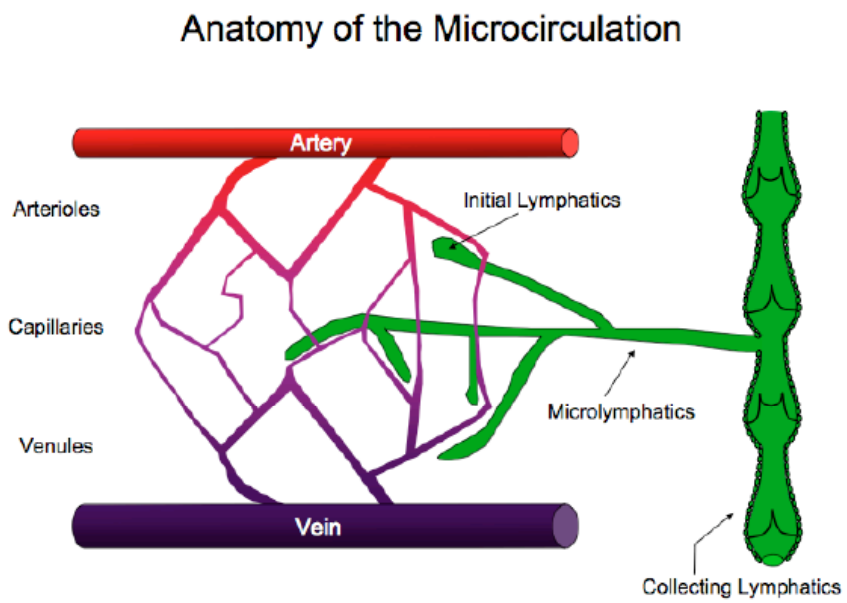

Figure 1. Cartoon depicting the architecture of lymphatic microvessels in relation to the blood microvessels as they appear in the rat mesentery. Ideally, the feeding artery would lie adjacent to the draining vein, and both would lie adjacent to a collecting lymphatic vessel to form a triad of parallel vessels. Interstitial fluid formed by the capillary filtrate first encounters the initial lymphatic bulbs, which transport this fluid to the microlymphatic vessels. The fluid, called lymph, then travels through the collecting lymphatic vessels until it finally arrives at the thoracic duct that empties into the left subclavian vein in mammals.

Lymph Formation

Lymph formation refers to the entry of fluid and protein into the initial lymphatics from the surrounding tissue. The mechanisms responsible for this process are poorly understood, but two main hypotheses have been proposed. The first is that an osmotic gradient becomes established across the initial lymphatic wall through sieving of protein that then generates its own convective flow by pulling in protein-containing interstitial fluid *against* a concentration gradient (20). Very little, if any, experimental support exists for this theory, which is in direct violation of the second law of thermodynamics, despite its original appearance nearly four decades ago. Therefore, the following discussion will focus on the second hypothesis, that a hydrostatic pressure gradient is needed to fill the initial lymphatics.

As stated before, the initial lymphatics possess overlapping endothelial cells tethered to the tissue. Thus, when the tissue becomes hydrated it swells and pulls apart the endothelial cells to form ~2 μm diameter pores that act like a nonselective one-way valve, trapping fluid, solute, and cells passively (124). Considering their unique structure, one would arrive at the logical conclusion that a pressure gradient across the interstitium drives fluid and solute accumulation within the initial lymphatics. From the few studies of interstitial pressure gradients it was shown that a gradient of 0.2 to 0.8 cmH_2O exists (48, 136). At first glance this pressure gradient seems small, but others have calculated that a pressure head of only 0.12 cmH_2O is adequate to drive the capillary filtrate into the low resistance initial lymphatics (113). One foreseeable problem with this hypothesis is that the interstitial pressures measured routinely are negative values relative to

atmospheric, which would cause water to flow out of any vessel into the interstitium (24, 44). Significant overlap of interstitial and initial lymphatic pressures measured simultaneously was observed (24), depending on the superfusion solution and the time of measurement (immediately following exteriorization or 30 minutes later). Particularly interesting was that 30 minutes after exposure of the mesentery, superfused with oil to preserve natural tissue hydration, respective pressures in the interstitium and initial lymphatics were -0.2 and -0.25 mmHg. Therefore, it is possible that a positive pressure gradient can allow fluid to enter the initial lymphatics even in the face of a negative interstitial pressure. More current support for this hypothesis has been reported (85).

A passive interstitial pressure gradient, while sufficient, does not provide a complete description of every mechanism contributing to the formation of lymph. Pulsation of arteries was shown to aid in removal of interstitial tracer, which ceased after application of a steady arterial pressure (92). Likewise, in the bat wing preparation, cyclical dilatation of the venules provides a form of extrinsic pumping that also stimulates intrinsic spontaneous contractions of collecting lymphatics (35). Other factors that increase local tissue pressure and facilitate lymph formation include respiration, muscle contraction (e.g., peristalsis, walking), elevation of capillary filtration (e.g., venous hypertension, increased capillary permeability), and massage. Opposite to an increase in interstitial pressure, a variant of the hydrostatic pressure hypothesis posits that spontaneously contractile collecting lymphatic lymphangions, during their relaxation phase, are able to generate a suction that draws interstitial fluid into the initial lymphatics (99). Negative pressures produced by isolated bovine mesenteric collecting lymphatics

under “low filling” states have been reported (37), but direct evidence for transmission of this suction to the initial lymphatics is needed.

Further support for the hydrostatic pressure gradient hypothesis is derived from studies demonstrating a positive correlation between interstitial pressure and lymph flow, which are discussed next.

Interstitial Fluid Pressure and Its Influence on Lymph Flow

A convincing argument for an interstitial pressure gradient to drive lymph formation has been outlined in the previous section. The potential of the initial lymphatic lumen to collapse under a positive pressure difference is minimized by their unique anatomy. Initial lymphatic endothelial cells are tethered to the interstitium by anchoring filaments (68) responsible for holding the lumen open during conditions of increased tissue pressure or swelling, creating large (~ 2 μm diameter) interendothelial pores. The pores are a consequence of the “button”-like pattern of endothelial junctional adhesion proteins, in contrast to the contiguous expression of these molecules in blood vessel and collecting lymphatic endothelium (9). Thus, interstitial fluid is able to access the initial lymphatic lumen especially during edematous states when tissue pressure becomes positive.

Possibly as a result of the direct communication of the interstitial fluid and the lumen of the initial lymphatics, interstitial pressure and lymph flow are positively related. Several studies where tissue pressure was measured using the capsule technique provide direct evidence for this relationship (40, 121). Figure 2A, from Taylor *et al.* (122), shows

that the rise of lymph flow in the dog hind leg is steepest at tissue pressures of ~ 0-1 cmH_2O and attains a sustained maximal value when tissue pressure reaches 2 cmH_2O. The importance of this curve is that it maintains a constant interstitial volume due to the tight correlation between interstitial volume and interstitial pressure shown in Figure 2B (42). Two mechanisms protecting against edema (i.e., edema safety factors) are evident from Figure 1, assuming that interstitial pressure is normally negative: 1) Since interstitial pressure must rise above 2 cmH_2O for lymph flow to plateau, large changes in interstitial pressure can be accommodated before edema develops, and 2) an elevated lymph flow will return quickly the interstitial volume back to normal levels, as long as the excess volume does not exceed the capacity of the lymphatic circulation. Thus a small increase in interstitial volume greatly increases its pressure, promoting lymph flow that acts to restore the interstitial volume to normal.

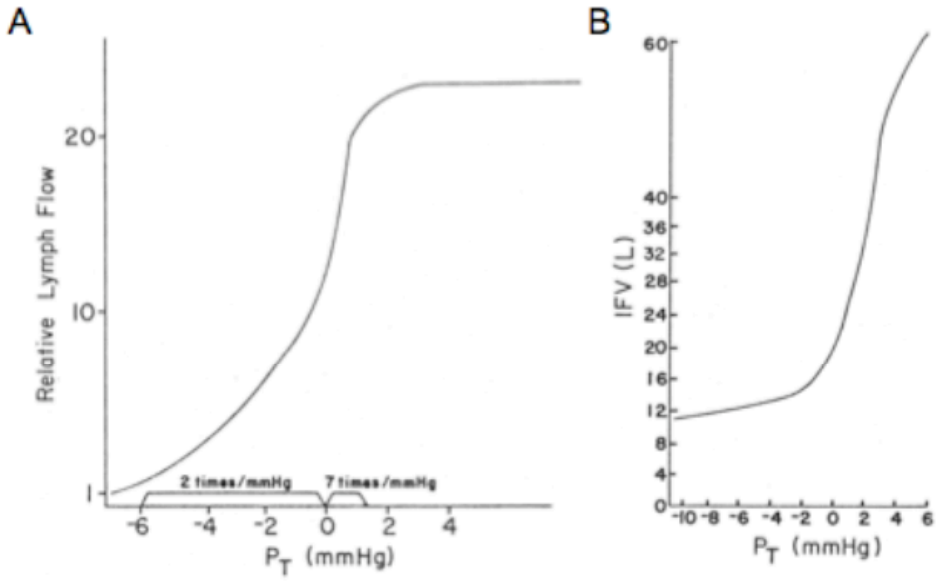

Figure 2. A, Relative increase in lymph flow versus tissue hydrostatic pressure (P_T, mmHg) during an experimental edema produced by intravascular infusion of Ringer's into a canine limb. **B**, Interstitial fluid volume (IFV in liters, L) versus P_T determined in man. Reprinted from Taylor *et al*. (123).

Propulsion of Lymph by the Lymphatic Muscle Pump

The field of research examining the functional and molecular control of lymphatic contractility has been productive in the past two decades. One key discovery is that lymphatic muscle may act as a functional hybrid between smooth and cardiac muscle because it contains molecular machinery from both cell types (84). This has stimulated new hypotheses about how collecting lymphatics are able to independently regulate both tonic and phasic contractions.

Hydrostatic pressure increases progressively as lymph moves downstream into larger vessels of the lymphatic vasculature. In contrast, peripheral veins in the human experience a greater hydrostatic pressure than the downstream central veins, especially when standing, owing to the effects of gravity. Restated, the pressure gradient produced by the heart, in addition to the extrinsic venous pump, provides the driving force for venous return (8). The lymphatic vasculature has no such pressure head (i.e., *vis a tergo*) so lymph does not – and cannot – *drain* passively through the lymphatic vessels, but requires propulsion. However, under edematous conditions, the interstitial pressure rises so that lymph may flow down a pressure gradient.

Lymph is transported throughout the lymphatic vasculature by intrinsic phasic contractions generated by the lymphatic muscle of collecting lymphatics that, along with valves, are necessary for unidirectional lymph flow. The spontaneous contractions are analogous to the cardiac contraction cycle consisting of a contraction and relaxation phase, stroke volume, and ejection fraction (12). For comparison, the measured ejection fraction and frequency of rat mesenteric collecting lymphatics were ~67% and 6 min^{-1},

respectively (12). Understanding the functional and molecular regulation of lymphatic spontaneous contractions is essential for developing therapeutic treatments for edema (and lymphedema) centered on augmenting contraction amplitude and/or frequency.

Since the walls of collecting lymphatics are vested with muscle cells, they are able to regulate their diameter and tone, therefore modulating lymph flow resistance. Several factors, both mechanical and chemical, are able to regulate collecting lymphatic tone (133). Mechanical stimuli include lymph flow, shear stress, hydrostatic pressure, and temperature. Hydrostatic pressure has been shown to elicit a myogenic response in collecting lymphatic muscle (measured during the relaxation phase) analogous to the arteriolar myogenic response (32). In that study an elevation in hydrostatic pressure induced constriction, thus reducing the end diastolic diameter of isolated collecting lymphatics, similar to the arteriolar myogenic response to pressure. Chemical factors influencing collecting lymphatic tone include neurotransmitters, neuropeptides, hormones, and metabolites. For instance, addition of the neuropeptide substance P to the superfusion bath potentiates the effect of pressure on myogenic tone and increases basal collecting lymphatic tone (4, 31).

Similar to cardiac myocytes, length-tension curves have been determined for the perivascular muscle of collecting lymphatics, arterioles, and venules (142). Wall tension and stress derived from these curves were found to be lowest in rat mesenteric lymphatics, while mesenteric veins possessed higher tension and stress, and that of mesenteric arteries was the highest. Functionally, this makes sense in that arterioles, the resistance vessels, constrict to regulate pressure and flow; venules and lymphatics possess

lower hydrostatic pressures reflecting their roles as capacitance vessels. The same group estimated the optimal preload (or hydrostatic pressure) for collecting lymphatic tone during peak active force to be ~ 5-13 cmH_2O, which compares well with measures of *in vivo* hydrostatic pressure (110, 143).

Other research has focused on the regulation of collecting lymphatic phasic activity. Functional studies demonstrated that lymph flow inhibits spontaneous contraction frequency and amplitude of both collecting lymphatic and thoracic duct isolated vessels (38). However, the conclusion was that *in vivo* total lymph flow (defined as passive flow plus contraction-generated flow) would not be diminished as expected. Instead, a reduction of pumping activity was suggested as a mechanism to reduce the outflow resistance in the presence of high passive flows.

Another vessel possessing spontaneous contractile activity besides the collecting lymphatics is the portal vein. Like the portal vein, collecting lymphatics were more sensitive to the rate rather than to the magnitude of circumferential stretch (33, 58). These characteristics are consistent with developmental work showing that lymphatic endothelial cells are derived from the cardinal vein (114). In experiments where isolated mesenteric collecting lymphatics were exposed to pressure ramps of different rates, bursts of increased contraction frequency were observed with increasing hydrostatic pressure ramps while inhibition of contraction frequency was observed for ramps decreasing pressure (33). When the effects of substance P on collecting lymphatic sensitivity to stretch were assessed, both contraction amplitude and frequency were enhanced under basal conditions and in response to elevations in pressure (4, 31).

The molecular basis for lymphatic spontaneous contractions has just begun to be explored. Nitric oxide (NO) has been implicated in the modulation of collecting lymphatic spontaneous contractions (38). Application of NO to the solution bathing isolated collecting lymphatics blunted spontaneous contraction frequency, amplitude, and ejection fraction in a fashion that imitated the effects of lymph flow. However, when the effect of elevated flow was investigated after the addition of the NO synthase inhibitor, L-NAME, NO did not fully account for the inhibition of contraction amplitude and frequency. NO involvement in the regulation of lymphatic spontaneous contractions is discussed in more detail in a recent review (141).

Importantly, calcium has been studied in the context of lymphatic phasic activity. Several different Ca^{2+} channels have been identified in lymphatic muscle, including L-type and T-type channels (49). A hypothesis for spontaneous transient depolarizations (STD) in the generation of spontaneous contractions has been proposed (131). At present it is likely that summation of several STD leads to a spontaneous contraction, with several ion channels appearing to be involved (131, 134). Another hypothesis states that pacemaker cells generate a current which spreads throughout the lymphatic muscle (89). The precise location of these cells, though, was made difficult by the diffusion of current (64). A newer study, however, has identified a subpopulation of lymphatic muscle cells that may act as pacemaker cells (76). While evidence for the sympathetic innervation of lymphatic muscle is abundant, its role in altering spontaneous contractions has not been fully investigated. Several current reviews cover this topic in greater detail (78, 128, 131, 141).

The benefits of studying the mechanisms of lymphatic contractions are obvious – during edema, when the lymphatic vessels appear overwhelmed, an increase in pumping efficiency would be expected to recover proper fluid balance.

Lymphatic Solute Permeability

Many studies have probed the 'solute permeability' of initial lymphatics in a qualitative fashion, in that absolute values of permeability were not measured directly. Instead, after injection of colloid or radiolabeled protein, inferences were made from visualizing tracer uptake, analyzing downstream lymph samples, or viewing histological sections. As previously stated, both interendothelial pores (70) and transendothelial vesicles (1, 70) have been implicated in solute and fluid removal from the interstitium by initial lymphatics. The physiological role for vesicles in the lymphatic vasculature remains unknown, but their appearance may reflect the anatomic variation in lymphatic morphology (41). Leak (70) favored the view that the interendothelial route was the major conduit for solute transport, whereas vesicles facilitated digestion of interstitial protein by the initial lymphatic endothelium. Generally, it is now believed that initial lymphatics are able to passively absorb particles, protein, cells, and fluid from the interstitium through large pores without regard for molecular size. Consequently, the lymph protein concentration of *initial* lymphatics probably approximates the protein concentration of the interstitium (120, 140). Much controversy still surrounds the question of whether the protein concentration of lymph from *collecting* lymphatics is

equal to that of interstitial fluid; i.e., whether collecting lymphatics possess the ability to concentrate solute along their length (17, 56, 119, 120).

Unlike initial lymphatic solute uptake, flux of solute across the collecting lymphatic walls depends on molecular size (75). Studies performed by Mayerson (75) were initially aimed at answering questions regarding blood capillary permeability, using the lymphatic circulation as a "window into the interstitium," but became focused on how efficiently lymph is transported through the lymphatic vessels. By injecting a known amount of radiolabeled albumin directly into a canine limb collecting lymphatic duct (of unknown diameter, but likely much larger than the peripheral collecting lymphatics, which average ~100 μm) and analyzing thoracic duct lymph, the percent albumin lost across the vessel wall was estimated (94). Not only is this method less sensitive than microfluorometric methods used today (50), but it almost certainly reflects the 'permeability' of the larger collecting lymphatic ducts and lymph nodes, not the prenodal microlymphatics or collecting lymphatic vessels. However, these studies were novel for the time and provided a first approximation of the size selectivity of the lymphatic ducts up to and including the thoracic duct. What Mayerson (75) discovered was that macromolecules equal to or greater than 6000 daltons (6 kDa) did not leave the larger ducts in 'great' quantity (albumin lost < 3%), while molecules smaller than 6 kDa escaped the vessels with ease. Simply put, large lymphatic ducts seemed to possess a relatively low 'permeability' to large macromolecules and a higher 'permeability' to molecules smaller than insulin.

Physiological Importance of Maintaining Lymph Flow

As summarized by Drinker (36), the main function of the lymphatic vasculature is to be:

> "…engaged steadily in returning blood proteins to the blood, and that in the absence of normal lymph function these substances will accumulate extravascularly."

Therefore, because approximately 50% of the plasma proteins are filtered by the blood microvessels per day, and are *not reabsorbed by the venules* (72, 82), the lymphatic circulation alone is left with the task of returning these proteins to the blood (41, 100). Extravascular accumulation of plasma proteins, if unchecked, leads to the osmotic flow of water into the interstitium, producing edema. Further, Drinker (36) found that if thoracic duct lymph flow is diverted into a test tube, then the blood microvasculature "simply converts all the plasma to lymph." Such a circumstance is not compatible with life and illustrates the importance of a properly functioning lymphatic vasculature that returns protein and fluid to the blood.

In reality the extreme circumstance of stopping systemic lymph flow is rarely encountered, but several other mechanisms are known to diminish regional lymph transport: vessel regression or damage (including radiation and surgical transection), valvular incompetence of the collecting lymphatics, vessel obstruction either by parasites (filariasis) or cancer cells (metastasis), and inhibition of spontaneous contractions (e.g., by calcium channel blockers (15)). Because lymph flow is needed to return plasma proteins and water to the blood circulation, these events cause a backup of the capillary

filtrate into the interstitium. Eventually, sufficient fluid accumulates in the interstitium to increase the interstitial hydrostatic pressure until it matches the capillary pressure and water ceases to be filtered into the interstitium. Solute continues to diffuse down its concentration gradient into the interstitium until the protein concentration matches that of the blood flowing through the capillaries. When this occurs, fluid and solute are at equilibrium between the interstitium and blood. This type of edema is called "lymphedema", as it originates from a deficiency in lymphatic function.

However, another mechanism exists that could reduce lymph flow enough to produce lymphedema – a change in lymphatic vessel permeability to water and solute. Here the phrase 'lymphatic permeability' is meant to be analogous to that of blood microvessels because it refers to the permeability of the lymphatic vessel endothelium, not the permeability of the large initial lymphatic pores as is commonly assumed. As the permeability of the collecting lymphatic vessels to protein is the focus of this dissertation, the next section will explain how alterations in lymphatic permeability would be expected to lead to a diminished lymph flow.

Microvessel Solute Permeability Theory

To explain how Mayerson's observations (75) differ from direct measures of permeability, we must first understand what 'permeability' means. The terminology here will be the same as that used for the blood microvessels (50).

The diffusion of a solute across a semi-permeable membrane is described by Fick's first law:

$$P_s = J_s/S\Delta C, \quad (1.1)$$

where membrane permeability to a solute ($\mathbf{P_s}$, $cm \cdot s^{-1}$) is defined by the rate at which solute crosses the membrane (solute flux, $\mathbf{J_s}$, $mmol \cdot s^{-1}$) over its finite surface area ($\mathbf{S}$, cm^2) with a constant concentration gradient between the two sides of the membrane ($\Delta\mathbf{C}$, $mmol \cdot mL^{-1}$). This relationship accurately describes the diffusional permeability of a vessel to a solute in the absence of a hydrostatic pressure gradient across the vessel wall. Blood vessels, however, have both hydrostatic and oncotic pressure differences across their walls, with the net effect of filtering water into the interstitium. If water and solute share the same pathway, then water movement can force solute across the vessel wall faster than it would occur by diffusion alone. The name for this process is convective transport and can lead to a pressure-dependent increase in solute flux.

A separate relationship describes the movement of water across the blood vessel wall. In 1896 Starling (116) hypothesized that the balance of two forces ($\mathbf{P}$, hydrostatic pressure; and $\boldsymbol{\pi}$, oncotic pressure; both in cmH_2O) determine water flux ($\mathbf{J_v}$, $mL \cdot s^{-1}$) leading to the modern day form of the Starling equation:

$$J_v/S = L_p[\Delta P - \sigma\Delta\pi], \quad (1.2)$$

where ΔP and $\Delta\pi$ refer to the differences in hydrostatic and oncotic pressures, respectively, between the blood vessel lumen and the interstitium. The probability that a solute traveling towards the vessel wall will pass through or be reflected back into the lumen is denoted by the reflection coefficient, $\boldsymbol{\sigma}$, and is a value between 0 and 1. If a protein were to have a reflection coefficient of 0, every molecule encountering the wall would pass through to the interstitium so that no oncotic pressure difference would be

observed. Conversely, if the reflection coefficient were 1 for a protein, then every molecule would be retained in the lumen, water could move, and the full oncotic pressure difference would be exerted across the wall. In actuality, the value is between 0 and 1 for proteins so that some fraction of the oncotic pressure is expressed (i.e., effective oncotic pressure). For the macromolecule albumin, this value is in the range of 0.85 – 0.95 depending on the animal species, vessel type, or charge of the protein. The L_p term in Equation 2 is a measure of the porosity, or permeability, of the vessel wall to water and is called hydraulic conductivity (**L_p**, $cm \cdot s^{-1} \cdot cmH_2O^{-1}$).

Equation 1.1, then, is an incomplete description of all the forces involved in solute flux across the endothelial barrier. We can rewrite the equation to include the convective component of solute flux as:

$$P_s = J_s/S\Delta C = P_d[Pé/(e^{Pé} - 1)] + J_v/S(1 - \sigma), \qquad (1.3)$$

where P_s is the apparent permeability to solute (at a particular hydrostatic pressure), **Pé** stands for the Péclet number, a (unitless) ratio between the convective and diffusive driven solute flux. Specifically, the ratio is defined as:

$$Pé = [(J_v/S)(1 - \sigma)] / P_d. \qquad (1.4)$$

The other new term introduced in Equations 1.3 and 1.4 is the diffusional permeability (**P_d**, $cm \cdot s^{-1}$), and is defined as the permeability measured when only diffusion is driving solute flux; i.e., when no other forces, such as convection, are present.

Returning now to Mayerson's experiments (75), we can see that his observations cannot suffice as substitutes for permeability measurements because changes in pressure, surface area, or concentration could result in changes in *solute flux* that have no

corresponding physiologically relevant meaning relative to the structure of the exchange barrier, whereas changes in *permeability* accurately reflect physiological processes that alter the rate at which solute crosses the endothelial barrier. What he was really measuring was the amount of solute lost per unit time and is equivalent to J_s ($mmol \cdot s^{-1}$). To calculate permeability, he would have needed three additional pieces of information – the surface area of the vessel, the concentration difference across the vessel wall, and the pressures of the vessel where the solute was lost. Thus, we can see from Equation 1.3 that while several extraneous factors could alter *falsely* a measure of solute flux, permeability measurements are inherently more accurate at describing solute movement as they account for pressure, convection, surface area, and solute concentration.

Typically, solute leaks from the blood microvessels down its concentration and pressure gradient; i.e., the solute concentration is greater in the vessel lumen than in the interstitium (see Eqn 1.1). For most plasma proteins this is the case and they leak into the tissue spaces, albeit slowly. However, the concentration gradients for proteins in lymph have not been established throughout the lymphatic vessel network, making it difficult to know whether increasing permeability to a solute will result in a faster transport of solute *into* or *out of* the vessel.

Natriuretic Peptides and their Influence on Microvascular Permeability

The natriuretic peptides are peptide hormones secreted predominantly either by the heart or by the vascular endothelium with the net effect of reducing cardiovascular volume. Multiple isoforms are secreted by the heart – atrial natriuretic peptide (ANP) is

secreted mainly by the atria and the majority of brain natriuretic peptide (BNP) is secreted by the ventricles. Precursor proteins are cleaved to give rise to both active isoforms whose plasma concentrations increase in response to myocardial stretch. The third isoform, C-type natriuretic peptide (CNP), is produced by and acts on the endothelium in an autocrine manner. The actions exerted by ANP are well documented and include natriuresis and inhibition of the renin-angiotensin-aldosterone axis, which serve to reduce the vascular volume (101). This is particularly important in lowering vascular volume in response to vascular volume expansion or fluid shifts (e.g., microgravity and congestive heart failure).

ANP has also been reported to increase the vascular permeability of microvessels to water and solute (51, 80). By increasing vascular permeability, both water and protein leave the vasculature faster with the effect of displacing some of the vascular volume into the interstitium. Another name for this process is "third-spacing," as the interstitium represents the third compartment in the body, after the vascular and cell compartments. When capillary and venular responses to ANP were compared, no difference in sensitivity was observed (53). While the effects of BNP on mammalian microvessel permeability were never tested, the permeability responses of frog capillary venules to BNP is similar to that of ANP (79).

An important question to answer is whether ANP or BNP alter lymphatic vessel permeability to either solute or water, since the lymphatic vessels are important in regulating fluid homeostasis. One recent study provides evidence that upon ANP infusion into the splenic artery, extrasplenic lymphatic solute flux increased (18), suggesting that

these peptides may target the lymphatic circulation as an additional mechanism to reduce cardiovascular volume.

Hypotheses

The most recent understanding of lymphatic permeability has been presented, demonstrating that several important questions remain to be answered. Are lymphatic vessels absorptive, leaky, or perhaps are they impermeable as textbooks propose? Would an increase (or decrease) in lymphatic permeability be expected to resolve or create edema? Does lymphatic permeability change significantly in response to vasoactive agents known to alter vessel tone or in any cardiovascular diseases? Are there regional differences in lymphatic permeability (e.g., between micro- and collecting lymphatics)? Do collecting lymphatics really concentrate solute along their length?

The current dissertation answered several of these questions by testing the following two hypotheses based on the fact that lymphatic endothelial cells originate from the venous endothelium (114) and the inference that functional similarity exists between the lymphatics and venules:

1) The collecting lymphatic permeability to albumin will not differ from that of venules in the same tissue.

2) A vasoactive peptide hormone encountered during volume expansion/shifts as occurs in congestive heart failure (specifically, 100nM atrial or brain natriuretic peptide) known to increase venular permeability to albumin will elevate collecting lymphatic vessel permeability to albumin to a similar magnitude and with similar kinetics.

CHAPTER 2: *IN VIVO* DETERMINATION OF COLLECTING LYMPHATIC VESSEL PERMEABILITY TO ALBUMIN: A ROLE FOR LYMPHATICS IN EXCHANGE

Abstract

While it is well established that the lymphatic vasculature is central to fluid and solute homeostasis, how it accomplishes this task is not well defined. To clarify the basic mechanisms underlying basal fluid and solute homeostasis, we assessed permeability to rat serum albumin (P_s^{RSA}) in mesenteric collecting lymphatic vessels and venules of juvenile male rats. Using the quantitative microfluorometric technique originally developed for blood capillaries, we tested the hypothesis that as a consequence of venules and collecting lymphatics sharing a common embryological origin, their P_s^{RSA} would not differ significantly. Supporting our hypothesis the median collecting lymphatic P_s^{RSA} ($3.5\pm1.0 \times 10^{-7}$ cm·s^{-1}, N=22) did not differ significantly from the median venular P_s^{RSA} ($4.0\pm1.0 \times 10^{-7}$ cm·s^{-1}, N=8, p=0.61). For collecting lymphatics the diffusive permeability ($P_d = 2.5 \times 10^{-7}$ cm·s^{-1}) was obtained from the relationship of apparent P_s^{RSA} and pressure. While the measured P_s^{RSA}, P_d, and estimated hydraulic conductivity of collecting lymphatics and venules were similar, the contribution of convective coupling differs as a result of the higher hydrostatic pressure experienced by venules relative to collecting lymphatics *in vivo*. In summary, the data demonstrate the capacity for collecting lymphatics to act as exchange vessels, able to extravasate solute and filter fluid. As a

consequence these data provide experimental support for the theory that prenodal lymphatic vessels concentrate intraluminal protein.

Introduction

The lymphatic system is known to be vital for fluid homeostasis, lipid absorption, and immune surveillance under conditions of health (41, 74, 75). Less widely understood is the role of the lymphatic system in disease states such as edema, inflammation, cancer, and obesity (2, 46, 115). A recent upsurge in interest, likely reflecting the development of novel molecular markers specific for lymphatic vessels and realization of their importance to disease, has led to significant advances in this field (26). Knowledge of lymphatic vessel function, though, still lags behind that of the blood vessels given the difficulty in studying these structures that are sensitive to both mechanical and chemical stress (75). While lymphangiogenesis, lymphatic pumping, and lymph node function are receiving current attention, other elusive aspects of the lymphatic system that deserve attention still remain.

One aspect of lymphatic function relates to its role in exchange, in particular, lymphatic vessel permeability to solute. Lymphatic permeability was studied in the 1960s predominantly as a means for gaining insight into blood capillary permeability. The few experiments performed during that era concluded that the lymphatic system retains all solutes with molecular weights larger than 2300-6000 (75). Because radiometric methods used at that time had limited sensitivity compared to present day microfluorometric methods that facilitate quantitative measurement of solute flux in living tissue (51), we

decided to use the latter approach to test the hypothesis that lymphatic vessels possess a macromolecular permeability analogous to that of the blood microvessels, particularly venules, under basal conditions.

Blood microvessels are permeable to solute and water. In health, microvessel permeability is influenced by tissue function and can be modestly regulated both positively and negatively. Microvessels possess a barrier of finite permeability to provide adequate perfusion of the tissues with nutrients, oxygen, and lipids. However, it is widely taught that the processes controlling exchange, whether water or solute, are passive and that only under inflammatory states does permeability change – usually an increase whereupon materials contained in the vascular compartment leak into the tissue space, thereby compromising function. Furthermore, microvascular exchange has been represented pictorially in multiple texts by a single exchange vessel, a capillary, connecting a single arteriole with a single draining venule (13, 16). In this oversimplified model, filtration of fluid occurs on the arterial (high pressure) end of the capillary and reabsorption of 90% of this filtrate occurs on the venous side of the capillary (16, 43). In opposition to this view, many experimental studies have provided evidence that filtration occurs throughout the microvascular network of vessels, with reabsorption only occurring during special states (e.g., increased tissue hydrostatic pressure) or in encapsulated organs (72, 82, 100). Appreciation of this discrepancy is important because the mental picture of a single capillary replacing a microvessel network obscures the clinically important role that the missing constituents, the lymphatic vessels, play in the establishment and maintenance of proper fluid homeostasis. Thus, the fact that the microvessels filter

approximately 50% of the circulating plasma proteins per day – all of which is returned to the circulation by the lymphatic system – reinforces this assertion (36, 41, 100).

The focus of this manuscript, the collecting lymphatic vessels, share important features with veins, including presence of valves, smooth muscle, and chronic exposure to a low hydrostatic pressure environment. Notably, the developmental origin of lymphatic endothelium has recently been shown to be the veins (114). Given their morphological similarity and common embryological origin, we hypothesized that the permeability of collecting lymphatic vessels and venules to albumin would not differ in a given tissue. Additionally, given that collecting lymphatics exhibit a greater hydrostatic pressure than microlymphatics, we posited that collecting lymphatics were a potential site for solute exchange (143). Here, for the first time, we measure basal permeability values to rat serum albumin for *in vivo* rat mesenteric collecting lymphatics. To accomplish this task we developed and validated a reliable method for cannulation and perfusion of collecting lymphatics in rat mesentery.

From measurements of albumin flux at multiple hydrostatic pressures, we determined the diffusive permeability to albumin (P_d) and the convective coupling of albumin flux to transmural fluid flux of collecting lymphatic vessels from rat mesentery. Utilizing these data, estimates of volume flux of the collecting lymphatics over a range of physiological pressures were determined. We found, consistent with our hypothesis, that permeability to albumin does not differ between venules and collecting lymphatic vessels. Preliminary results from this study have been presented in abstract form (109).

Methods

Ethical Approval:

Animal protocols were approved by the Institutional Animal Care and Use Committee (IACUC) at the University of Missouri and conducted in accordance with the National Institutes of Health's *Guide for the Care and Use of Laboratory Animals*. All animals were killed after the experiment by an overdose of anaesthetic followed by bilateral pneumothorax and aortic transection in agreement with the protocol.

General Surgical Preparation:

All experiments were performed *in situ* on juvenile male (35-55 days, 200-250g) Sprague Dawley rats (Hilltop Lab Animals, PA, USA) housed 3 to a cage for a minimum one-week acclimation period prior to the experiment. For these initial studies, juvenile males were chosen for their lack of visceral fat, which facilitated location and subsequent cannulation of collecting lymphatics. One venule or collecting lymphatic was cannulated per animal.

Following induction of anesthesia with Inactin (IP, thiobutabarbital, Research Biochemicals Int., MA, USA, 128 mg/kg body weight), surgical exteriorization of the mesentery and continuous superfusion (2-3 mL/min) with mammalian Krebs at 37 ± 0.5°C, a vessel was located under the Zeiss dissection microscope. The animal on a custom, heated Plexiglas™ board was then transferred to a Leitz Diavert inverted microscope and the suffused preparation was allowed to equilibrate for approximately 30 minutes prior to vessel cannulation and data collection.

Venular and Lymphatic Microvessel Classification:

To facilitate comparison of our data with previously published measurements of mammalian venular permeability (104, 107), only relatively straight, unbranched venules with brisk flow and fewer than 2 adherent leukocytes were used. Vessels enveloped by adipose tissue were avoided because the fat cells make cannulation nearly impossible. Venules were identified by size, paucity of smooth muscle, and converging flow on either side of the vessel segment as described by Chambers and Zweifach (22). Collecting lymphatic vessels were identified by the presence of valves, spontaneous contractions, and their transparent contents (143). Leukocytes were often visualized in collecting lymphatics, which were not studied if more than 2 adherent cells were seen.

Solutions:

Mammalian Krebs. All superfusion and perfusion solutions were prepared fresh and used on the same day. Unless otherwise stated all materials were purchased from Sigma (MO, USA). The Krebs solution consisted of (in mmol): 141.4 NaCl, 4.7 KCl, 2.0 $CaCl_2 \cdot 2H_2O$, 1.2 $MgSO_4$, 1.2 $NaH_2PO_4 \cdot H_2O$, 5.0 d-glucose, 3.0 $NaHCO_3$, and 1.5 NaHEPES. The pH of the solution was 7.4 ± 0.05 at 37°C.

Krebs-BSA. Dialyzed (Supplemental Methods) bovine serum albumin (BSA, Sigma cat# A7906) was added to the Krebs solution to achieve a final concentration of 1 mg/mL on the day of the experiment. The osmolarity, measured by freezing point osmometry, was generally between 292-297 mOsm after the addition of BSA.

Labeled Protein. The macromolecular probe used in this study, rat serum albumin (RSA, Sigma cat# A6272), was bound to the Alexa-488® fluorophore (Invitrogen, CA, USA) by modifying the manufacturer's protocol (see Supplemental File). The perfusate solution contained 10% (w/v) labeled RSA (1 mg) with 9 mg of unlabeled RSA and was brought to a volume of 1 mL with freshly made Krebs solution so that the final total protein concentration was 10 mg/mL. A washout solution was made, with unlabeled protein, at an identical total protein concentration. Both solutions of 10 mg/mL RSA possessed an oncotic pressure of 4.1 cmH_2O calculated from the Landis-Pappenheimer equation (67).

Assays for Total Protein and Albumin Concentration of Lymph:

The concentration of albumin and total protein were measured in samples of lymph, peritoneal fluid, and plasma (N=4). Lymph was obtained after cannulation with an empty siliconized single lumen micropipette (tip diam. = 25 μm) of collecting lymphatic vessels in rat mesentery covered with mineral oil. Peritoneal fluid was obtained by swabbing the mesentery with a hematocrit tube immediately following the midline incision. Approximately 20-60 μL of blood-free lymph and peritoneal fluid were obtained using these methods. Plasma was obtained by centrifuging ~3 mL of blood (taken by intracardiac puncture) for 10 minutes at 3220×g.

Total protein concentration of each sample was determined (Supplemental File) by the Micro BCA Protein Assay, while albumin concentration was determined by the Albumin Blue 580 Fluorescence assay (62). All solutions were made fresh on the day of

use. The albumin or total protein concentration was then used to calculate the albumin or total protein oncotic pressures, respectively, for each sample using the Landis-Pappenheimer equations (67).

Measurement of Microvessel Protein Flux:

The method for determining solute permeability (P_s) to proteins in mammalian blood microvessels and its limitations is described in several publications (50, 104, 107). In short, collecting lymphatics and venules studied here were cannulated with custom made pipettes and perfused with either fluorescently labeled RSA (dye) or unlabeled RSA (washout) in Krebs solution. Details of the pipette fabrication and cannulation procedures are to be found in the Supplemental Methods. In experiments using theta pipettes the vessel was perfused at constant, selected pressures under user control. Switching a valve changed the perfusate from the washout solution to the dye solution for a time sufficient to make measurements of fluorescence intensity without altering pressure. Additionally, this system allowed the native vessel pressure (P_{Lumen}, Table 1) to be measured prior to assessment of solute flux by keeping the fluorescent dye front from moving within the pipette. Pressure in spontaneously contracting collecting lymphatics is constantly changing so only diastolic pressure (during relaxation) was recorded. Importantly, one must understand that these native pressure measurements (Table 1) were made before measuring solute flux to establish the native pressure range for collecting lymphatics. To measure solute flux the pipette pressure was raised above that of the vessel in order to elicit flow of the perfusate. During the solute flux measures, the

perfusion pressure of the theta pipette was measured when there was zero flow through the non-perfusing side. This pressure was plotted in Fig. 5, but was not reported in Table 1.

Direct measures of solute flux (J_s, mmol/s) were made over an area of vessel defined by a rectangular diaphragm (width ≥4 vessel diameters, length = 8 vessel diam.). When dye labeled solute filled the vessel lumen there was an initial step increase in fluorescence intensity (I_o), followed by a gradual, but linear, increase in intensity as fluorescent probe accumulated in the interstitial space over time (dI_f/dt) in addition to the signal generated from the fluorophore flowing through the vessel lumen. Apparent solute permeability (P_s, $cm \cdot s^{-1}$) was calculated from the equation relating solute flux (J_s, $mmol \cdot s^{-1}$) to surface area (S, cm^2) at a constant concentration difference (ΔC, $mmol \cdot mL^{-1}$)(50):

$$P_s = J_s/S\Delta C = (1/I_o)(dI_f/dt)(D/4) \qquad (2.1).$$

Vessels were assumed to be circular and to have a volume-to-surface area ratio of D/4.

Triplicate measures of flux were attempted in each vessel. In some vessels solute flux was measured at different hydrostatic pressures to assess the relationship between convective and diffusive flux. Previously, we and others (27, 50) have shown that when convective water movement contributes to J_s, measures of P_s overestimate the true diffusive permeability (P_d). These terms are related by the equation:

$$P_s = J_s/S\Delta C = P_d[Pé/(e^{Pé} - 1)] + J_v/S(1 - \sigma) \qquad (2.2),$$

where Pé is the Péclet number:

$$Pé = [J_v/S(1 - \sigma)]/P_d \qquad (2.3).$$

Eqn. 2.2 is a modified form of the Patlak, Goldstein, and Hoffman equation (93). Assuming a homoporous barrier and a small constant interstitial oncotic pressure,

$$P_s = J_s/S\Delta C = P_d[Pé/(e^{Pé} - 1)] + L_p(1 - \sigma)(\Delta P - \sigma\Delta\pi) \quad (2.4),$$

where ΔP (cmH_2O) is the hydrostatic pressure difference between the vessel lumen and the interstitium ($P_c - P_i$), L_p is the hydraulic conductivity ($cm \cdot s^{-1} \cdot cmH_2O^{-1}$), σ is the unit-less reflection coefficient for solute, and $\Delta\pi$ (cmH_2O) is the oncotic pressure difference ($\pi_c - \pi_i$) exerted across the vessel wall. Plotting P_s against hydrostatic pressure and simultaneously solving for P_d and $L_p(1 - \sigma)$ from Eqn. 2.4 yields a curve describing the data. When the net filtration pressure ($\Delta P - \sigma\Delta\pi$) is equal to zero, the y-intercept becomes P_d. The limiting slope of this line is $L_p(1 - \sigma)$ and labeled in Fig. 5 (52).

Volume flux (J_v, $cm^3 \cdot s^{-1}$) across a semipermeable membrane of surface area (S) is described by the modern form of the Starling equation:

$$J_v/S = L_p(\Delta P - \sigma\Delta\pi) \quad (2.5),$$

where L_p, ΔP, σ, and $\Delta\pi$ are as defined above. However, this equation describes J_v during transient (i.e., when pressure is changing) rather than steady state conditions. Another equation has been developed that describes steady state J_v (82):

$$J_v/S = L_p[\Delta P - \sigma^2\pi_c(1 - e^{-Pé})(1 - \sigma e^{-Pé})^{-1}] \quad (2.6a).$$

Eqn. 2.6a can be rewritten to group the unknown terms on one side of the equation:

$$\Delta P = (J_v/L_pS) + \sigma^2\pi_c(1 - e^{-Pé})(1 - \sigma e^{-Pé})^{-1} \quad (2.6b),$$

where π_c is the colloid osmotic pressure in the vessel. Neither eqn. 2.5 nor 2.6 assume large hydrostatic pressures or large Pé values.

Statistical Analyses:

Prism™ (GraphPad Software, CA, USA) software was used for all statistics. To determine whether the P_s to albumin (P_s^{RSA}) in collecting lymphatic vessels differed significantly from the venular P_s^{RSA}, the nonparametric Mann-Whitney U test was performed at a 95% confidence level to compare the medians because data from both groups were left skewed (i.e., not normally distributed). Distribution normality was determined by the D'Agostino-Pearson K^2 test. The Kolmogorov-Smirnov Two Sample test was performed (30) to compare the distributions of collecting lymphatic and venular P_s^{RSA} values with 95% confidence. To compare the medians of all three skewed data sets, the nonparametric one-way ANOVA Kruskal-Wallis test was performed at a 95% confidence level. Medians were reported as median ± median absolute deviation (MAD). Means were compared with the Student's unpaired t-test and reported as means ± standard error (SE) to compare the present permeability data with published values. For comparisons of total protein and albumin concentration differences between peritoneal fluid and lymph, Student's paired t-tests were performed and the means ± standard error (SE) were reported.

Power analysis performed beforehand indicated that to detect a 20% change between the two groups (1×10^{-7} cm·s^{-1}), with a 95% confidence (significance level $P<0.05$), approximately 21 animals were needed in each group (86).

Results

Raw Tracings of Solute Flux

Figure 3 illustrates a raw data tracing of the fluorescence intensity of the probe (Alexa-488® conjugated RSA) as a function of time from experiments on two separate animals. The tracing on the left is from a collecting lymphatic vessel perfused at a pressure of 5 cmH_2O and the tracing on the right is from a similar vessel perfused at a pressure of 15 cmH_2O. Visible spontaneous contractions, shown in the expanded view as fluctuations in the fluorescence intensity, are evident from tracing A, while tracing B lacks these fluctuations. Both patterns were encountered in the present study only after cannulation, since prior to cannulation all collecting lymphatic vessels exhibited spontaneous contractions.

Basal Albumin Permeability of Collecting Lymphatics and Venules

Table 1 reports the apparent albumin permeability values (P_s^{RSA}) of all vessels in this study along with their respective native pressure and diameter measurements. The P_s^{RSA} of collecting lymphatics and venules did not differ significantly whether analyzed as means (p = 0.80, 5.0±0.9 x 10^{-7} $cm \cdot s^{-1}$ (N=22) vs. 4.6±0.9 x 10^{-7} $cm \cdot s^{-1}$ (N=8)) or medians (p = 0.61, 3.5±1 x 10^{-7} $cm \cdot s^{-1}$ vs. 4.0±1 x 10^{-7} $cm \cdot s^{-1}$) consistent with our hypothesis. As anticipated from the work of Zweifach & Prather (143), collecting lymphatic native pressure (P_{Lumen}) correlated with diameter (p = 0.03, Table 1). When P_{Lumen} and diameter of collecting lymphatics was compared to that of venules, lymphatic pressure was significantly lower ($p < 0.0001$) and diameter was significantly greater ($p < 0.0001$).

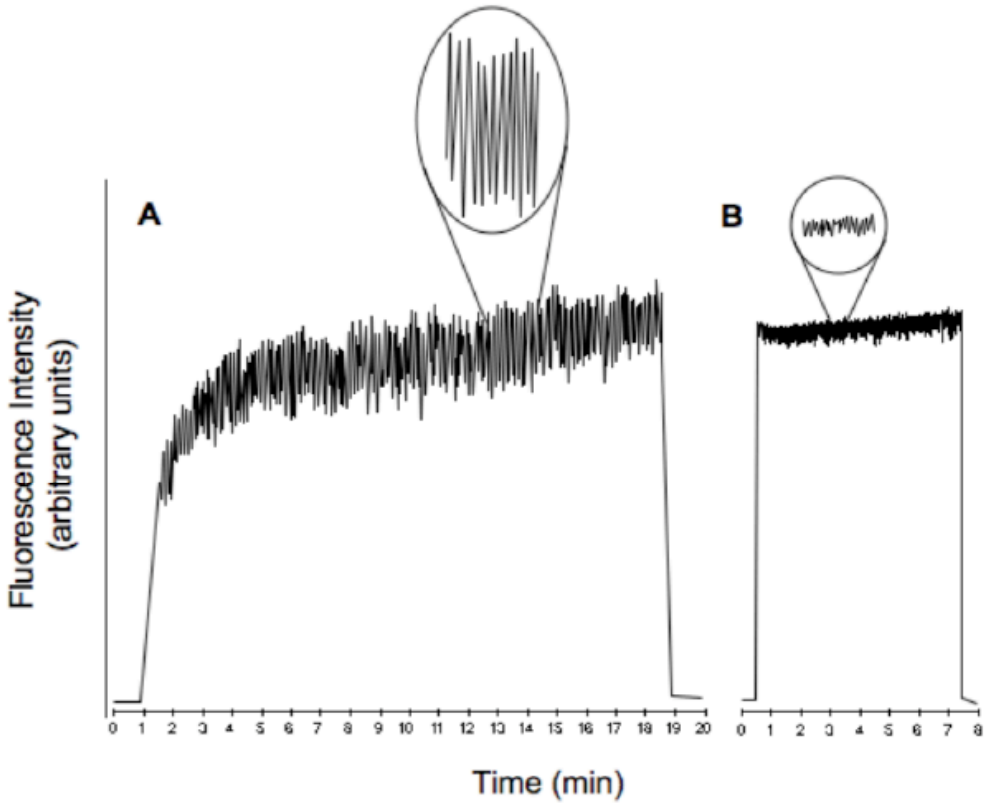

Figure 3. Raw data tracings from two different rat mesenteric collecting lymphatics. **A**: Collecting lymphatics perfused at low pressures exhibit spontaneous contractions at a frequency of ~15 min^{-1} (see ~90 s tracing in insert). In this case perfusion pressure was 5 cmH_2O. **B**: Upon perfusion at a higher pressure of 15 cmH_2O, spontaneous contractions are greatly attenuated so that only noise is evident (see ~60 s insert).

Comparing frequency distributions for all 22 collecting lymphatic P_s^{RSA} values reported in Table 1 (Fig. 4A) and 26 rat mesenteric venular P_s^{RSA} values (Fig. 4B) (102, 104) provides additional support for the hypothesis. Both frequency distributions were strikingly similar and left skewed. The Kolmogorov-Smirnov Two Sample test (30) concluded that these two distributions did not differ ($p = 0.37$). Since the distributions are not statistically normal ($p < 0.0001$), it is more accurate to compare the medians instead of the means of the two populations (86, 104). The Mann-Whitney U test was performed and demonstrated that the median collecting lymphatic ($P_s^{RSA} = 3.5\pm1 \times 10^{-7}$ cm·s^{-1}, N=22) and median venular ($P_s^{RSA} = 5.6\pm2 \times 10^{-7}$ cm·s^{-1}, N=26) values for albumin permeability did not differ significantly ($p = 0.12$). When we tested for any differences between all three groups by performing the Kruskal-Wallis test, none were observed ($p = 0.24$). Finally, when we compared our measured venular values to those previously reported (102, 104), we discovered that they did not differ ($p = 0.31$).

Convective Coupling of Albumin Flux

All apparent P_s^{RSA} values from collecting lymphatics were graphed in Fig. 5 to illustrate the dependence of solute flux on hydrostatic pressure. The dashed line demarcates the effective osmotic pressure ($\sigma\Delta\pi = 3.85$ cmH_2O) of the perfusion solution when σ is 0.94. Where it meets the solid line is the true diffusive permeability to albumin ($P_d = 2.5 \times 10^{-7}$ cm·s^{-1}). The limiting slope of the solid line is equal to $L_p(1 - \sigma) = 1.3 \times 10^{-8}$ cm·s^{-1}·cmH_2O^{-1}, and is used to calculate the Péclet number. Additionally, the L_p of the pathway conducting both solute and water can be estimated from this term if σ is known.

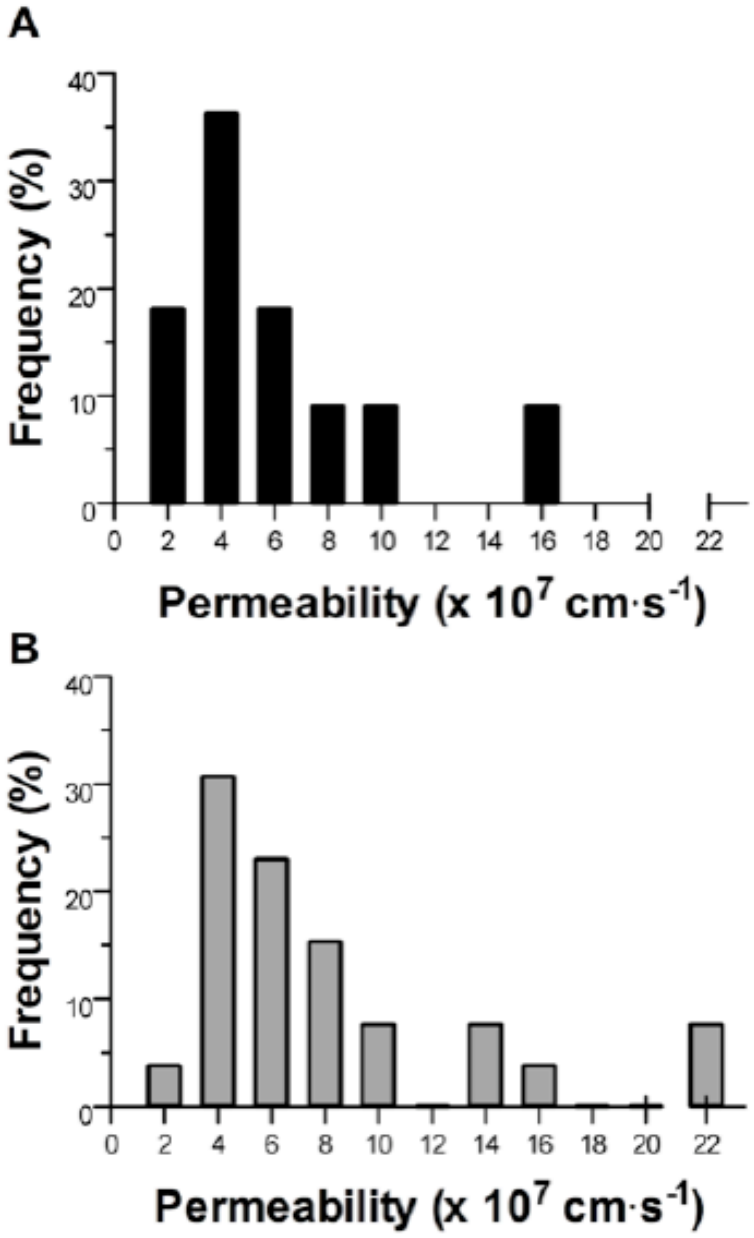

Figure 4. Frequency distribution of basal apparent permeability (P_s^{RSA}, x 10^{-7} cm·s^{-1}) values of juvenile male rat mesenteric collecting lymphatics (**A**) and venules (**B**). Venular data are redrawn from a dissertation (102) and do not contain any venular measures from this study. All data are plotted as a percentage of the total.

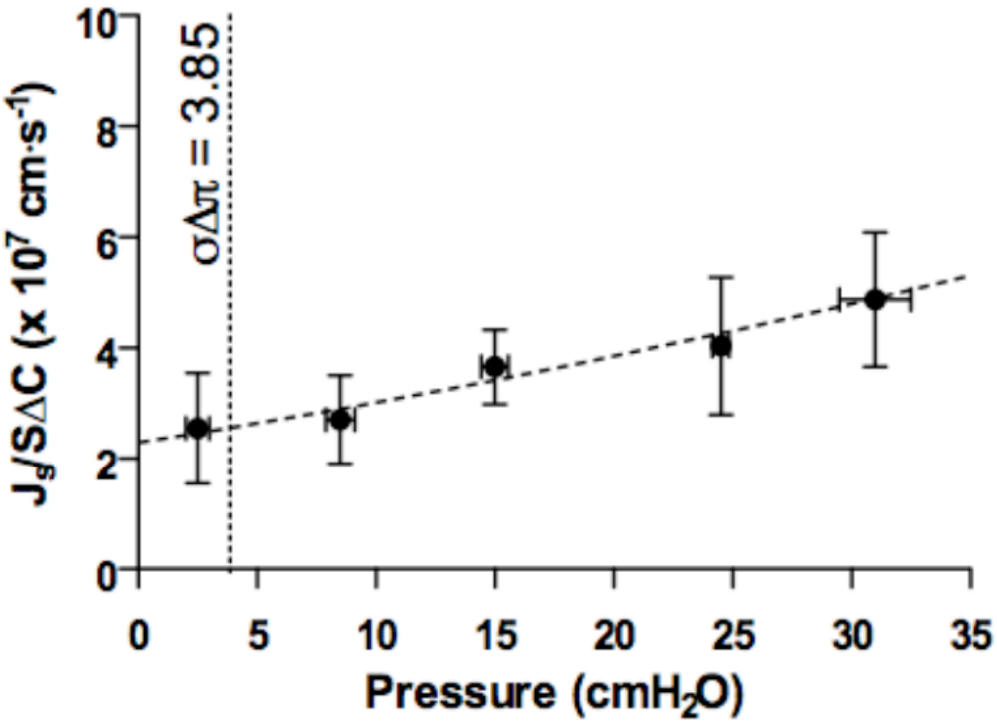

Figure 5. Juvenile rat mesenteric collecting lymphatic permeability to albumin (P_s^{RSA}) plotted as a function of hydrostatic pressure (cmH_2O) to determine the contribution of (pressure driven) convective coupling to solute flux. The predicted relationship (solid line) was obtained from simultaneous solution for P_d ($cm \cdot s^{-1}$) and $L_p(1 - \sigma)$ ($cm \cdot s^{-1} \cdot cmH_2O^{-1}$) in Eqn. 2.2. The dashed line marks the effective oncotic pressure ($\sigma\Delta\pi$, cmH_2O). The apparent permeability (P_s^{RSA}) is equal to the diffusive permeability (P_d) at zero net filtration pressure (intersection of solid and dashed lines) and the limiting slope is equal to $L_p(1 - \sigma)$.

Predicted Solute and Volume Flux from the Albumin Concentration of Lymph and Peritoneal Fluid

Figure 6 (from Table 2) summarizes the measured albumin and total protein concentration of lymph, peritoneal fluid, and plasma from 4 animals. The calculated oncotic pressures for total protein and albumin, given for each compartment, were then used to predict the relationships illustrated in Fig. 7.

Predicted solute flux per unit surface area per concentration difference ($J_s/S\Delta C$) was plotted over pressure in Fig. 7A. To accomplish this P_d and J_v/S (obtained below) were substituted into Eqn 2.2. The limiting slope of this line is equal to $L_p(1 - \sigma)$.

The volume flux per unit surface area (J_v/S) as a function of pressure was predicted for transient and steady state conditions by substituting P_d and L_p into Eqns. 2.5 and 2.6b (shown in Fig. 7B). The calculated oncotic pressure difference for albumin ($\Delta\pi$) was substituted into Eqn. 2.5, while the calculated oncotic pressure of lymph albumin (π_L) was appropriately substituted into Eqn. 2.6b. Both the steady state and transient state curves are shown over a wide range of pressures. The x-intercepts correspond to the transmural effective oncotic pressures and are labeled. The limiting slope of all lines is equal to L_p.

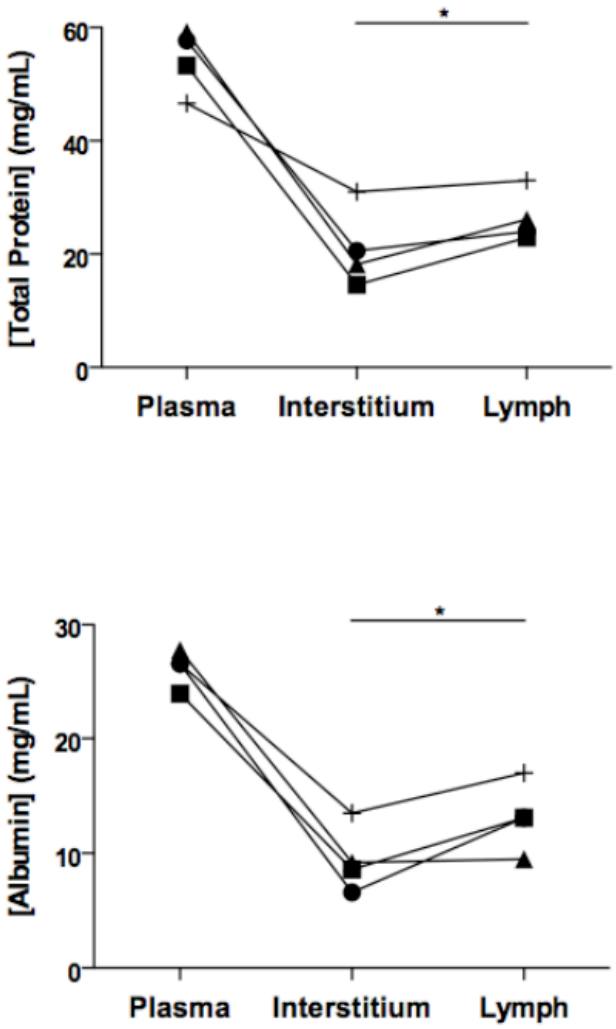

Figure 6. Simultaneous measures of total protein and albumin concentrations of plasma, interstitial, and lymph. Data are graphed from Table 2 (see Appendix) and indicate that for every animal examined (N=4), a positive protein concentration gradient existed across the lymphatic wall, such that total protein and albumin are expected to diffuse from the lumen to the interstitium.

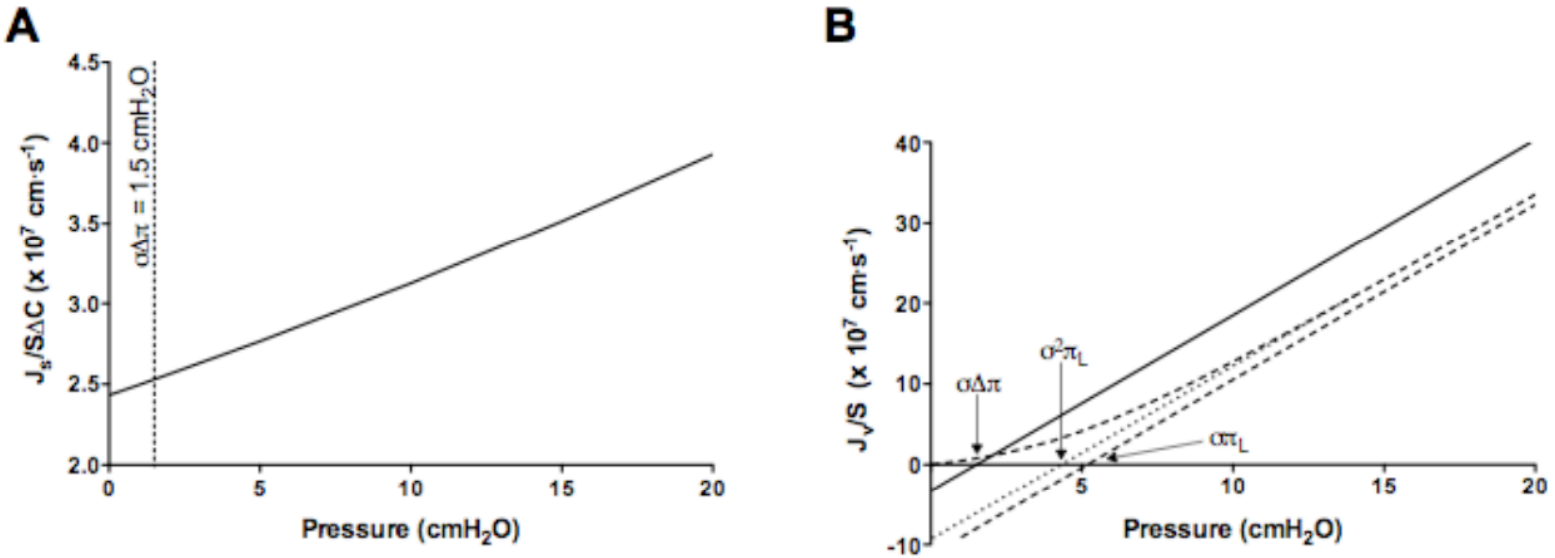

Figure 7. Predicted solute and volume flux of mesenteric collecting lymphatics over pressure using the average concentration differences reported in Table 2. Positive and negative values indicate fluid filtration and reabsorption, respectively. **A**: Solute flux per unit surface area and concentration difference ($J_s/S\Delta C$) is graphed as a function of hydrostatic pressure using Eqn. 2.2. The dashed line is the effective oncotic pressure calculated from the measured albumin concentration using the Landis-Pappenheimer equation (Landis & Pappenheimer, 1963). Where it intersects the solid line is the true diffusive permeability, P_d. **B**: Volume flux per unit surface area as a function of hydrostatic pressure is calculated by substitution of P_d and L_p into Eqn. 2.5 (solid line, transient state) and Eqn. 2.6b (dashed curve, steady state). Reflection coefficient (σ) was assumed equal to 0.94 (Kendall & Michel, 1995). The effective oncotic pressure for each condition is labeled at the x-intercept. The dashed line parallel to the steady state graph is to illustrate how transient state volume flux would appear when interstitial protein is negligible as occurs in many experimental, but not *in vivo*, conditions. The dotted line tangent to the steady state graph is only to show where the effective oncotic pressure lies. The limiting slope of each line is the hydraulic conductivity, L_p.

Discussion

The present study was a test of the null hypothesis that the albumin permeability of collecting lymphatic vessels would not differ from venules. To our surprise we accepted our hypothesis, since the P_s medians between the two groups did not statistically differ. Additionally, we noted a remarkable similarity in the distributions of the data sets, which were both left skewed. From the plot of apparent permeability data over pressure we were able to estimate the true diffusive permeability (P_d) to albumin of rat mesenteric collecting lymphatics.

Methodological Limitations for the Measurement of Solute Flux

Measurement of solute flux is determined from the step change in fluorescence intensity upon filling of the vessel and subsequent change in intensity over time. This measurement could be compromised if there were to be photobleaching of the dye during the measurement period. Further, photobleaching of the dye is associated with free radical formation, which itself could alter barrier properties.

Photobleaching of the fluorescent probe was evaluated on the same equipment as used for experiments by exciting a sample of the conjugated probe on a standard glass slide with a spacer (thickness of 150-microns) and coverslip. Emission of the fluorescent probe, measured over 4 hours of constant excitation *in vitro*, did not vary, demonstrating the photostability of this labeled macromolecular probe. During experiments *in vivo* the longest time the interstitial probe was excited was 30 minutes; probe in the vessel lumen was only excited for seconds because flow carried it out of the measuring window.

All experiments were performed on juvenile male rats (< 60 days) to take advantage of their lack of perivascular adipose tissue. To calculate the effective oncotic pressure for the perfused albumin solution, σ of albumin must be known for collecting lymphatics. Because this value has never been measured we assumed that it was equal to that of rat mesenteric venules (0.94, (61)). Finally, for all graphs of flux we assumed that P_i was equal to an atmospheric pressure of zero.

Similarity of Collecting Lymphatic and Venular Permeability

The median collecting lymphatic P_s^{RSA} (3.5±1 x 10^{-7} cm·s^{-1}) did not differ significantly from the P_s^{RSA} of venules in this study (4.0±1 x 10^{-7} cm·s^{-1}) or venules from a previous study (5.6±2 x 10^{-7} cm·s^{-1}, (104)). Strikingly, even the frequency distributions of lymphatic and venular P_s did not differ (Fig. 4). No correlation was observed between P_s^{RSA} and vessel diameter or time of year, ruling out seasonal variation of solute permeability in the rat (data not shown). However, as for venules, a correlation was found between collecting lymphatic P_s^{RSA} and the perfusion pressure at the time of the flux measurement, a result of the coupling of solute flux to volume flux.

When the P_s^{RSA} values are graphed against hydrostatic pressure, one can determine the true diffusive permeability (P_d) under the special condition of zero net filtration pressure. We found that collecting lymphatic P_d was 2.5 x 10^{-7} cm·s^{-1} after adjusting the graph for the effective osmotic pressure of our perfusate. While not very different from the P_d to bovine serum albumin (BSA) for frog mesenteric venules (2.3±0.25 x 10^{-7} cm·s^{-1} (28)), our collecting lymphatic P_d must be compared to rat mesenteric venular P_d, for which no reported measures exist. The scarcity of mammalian

P_d data underscores the need for future experiments to elucidate P_d to albumin in rat mesenteric microvessels to form a complete description of the network permeability, inclusive of all vessel types.

The Péclet number describes the ratio of convective to diffusive transport of solute. In these experiments albumin, a carrier of free fatty acids, hormones, and drugs, was used because it is the major determinant of oncotic pressure in intact, autoperfused tissues. At the mean hydrostatic pressure for collecting lymphatics (7 cmH_2O, Table 1) the calculated Pé = 0.36, meaning that ~40% of albumin transport was mediated by convection through pathways/structures through which water and solute travel together and ~60% of albumin crosses by pressure-independent mechanisms. If the permeability properties of rat mesenteric venules and collecting lymphatics are similar, the venular Pé value would be ~1 at their greater hydrostatic pressure of 20 cmH_2O. In contrast, Pé for isolated rat skeletal muscle venules at 20 cmH_2O is 0.13 (107). It is notable that the difference between these two values likely reflects the fact that P_s^{BSA} of skeletal muscle venules is an order of magnitude greater than mesenteric venular P_s^{RSA}, indicative of the difference in metabolic demand of the two tissues (107) or the difference in permeability to BSA relative to RSA as a result of differing charges (14, 102).

Others have reported P_s to BSA ($14\pm7 \times 10^{-7}$ $cm \cdot s^{-1}$, (98)) from a confluent tube of lymphatic endothelial cells (D = ~100μm). Though this P_s^{BSA} is from a vessel with a diameter similar to that of rat mesenteric collecting lymphatics, it likely represents microlymphatic vessel permeability due to the lack of basement membrane, smooth muscle, and pericytes. In support of this notion, from a single microlymphatic vessel

cannulated *in vivo* we measured a P_s^{RSA} of 12 x 10^{-7} cm·s^{-1} (D = 37.8 μm, P_{Lumen} = 3 cmH_2O). While cell culture is a valuable system for studying the molecular mechanisms regulating permeability, caution should be exercised when interpreting these P_s values.

Influence of Pressure on Collecting Lymphatic Spontaneous Contractions

Figure 3 demonstrates the effect of hydrostatic pressure, and hence flow, on the spontaneous contraction frequency of collecting lymphatics. Studies show (38) that with increased flow, there is a decrease in spontaneous contraction frequency mediated in part by nitric oxide. Others (142) have demonstrated that in the absence of flow, elevation in pressure alone is sufficient to diminish contraction amplitude. Fig. 3A shows that a collecting lymphatic vessel perfused at a relatively low pressure possesses spontaneous contractions compared to a vessel in Fig. 3B with a higher perfusion pressure lacking spontaneous contractions. Both forces are likely involved. After cannulation approximately half of the P_s recordings exhibited spontaneous contractions, while absent in the other half. Since solute flux is affected by pressure as a result of convective coupling, the P_s^{RSA} values between contracting and non-contracting vessels differed, although the direct effect of spontaneous contractions versus a contribution of flow cannot be extracted from these data. While some vessels lacked spontaneous contractions, this occurred invariably after cannulation and only at relatively high pressure and/or flow.

Assumptions for Modeled Solute and Volume Flux Over Pressure

With knowledge of L_p and P_d the graph of volume flux against pressure can be constructed once we know the reflection coefficient (σ) of the vessel and the oncotic

pressure difference ($\Delta\pi = \pi_L - \pi_i$). As a first approximation, given the similarity in solute permeability parameters P_s and P_d, we assumed that σ for albumin does not differ between the two vessel types. The value that has been measured for rat mesenteric venules is 0.94 (61). The other parameter that must be known is the oncotic pressure difference across the lymphatic vessel wall ($\pi_L - \pi_i$), for which the reported values vary considerably. Therefore, the albumin concentrations of lymph, peritoneal fluid, and plasma were measured directly (Table 2), facilitating the calculation of the oncotic pressure difference for albumin. Ideally, interstitial fluid should be sampled instead of peritoneal fluid, but the latter has been shown to be only modestly more concentrated than the former (10). For all graphs of flux, the interstitial pressure (P_i) is assumed to equal zero.

Estimation of Collecting Lymphatic Vessel Hydraulic Conductivity (L_p)

Although these studies were aimed at determining permeability to solute, the question remains: what is the magnitude of the 'hydraulic permeability coefficient', L_p, and does that differ from rat mesenteric venular L_p? To address this, we examined the limiting slope of Fig. 5, which defines $L_p(1 - \sigma)$, and assumed that collecting lymphatic σ was identical to the rat mesenteric venular σ of 0.94 (61). The calculated L_p is 2.2 x 10^{-7} $cm \cdot s^{-1} \cdot cmH_2O^{-1}$, similar to basal values measured in rat mesenteric venules (2.4±0.2 x 10^{-7} $cm \cdot s^{-1} \cdot cmH_2O^{-1}$, (61); 2.6±0.3 x 10^{-7} $cm \cdot s^{-1} \cdot cmH_2O^{-1}$, (63); 2.4 x 10^{-7} $cm \cdot s^{-1} \cdot cmH_2O^{-1}$, (103)). To validate this estimation, experiments are needed to measure hydraulic conductivity for rat mesenteric collecting lymphatics, which will provide the remaining permeability values for both albumin (σ) and water (L_p).

Predicted Solute and Volume Flux from Measured Albumin Concentration Differences

Table 2 (Fig. 6) provides evidence that lymph taken from a typical rat mesenteric collecting lymphatic can possess a greater concentration of albumin than that found in surrounding peritoneal fluid. Since interstitial fluid is slightly less concentrated than peritoneal fluid (10), we can confidently state that the albumin concentration in lymph is greater than the interstitial concentration, at least for vessels in rat mesentery. The total protein lymph-to-plasma ratio of 77% agrees well with previous studies reporting 70% in the rat tail (7). More interestingly, the albumin-to-total protein ratio for each compartment differed, suggesting non-uniform albumin handling within each compartment.

Figure 7A shows that albumin flux (J_s) is outwardly directed since ΔC is a positive value, where the positive direction is from the vessel to the interstitium. Finding *in vivo* evidence supporting solute extravasation is intriguing since collecting lymphatics are believed to only absorb protein and fluid (13, 16, 43). Fig. 7B indicates an outwardly directed volume flux in both the transient (solid line) and steady state (dashed curve) conditions. The steady state relationship shows that constitutive reabsorption of fluid by collecting lymphatics cannot occur, which confirms that proposed by Michel for microvessels (82). However, collecting lymphatics of this study were observed to contract spontaneously at frequencies of 10-15 min^{-1}; consequently, a steady state pressure is never attained. Thus, description of physiological collecting lymphatic volume flux is better represented by the transient graph of volume flux on pressure (Fig. 7B).

While filtration of fluid occurs over most of the pressures observed in this study, at low pressures (< 1.5 cmH_2O) reabsorption of fluid is possible.

Physiological Significance of Collecting Lymphatic Permeability Properties

The measured values of albumin flux led us to accept our hypothesis that rat mesenteric collecting lymphatics are no different than venules with respect to albumin permeability, which supports the proposal that the cardinal vein is the origin of lymphatic endothelium (114). Further, our data show that a positive concentration difference is possible (Table 2) such that solute moves from the vessel lumen towards the interstitium, a result that opposes the current expectations that lymphatic vessels should only absorb protein and fluid. While the concentration differences for lymphatic vessels of every organ may not be positive, these data demonstrate that the capacity for lymphatic solute exchange exists. A consequence of an outwardly directed and convectively coupled albumin flux is that during increased lymphatic hydrostatic pressure a greater amount of albumin is extravasated, increasing the interstitial albumin concentration and likelihood for edema formation. Therefore, additional studies are needed to elucidate the regulation of lymphatic solute permeability in the context of edema formation.

If the ideal graphs of volume flux represent the behavior of most rat mesenteric collecting lymphatic vessels, they have important implications for edema and overall fluid balance. For instance, collecting lymphatic hydrostatic pressure is elevated during lymphedema and according to Fig. 7B enhances fluid filtration that, if sufficient, is expected to produce a low-protein edema. Further, a higher hydrostatic pressure inhibits spontaneous contractions so that volume flux follows the steady state curve (Fig. 7B) for

which fluid reabsorption is no longer possible. Although the volume flux predictions are approximations, and it is probable that not all collecting lymphatic vessels possess the same oncotic pressure difference, the albumin concentration data in Table 2 show that it is likely that macromolecules in lymph of prenodal collecting lymphatics are more concentrated than in the surrounding interstitial fluid. Together our solute flux data and volume flux estimates support the theory that prenodal collecting lymphatics concentrate their luminal protein (17, 56, 119) by preferentially losing water over solute (depicted in Fig. 8). Experiments to determine collecting lymphatic hydraulic conductivity are needed to fully delineate the conditions that produce edemas of lymphatic origin.

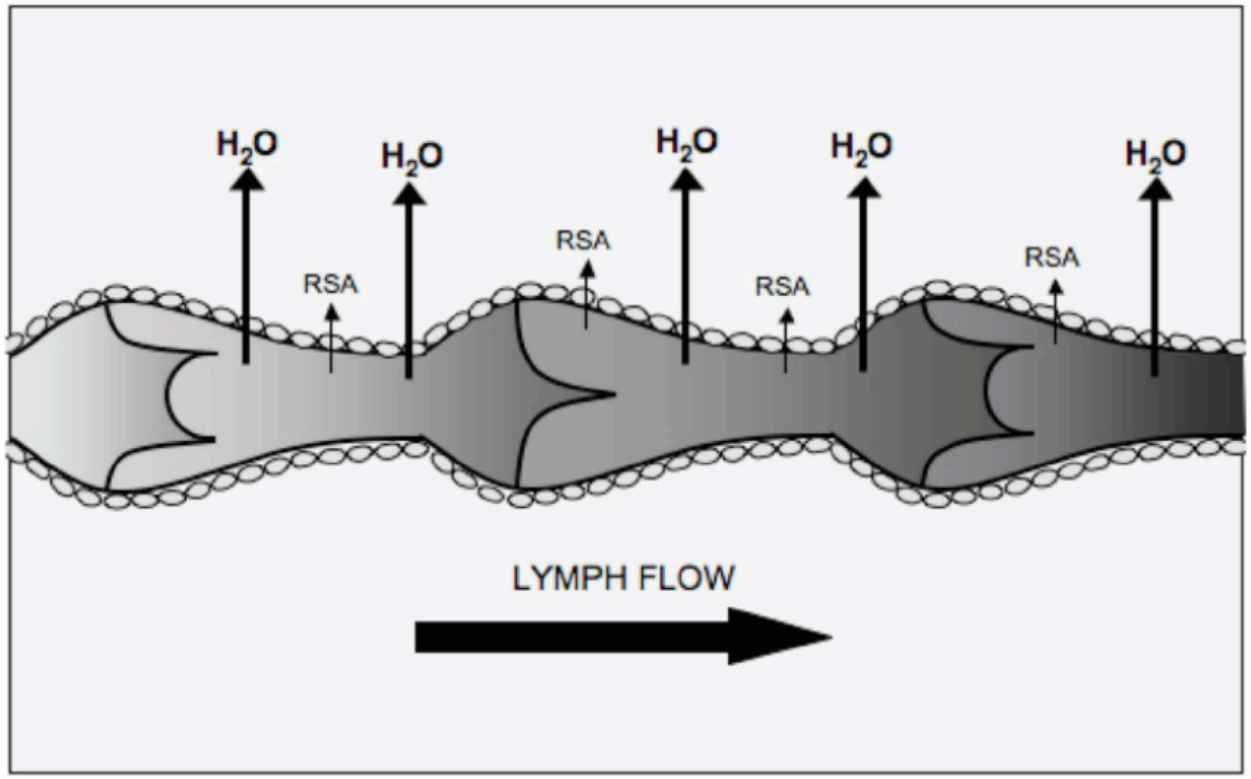

Figure 8. Idealized schematic of predicted collecting lymphatic solute and volume flux for the concentration difference in Table 2. Lighter shading corresponds to a lower albumin concentration and vice versa. The lymph rat serum albumin (RSA) concentration is believed to increase along the vessel length as water is filtered.

Supplemental Methods

Surgical Preparation

All experiments were performed *in situ* on juvenile male (35-55 days, 200-250g) Sprague Dawley rat mesenteric microvessels (Hilltop Lab Animals, PA, USA). Animals were housed 3 to a cage for a minimum one-week acclimation period prior to the experiment. For these initial studies, juvenile male animals were chosen for their lack of visceral fat, which facilitated location and subsequent cannulation of collecting lymphatics. One venule or collecting lymphatic was cannulated per animal. On the day of the experiment, the animal was weighed and anesthetized by intraperitoneal injection of Inactin (thiobutabarbital, Research Biochemicals Int., MA, USA, 128 mg/kg body weight). After the abdomen was shaved, the animal was placed atop a custom Plexiglas™ board in the supine position on a layer of Sylgard™ that contained coiled Tygon™ tubing attached to a circulating heater to maintain body temperature at 37 ± 0.5°C. A small loop of intestine was exposed carefully through a midline abdominal incision prior to placing the rat in the left lateral decubitis position and draping the mesentery over a Sylgard™ pillar (2 cm diam.). The mesentery was superfused continuously (2-3 mL/min) with mammalian Krebs at 37 ± 0.5°C and the intestine was covered with small strips of Krebs-moistened gauze. After locating a vessel under the Zeiss dissection microscope, the animal and board were transferred to a Leitz Diavert inverted microscope and the suffused preparation was allowed to equilibrate for approximately 30 minutes prior to cannulation and data gathering.

In Vivo Collecting Lymphatic Vessel Cannulation

The instruments for *in situ* collecting lymphatic vessel cannulation, consisting of one beveled cannulating micropipette and one restraining rod, were fabricated according to the methods previously detailed by this lab (80). As with blood microvessels, it was discovered that the tip size of the micropipette was a major factor that determined successful cannulation and microvessel perfusion. For collecting lymphatics the two major considerations were that: 1) upon contact with the micropipette, the collecting lymphatic vessel would immediately constrict, presumably as a result of injury if the tip is too large; and 2) if the micropipette tip was too small, cannulation was relatively easy, but complete filling of the vessel lumen thereafter, a requirement for measurement of solute flux, was impossible. Therefore, the optimal micropipette size seemed to be approximately one third the diameter of the lymphatic vessel to obtain both ease of cannulation and complete filling of the vessel lumen.

The most successful micropipettes (success >90%) were made from single lumen capillary glass (WPI, FL, USA; cat# TW150-6) beveled at a 27.5° angle from the pipette axis (tip diameter, 25-30 μm) on a motorized grinding wheel (Narashige, Japan) using 0.3 μm diamond grit paper (AH Thomas, NJ). After grinding the pipettes were washed, siliconized with SurfaSil™ (Pierce Biotechnology, IL, USA), and dried with acetone. The first half of the experiments were performed with theta pipettes (Sutter Instrument, CA, USA; cat# BT-150-10) because they allowed a washout and a test solution to be used without recannulation. However, the cross section of a theta pipette is elliptical, instead of circular, causing greater trauma to the lymphatic vessel and dramatically reducing the success rate. Once it was determined that the likelihood of obtaining data was higher

using the single-lumen micropipettes, and that the absolute measures of flux did not differ with pipette type, the use of theta pipettes was discontinued.

To cannulate the vessel, a beveled pipette filled with the fluorescent perfusate solution was connected to a water manometer system, set to a low positive pressure (≤2 cmH_2O), and positioned (Prior micromanipulator with fine z-axis control, UK) near the cannulation site parallel to the vessel. A restraining rod, made from a pulled micropipette with the tip passed quickly through a flame and then also mounted on a Prior micromanipulator, was lowered onto the mesentery 20-50 μm away from the vessel and positioned at a ~90° angle to the vessel. The restraining rod was used to gently stretch the vessel axially and slightly radially. After the micropipette was lowered to barely make contact with the top surface of the vessel, it was advanced forward with the aid of a single dimension hydraulic drive (HAER, Brunswick, ME) along its axis in the direction of lymph flow while keeping the tip in the focal plane so that the vessel wall folded onto the micropipette. Care was taken to avoid touching the endothelium on the bottom surface of the vessel. If at any time a lymphatic vessel constricted during this process all movement was halted until the lymphatic recovered. Finally, the micropipette was advanced forward along the vessel axis to penetrate the wall. Once in the vessel lumen, the pressure in the micropipette was raised just enough to prevent aspiration of lymph.

Intravital Microscopy for In Vivo Measurement of Collecting Lymphatic Permeability

To make measurements of solute flux using theta pipettes, a baseline fluorescence was established with the washout solution, followed by a switch to 5-30 minutes of dye perfusion, and then switched back to the washout solution to prepare the vessel for

another measurement of flux. In the other half of the experiments the method we expect to use in future studies was employed. A siliconized, single lumen micropipette attached to the manometer system was used to perfuse the collecting lymphatic vessel with dye after measuring P_{Lumen}. To reestablish the baseline fluorescence, the vessel was quickly recannulated with a separate micropipette containing the washout solution.

The perfused microvessels were visualized with brightfield under Köhler illumination on a Leitz Diavert inverted microscope with a 10x objective (numerical aperture 0.22, UM10, Leitz, NJ, USA). Following cannulation, the brightfield illuminator was turned off, and a shutter was opened to allow epifluorescent illumination through an I2/3 filter cube for Alexa-488® (band pass: 450-490nm, long pass: 515nm, Leitz, NJ, USA). The light path was split 50:50, and projected simultaneously onto a black and white, low light CCD camera (IC-200, PTI, NJ, USA) and an analog photometer (D-104C, PTI, NJ, USA). Before reaching the photometer, the emitted fluorescence was reflected off a dichroic mirror (595nm, Chroma, VT, USA), and passed through an emission filter (band pass: 515-543nm, Chroma, VT, USA). The image of the low light camera was displayed on a 14" monitor (WV-BM 1400, Panasonic, NJ, USA) before being sent to a DVD recorder (DVO-1000 MD, Sony, NJ, USA).

Direct measures of solute flux (J_s, mmol/s) were made over an area of vessel defined by a rectangular adjustable diaphragm in the light path of the photometer (width ≥4 vessel diameters, length = 8 vessel diam.), which served to limit interference from stray light. Fluorescence filled the vessel lumen resulting in an initial step increase in fluorescence intensity (I_o), followed by a gradual but linear increase in intensity as the

fluorescent probe continuously flowing through the vessel segment began to accumulate in the interstitial space over time (dI_f/dt). Apparent solute permeability (P_s, $cm \cdot s^{-1}$) was calculated from the equation relating solute flux (J_s, $mmol \cdot s^{-1}$) to surface area (S, cm^2) at a constant concentration difference (ΔC, $mmol \cdot mL^{-1}$)(50):

$$P_s = J_s/S\Delta C = (1/I_o)(dI_f/dt)(D/4) \qquad (2.1).$$

Vessels were assumed to be circular and to have a volume-to-surface area ratio of D/4.

Preparation of Fluorescently Labeled Protein

Proteins, BSA or RSA, for use in the perfusate or suffusate solutions were "washed" with saline prior to use. In this procedure dialysis is achieved by ultrafiltration (Amicon 30kDa molecular weight cutoff, Millipore, MA, USA). The dialyzed BSA and RSA were stored in 10 mL and 100 µl aliquots, respectively, at a concentration of 100 mg/mL at -20°C until the day of the experiment.

Briefly, the Alexa-488® and RSA (3:1 molar ratio) were reacted for 30 minutes at room temperature. Free fluorescent dye was removed first by centrifugation using Vivaspin™ 20 (30kDa nominal molecular weight limit, VivaScience, Hanover, Germany); remaining free dye was removed by buffer exchange column chromatography. Protein concentration of the conjugate was determined by Micro BCA Protein Assay (Thermo Fisher Scientific, IL, USA) and stored at a final concentration of 10 mg/mL at -20°C.

Determination of Albumin and Total Protein Concentration from Lymph Samples

Total protein concentration of each plasma, lymph, or peritoneal fluid sample was determined by the Micro BCA Protein Assay utilizing BSA as a standard. Albumin

concentration of each sample was determined by the Albumin Blue 580 Fluorescence assay (62) using RSA as the standard. Volumes were adapted to a 96-well plate. The albumin or total protein concentration was then used to calculate the albumin or total protein oncotic pressures, respectively, for each sample using the Landis-Pappenheimer equations (67).

CHAPTER 3: COLLECTING LYMPHATIC VESSEL PERMEABILITY AND CONTRACTILE RESPONSES ELICITED BY ATRIAL AND BRAIN NATRIURETIC PEPTIDES

Abstract

Atrial and brain natriuretic peptides (ANP and BNP, respectively) are cardiac hormones released into the bloodstream in response to hypervolemia or fluid shifts to the central circulation. The actions of both peptides include natriuresis and diuresis, a decrease in systemic blood pressure, and inhibition of the renin-angiotensin-aldosterone system. Furthermore, ANP and BNP elicit modest, but significant increases in blood microvessel permeability, leading to protein and fluid extravasation into the interstitium (i.e. third spacing). Due to the importance of the lymphatic vasculature in maintaining fluid balance, we tested the hypothesis that perfusion with ANP or BNP increases lymphatic permeability (P_s) to rat serum albumin by 2-fold. Using a microfluorometric technique adapted to lymphatic vessels, we determined the rat mesenteric collecting lymphatic P_s responses to ANP and BNP were 2.0±0.4-fold (p=0.01, N=7) and 2.7±0.8-fold (p=0.07, N=7), respectively, consistent with the responses of other vessel types. In addition to measuring P_s responses, we were able to observe changes in spontaneous contraction amplitude and frequency from the albumin flux tracings. Notably, ANP abolished spontaneous contraction amplitude (p=0.005) and frequency (p=0.006), while BNP augmented both by ~2-fold (p<0.01 each). We conclude that ANP and BNP target collecting lymphatics by elevating their permeability to an extent similar to blood

microvessels and differentially altering their contractile function. In aggregate, our data support the theory that increases in collecting lymphatic permeability oppose the absorptive function of the lymphatic vasculature, trapping protein and fluid in the interstitial space as a compensatory response to volume expansion.

Introduction

Natriuretic peptides (NPs), a class of peptide hormones synthesized by the chambers of the heart, are released into the bloodstream upon cardiac stretch resulting from hypervolemia or fluid shifts favoring the central circulation (e.g. microgravity, swimming, cardiac failure) to reduce vascular fluid volume. As a result, NPs have been the focus of investigation for treatment of congestive heart failure (CHF) due to their numerous favorable physiological actions (77). Likewise, the lymphatic vasculature is a critical regulator of fluid distribution (19, 73, 110) and owing to this commonality the effects of NPs on lymphatic vessel function encourage study.

In healthy humans there is a constitutive low-level secretion of atrial (ANP) and brain natriuretic peptides (BNP), synthesized by the atria and ventricles of the heart, respectively (23). Notably, the heart is the main source for these circulating peptides although other organs are capable of secreting NPs (e.g. brain, lung), albeit at lower levels (39). C-type natriuretic peptide (CNP) is the exception to the rule, being synthesized and released mainly from the vascular endothelium as an autocrine hormone. Natriuretic peptide signaling occurs upon binding to one of the three natriuretic peptide receptors (NPR-A, -B, and -C). NPR-A and -B are the particulate, membrane-bound

guanylyl cyclase receptors, while NPR-C lacks this activity. ANP and BNP bind to NPR-A with similar binding affinities that are much greater than that of CNP (118). The NPR-C receptor, lacking the catalytic cytoplasmic tail, is believed to be a 'clearance' receptor and binds ANP with an affinity greater than CNP, which is greater than that of BNP (118).

Elevation of circulating ANP or BNP stimulates the well-established physiological responses of marked natriuresis and diuresis, a decrease in systemic blood pressure, inhibition of the renin-angiotensin-aldosterone system, and at high concentrations, vasodilatation (77, 101, 138). De Bold (34) observed an additional property of ANP infusion: a redistribution of vascular volume (increase in hematocrit) later shown to occur in the absence of the kidneys (3). It was then demonstrated that in selected tissues and portions of the vasculature, ANP elicited a rapid and sustained increase in microvascular permeability to both protein and water (29, 51, 80, 81). A response of this magnitude is sufficient to displace a significant portion of the circulating fluid and protein into the interstitium (125, 127), thus alleviating volume overload whether perceived (e.g. CHF) or real (e.g. microgravity). Another study investigating the permeability response of venular capillaries to BNP demonstrated a response mimicking that of ANP (79).

In a recent study, we confirmed that in the condition of health, collecting lymphatic vessel permeability to albumin does not differ from that of venules (110). Since a defining feature of the lymphatic vasculature is to control fluid distribution between the vascular and interstitial spaces, we hypothesized that collecting lymphatic

permeability to albumin would be elevated 2-fold upon exposure to 100 nM of either ANP or BNP, a response similar to that of venular capillaries (79, 80). Our rationale for hypothesizing equal lymphatic and venular responses arose from a study reporting that lymphatic endothelium is derived from the cardinal vein during embryological development (114), which led us to reason that a consequence of their similar genetic profiles may be comparable function.

Paired measures of albumin flux were made during perfusion of *in situ* rat mesenteric collecting lymphatics with control and natriuretic peptide solutions containing fluorescently labeled albumin, from which solute permeability was determined. We accepted our hypothesis that lymphatics would, like the venules, undergo a 2-fold increase in permeability to albumin (P_s) during ANP exposure and that lymphatic permeability responses to ANP and BNP would not differ. Additionally, we observed that the contractile features of collecting lymphatic vessels were altered differentially during ANP versus BNP treatment and tested whether nitric oxide played a role in the alteration of lymphatic contractile function in response to ANP. We conclude that the lymphatic vasculature represents an additional target of natriuretic peptide signaling and additional surface area from which protein and fluid may extravasate to relieve vascular volume expansion.

Methods

Ethical Approval:

Animal protocols were approved by the Institutional Animal Care and Use Committee (IACUC) at the University of Missouri-Columbia and conducted in accordance with the National Institutes of Health's *Guide for the Care and Use of Laboratory Animals*. All animals were killed after the experiment by an overdose of anaesthetic followed by bilateral pneumothorax and aortic transection to conform to the protocol.

General Surgical Preparation:

All experiments were performed *in situ* on juvenile male (35-55 days, 200-250g) Sprague Dawley rats (Hilltop Lab Animals, PA, USA) housed 3 to a cage for a minimum one-week acclimation period prior to the experiment. Juvenile males were chosen for their relative lack of perivascular fat, which facilitated location and subsequent cannulation of mesenteric collecting lymphatics. One collecting lymphatic (60-170 μm diameter) was cannulated per animal.

Following induction of anesthesia with Inactin (IP, thiobutabarbital, Research Biochemicals Int., MA, USA, 128 mg/kg body weight), the animal was placed on a custom, heated Plexiglas™ board that enabled transport of the animal from a dissection microscope to an intravital microscope. The mesentery was exteriorized and superfused continuously (2-3 mL/min) with mammalian Krebs at 37 ± 0.5°C while a vessel was located under the Zeiss dissection microscope. The animal and board were then

transferred to a Leitz Diavert inverted microscope and the suffused preparation was allowed to equilibrate for approximately 30 minutes prior to vessel cannulation and data collection.

Collecting Lymphatic Vessel Nomenclature and Identification:

The nomenclature of lymphatic vessels described in this manuscript conforms to that previously described (110). Collecting lymphatic vessels were identified by the presence of valves, spontaneous contractions, and their transparent contents (143). Additionally, leukocytes were often visualized in collecting lymphatics. Vessels shrouded by adipose tissue were not studied because the fat cells hinder cannulation.

Solutions:

Mammalian Krebs. All superfusion and perfusion solutions were prepared fresh and used on the same day. Unless otherwise stated all materials were purchased from Sigma (MO, USA). The Krebs superfusion solution consisted of (in mmol): 141.4 NaCl, 4.7 KCl, 2.0 $CaCl_2 \cdot 2H_2O$, 1.2 $MgSO_4$, 1.2 $NaH_2PO_4 \cdot H_2O$, 5.0 d-glucose, 3.0 $NaHCO_3$, and 1.5 NaHEPES. The pH of the solution was 7.4 ± 0.05 at 37°C.

Krebs-BSA. Dialyzed bovine serum albumin (BSA, Sigma cat# A7906) was added to the Krebs superfusion solution to achieve a final concentration of 1 mg/mL on the day of the experiment. The osmolarity, measured by freezing point osmometry, was generally between 292-297 mOsm after the addition of BSA.

Labeled Protein. The macromolecular probe used in this study, rat serum albumin (RSA, Sigma cat# A6272), was bound to the Alexa-488® fluorophore (Invitrogen, CA, USA) by modifying the manufacturer's protocol. Briefly, the Alexa-488® and RSA (3:1 molar ratio) were reacted for 30 minutes at room temperature. Free fluorescent dye was removed in two steps: first by centrifugation using Vivaspin™ 20 (30kDa nominal molecular weight limit, VivaScience, Hanover, Germany); second, any remaining free dye was removed by buffer exchange column chromatography. Protein concentration of the conjugate was determined by Micro BCA Protein Assay (Thermo Fisher Scientific, IL, USA) and stored at a final concentration of 10 mg/mL at -20°C. This approach removes unconjugated dye while preserving the primary structure of albumin (14).

The perfusate solution contained 10% (w/v) labeled RSA (1 mg) with 9 mg of unlabeled RSA and was brought to a volume of 1 mL with freshly made Krebs solution so that the final total protein concentration was 10 mg/mL. A washout solution was made, with unlabeled protein, at an identical total protein concentration. Both solutions of 10 mg/mL RSA possessed an oncotic pressure of 4.1 cmH_2O calculated from the Landis-Pappenheimer equation (67).

Dialysis Procedure for BSA and RSA. Proteins (BSA or RSA) for use in the perfusate or suffusate solutions were "washed" with saline to remove hydrophilic solutes carried on albumin prior to use. In this procedure dialysis is achieved by ultrafiltration (Amicon 30kDa molecular weight cutoff, Millipore, MA, USA). The dialyzed BSA and RSA were stored in 10 mL and 100 µl aliquots, respectively, at a concentration of 100 mg/mL at -20°C until the day of the experiment.

Perfusates Containing Natriuretic Peptide and/or L-NMMA. Rat atrial natriuretic peptide (ANP, Sigma cat# A8208) and brain natriuretic peptide (BNP, Sigma cat# B9901) were dissolved in saline to prepare 10 μM stock solutions. The 100x stock solutions were divided into 15 μL aliquots and stored at -20°C. On the day of the experiment, an ANP or BNP aliquot was thawed and 5 μL of stock solution were added to 500 μL (half) of the perfusion solution to a final concentration of 100 nM. The other half of the perfusion solution was used as the control. For natriuretic peptides the concentration of 100 nM was chosen to elicit a maximal P_s response (81). N^G-monomethyl-L-arginine (L-NMMA; Calbiochem, CA, USA; cat# 475886) was treated in a similar manner by dissolving it in saline to obtain a 1 mM stock solution. The 100x stock solution was aliquoted in 1 mL amounts and stored at -20°C. On the day of use, an aliquot was thawed and 10 μL of this stock replaced 10 μL of the Krebs superfusion solution that was used as a diluent for the 1 mL perfusion solution yielding a final concentration of 10 μM, a dose sufficient to eliminate nitric oxide production (38).

Microvascular Solute Flux Measurements:

The method we use for determining solute permeability (P_s) to proteins in lymphatic and blood microvessels and its limitations is described in several publications (50, 80, 104, 107, 110). Briefly, collecting lymphatics studied here were cannulated *in situ* with single lumen pipettes and perfused with unlabeled RSA (washout) followed by fluorescently labeled RSA (dye) in Krebs solution. Vessel diameter (D) was measured under brightfield via an ocular ruler following all measures of P_s. For all P_s and

contractile responses, recordings were taken from the same vessel segment throughout the experiment for accuracy.

Direct measures of albumin flux (J_s, mmol·s^{-1}) were made over an area of vessel defined by a rectangular diaphragm (width = 4 vessel diameters, length = 8 vessel diam.) in front of a photometer (PTI, Canada). When dye-labeled albumin filled the vessel lumen there was an initial step increase in fluorescence intensity (I_o), followed by a gradual, but linear, increase in intensity as fluorescent probe accumulated in the interstitial space over time (dI_f/dt) in addition to the constant signal generated from the fluorophore flowing through the vessel lumen. Solute permeability (P_s, cm·s^{-1}) was calculated from the equation relating solute flux (J_s, mmol·s^{-1}) to surface area (S, cm^2) at a constant concentration difference (ΔC, mmol·mL^{-1}) (50):

$$P_s = J_s/S\Delta C = (1/I_o)(dI_f/dt)(D/4) \qquad (3.1).$$

Contraction Amplitude and Frequency Assessment:

During the measurement of solute flux, we noticed that fluctuations in the fluorescence intensity tracing corresponded to collecting lymphatic vessel spontaneous contractions. To measure amplitude and frequency, the tracings were analyzed in the following manner: for measures of amplitude changes, the height of the fluorescent intensity oscillations were recorded as arbitrary units (blocks on the grid paper); the contraction frequency was obtained by counting the number of oscillations per unit time using the same chart recording paper. A similar method has been reported where total fluorescence intensity, which corresponds to volume, was used to control for vessel

cross-sectional area (129). One may object that changes in volume ($\pi r^2 l$) may not be the same magnitude as changes in diameter (r), but for these minute diameters volume varies linearly with diameter ($R^2 = 0.99$).

Experimental Protocols

Collecting lymphatic vessels were entered into one of three protocols. In the first, designed to measure the permeability responses to ANP and BNP, a vessel was cannulated and perfused with the washout solution to measure baseline fluorescence, then recannulated and perfused with the dye solution so that both I_o and dI_f/dt were obtained. This provided the control P_s measurement. The P_s response was obtained by recannulating the vessel with the washout solution for a period of time sufficient to return tissue fluorescence to baseline, and then recannulating the vessel a final time with a pipette containing the dye and natriuretic peptide solution. In the second protocol, designed to allow observation of the contractile responses to ANP and BNP, a vessel was cannulated and perfused with the dye solution at a hydrostatic pressure just above the native vessel pressure (to elicit flow without inhibiting contractions (38, 110, 142)). To obtain the contractile responses to NPs, the vessel was recannulated and perfused at the same hydrostatic pressure with a pipette containing both the dye and natriuretic peptide. In the third protocol, vessels were treated similarly to the first protocol (in an attempt to measure P_s along with contractile responses), except that they were cannulated again with a solution containing both ANP and L-NMMA after a washout period.

Statistical Analyses:

Prism™ (GraphPad Software, CA, USA) software was used for all statistics. The mean ± standard error of the mean (S.E.M.) was reported to facilitate comparison with published data. Student's paired t-tests were performed for the permeability and contractile function experiments where only two treatments were used. The Student's unpaired t-test was utilized to compare the P_s responses to ANP and BNP. To determine whether fitted curves differed between treatment groups, the extra-sum-of-squares F test was performed. When more than two treatments were employed, differences were determined by one-way ANOVA in conjunction with Tukey's post-hoc analysis for multiple pairwise comparisons.

Power analysis was performed beforehand using the mean and standard deviation from our previous study (110) as a first approximation. To detect a 40% change in collecting lymphatic P_s between groups (2.0×10^{-7} $cm \cdot s^{-1}$) with 95% confidence (significance level $p < 0.05$), approximately 6 animals were needed per group (86).

Results

Collecting Lymphatic Vessel Permeability Responses to Two Natriuretic Peptides

Figures 9A, 9B, and 9C each present data from 7 collecting lymphatic vessels. Solute permeability (P_s) was assessed during perfusion with a control (Krebs) solution followed by an identical solution containing 100 nM atrial (ANP; Fig. 9A,C) or brain natriuretic peptide (BNP; Fig. 9B,C). Both natriuretic peptide solutions induced increases in P_s to RSA ($p = 0.01$ for ANP and $p = 0.07$ for BNP) without eliciting appreciable

changes in vessel diameter. Because the distributions of P_s during peptide exposure appeared to differ slightly, the ratios were graphed in Figure 9C for further analysis. The fold changes in P_s elicited by ANP and BNP did not differ ($p = 0.44$) as the mean±S.E.M. P_s responses to ANP and to BNP were 2.0±0.4-fold and 2.7±0.8-fold increases, respectively. Further, when the one vessel that did not respond to BNP was excluded from the analysis, the permeability response reached statistical significance ($p = 0.04$).

Sensitivity of Collecting Lymphatic Permeability Responses to Natriuretic Peptides

Previous work from this laboratory with venular capillaries demonstrated that the response to ANP was more robust in vessels with a lower basal P_s (i.e. tighter barrier) (80). To determine whether collecting lymphatic vessels shared this feature, the fold increases in P_s to either ANP or BNP were graphed as a function of the control P_s in Fig. 10. Not only did lymphatic P_s responses to ANP recapitulate this characteristic of venular capillaries, but P_s responses to BNP also followed the same general trend. While the means of the responses did not differ between the two groups (Fig. 9C), the curve fitted to the BNP response data ($r^2 = 0.46$, N = 6) was shifted to the right compared to the ANP response curve ($r^2 = 0.91$, N = 7). An extra-sum-of-squares F test was performed to determine whether one curve was sufficient to fit all the data, and concluded that two curves were needed ($p < 0.05$), indicating that the right shift was statistically significant.

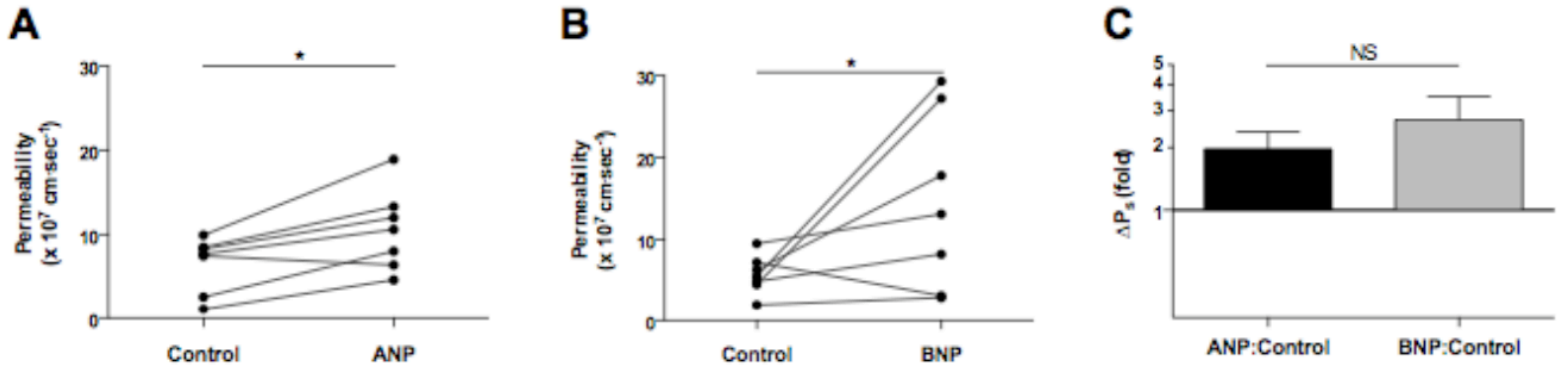

Figure 9. Collecting lymphatic vessel permeability increases upon exposure to either atrial or brain natriuretic peptide. **A and B**: Collecting lymphatic vessels underwent a significant increase in P_s to rat serum albumin versus control when perfused with either 100 nM ANP (p = 0.01) or BNP (p = 0.07). For each peptide N=7 paired measures. One vessel from each data set did not respond to the natriuretic peptide. **C:** P_s responses are graphed as the ratio of P_s during natriuretic peptide infusion to that measured during control conditions. The mean ± SEM fold changes for ANP and BNP are 2.0±0.4 and 2.7±0.8, respectively. Note the logarithmic y-scale. At y=1 there is no change from control, and lies where the x-axis is drawn. *, $p < 0.10$; NS, not significantly different.

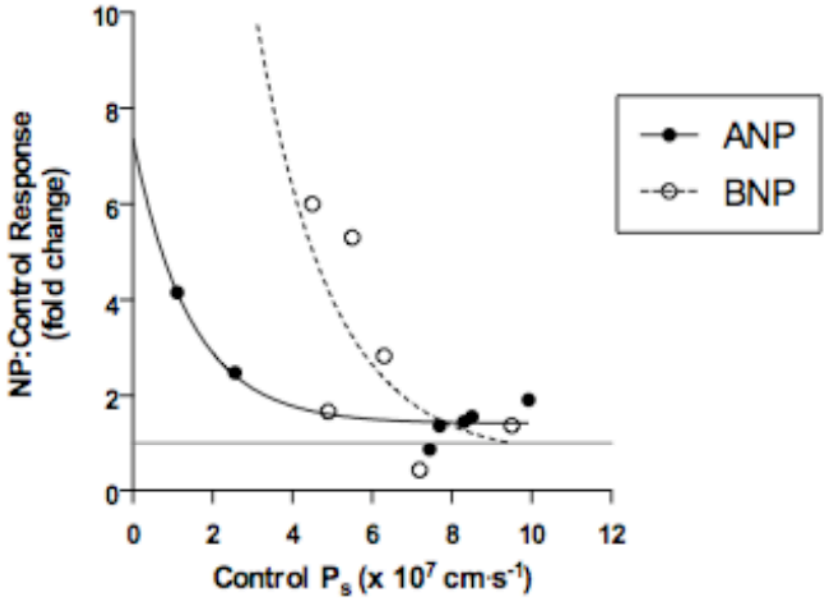

Figure 10. Sensitivity of the P_s response to natriuretic peptide infusion as a function of the control P_s. The fold increase in P_s is plotted on the y-axis for vessels exposed to either 100 nM ANP (solid circles, N=7) or BNP (open circles, N=6). The general trend is that vessels with a low basal P_s are more responsive to perfusion with natriuretic peptides. The dotted line drawn at y=1 marks where there is no change in P_s during perfusion with natriuretic peptides relative to control. The two curves are significantly different ($p < 0.05$).

Diffusion- and Convective-Mediated Albumin Flux are Similarly Affected by ANP

Solute moves across vessel walls chiefly by two mechanisms: by diffusion and/or by solvent (or convective) drag when solute becomes entrained by water movement. Figure 11 illustrates the contribution of each of these mechanisms to solute flux. In Fig. 11 the P_s responses to ANP (N = 6, excluding the one unresponsive vessel) were plotted as a function of the net pressure (difference between hydrostatic and oncotic pressures) at which they were assessed. The oncotic pressure of the perfusate, 3.85 cmH_2O, was calculated according to the Landis-Pappenheimer equations (67) as described previously (110). The axis intercept of each flux curve at the translymphatic pressure of zero defines the diffusional permeability, P_d, and the limiting slope is equal to $L_p(1 - \sigma)$, a measure of water permeability. While scatter in the data render the two curves as indistinguishable statistically, physiologically relevant information may still be obtained (Fig. 12), namely P_d and $L_p(1 - \sigma)$. The estimated values of P_d and $L_p(1 - \sigma)$ under control conditions were 3×10^{-7} $cm \cdot s^{-1}$ and 0.3×10^{-7} $cm \cdot s^{-1} \cdot cmH_2O^{-1}$, respectively (Fig. 12A and 12B). During perfusion with ANP, P_d and $L_p(1 - \sigma)$ rose to 5×10^{-7} $cm \cdot s^{-1}$ and 0.5×10^{-7} $cm \cdot s^{-1} \cdot cmH_2O^{-1}$, respectively. Of significance, P_d and $L_p(1 - \sigma)$ were almost doubled upon exposure to ANP with ~1.8 fold changes for each. The Péclet number (Pé), a unitless ratio describing the contributions of convective relative to diffusional solute flux, was calculated for the average collecting lymphatic hydrostatic pressure of 7 cmH_2O (refer to (110)) to yield remarkably similar values for control and ANP-modified Péclet numbers (0.66 vs. 0.70, respectively; Fig. 12C).

Collecting Lymphatic Contractile Parameters are Altered Upon Natriuretic Peptide Exposure in a Nitric Oxide-Dependent Manner

During measurement of albumin flux from collecting lymphatic vessels, we observed that the fluorescence intensity tracing recorded the amplitude and frequency of lymphatic spontaneous contractions, and could be used as a method to evaluate these parameters. The lymphatic contraction amplitude and frequency responses to either ANP (Fig. 13A and 13B) or BNP (Fig. 14C and 14D) were observed. Strikingly, in every vessel perfused with ANP spontaneous contractions were abolished completely (amplitude, $p = 0.005$; frequency $p = 0.006$). In marked contrast, perfusion with BNP resulted in stronger ($p = 0.01$) and more frequent ($p = 0.01$) contractions. The mean contraction amplitude and frequency responses to BNP were 2.2- and 2.1-fold increases, respectively.

Review of the literature revealed that spontaneous contractions of collecting lymphatic vessels appear to be mediated by nitric oxide (NO) (38, 66) and there is accruing evidence that ANP on binding to the natriuretic peptide "clearance" receptor initiates the NO signaling cascade (5, 25, 47, 83, 137). To test the hypothesis that NO mediated the inhibition of spontaneous contractions during exposure to ANP, we performed an additional set of experiments (N = 3). In this case the vessels were perfused with a control solution, followed by the same solution containing 100 nM ANP, and ending with an identical solution containing both ANP and 10 μM L-NMMA. Figure 15 summarizes the data from this group of experiments. Control amplitude and frequency differed from that during ANP infusion ($p < 0.05$), which eliminated spontaneous

contractions. L-NMMA treatment in the presence of ANP restored contraction amplitude and frequency, and thus differed significantly from the ANP group ($p < 0.05$) but not from the control ($p > 0.05$).

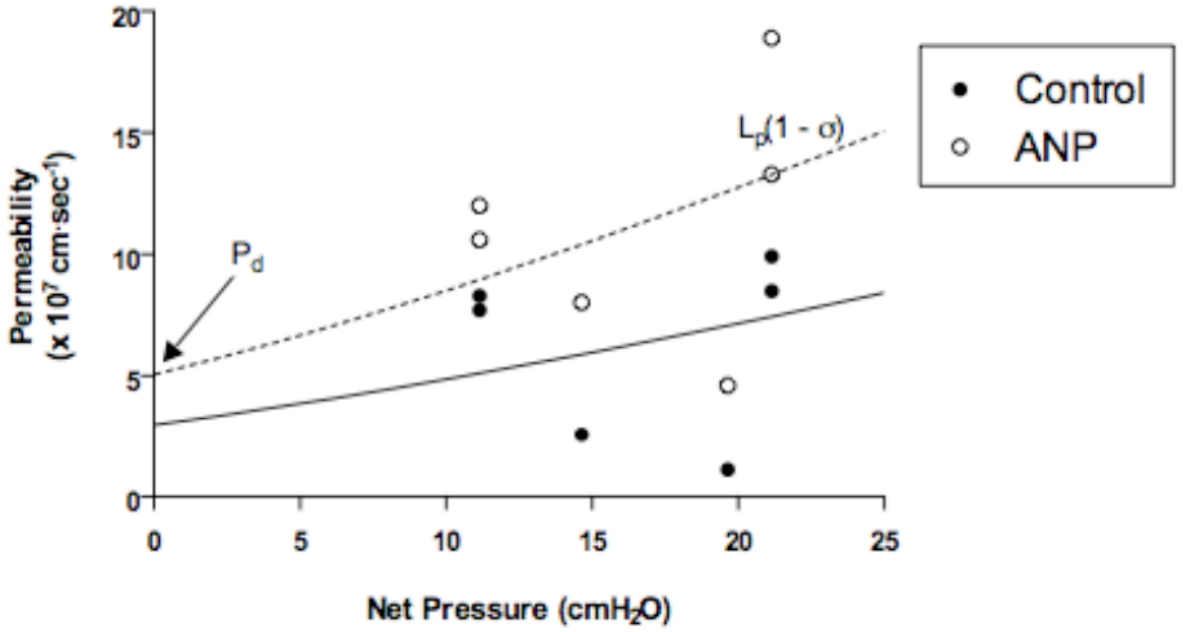

Figure 11. ANP increases the diffusion-mediated solute flux and convective (water driven) coupling of solute flux to water flux. The solid circles represent individual measures of control P_s, while the open circles represent the same vessels perfused with 100 nM ANP (N=6 measures per group). Net pressure, on the x-axis, is defined as the difference between the hydrostatic and effective oncotic pressures. The y-intercept is equal to the diffusional permeability (P_d), and the limiting slope of each fitted line is equal to $L_p(1 - \sigma)$. The fitted curves were not statistically significant, but were used to obtain the information in Fig. 11.

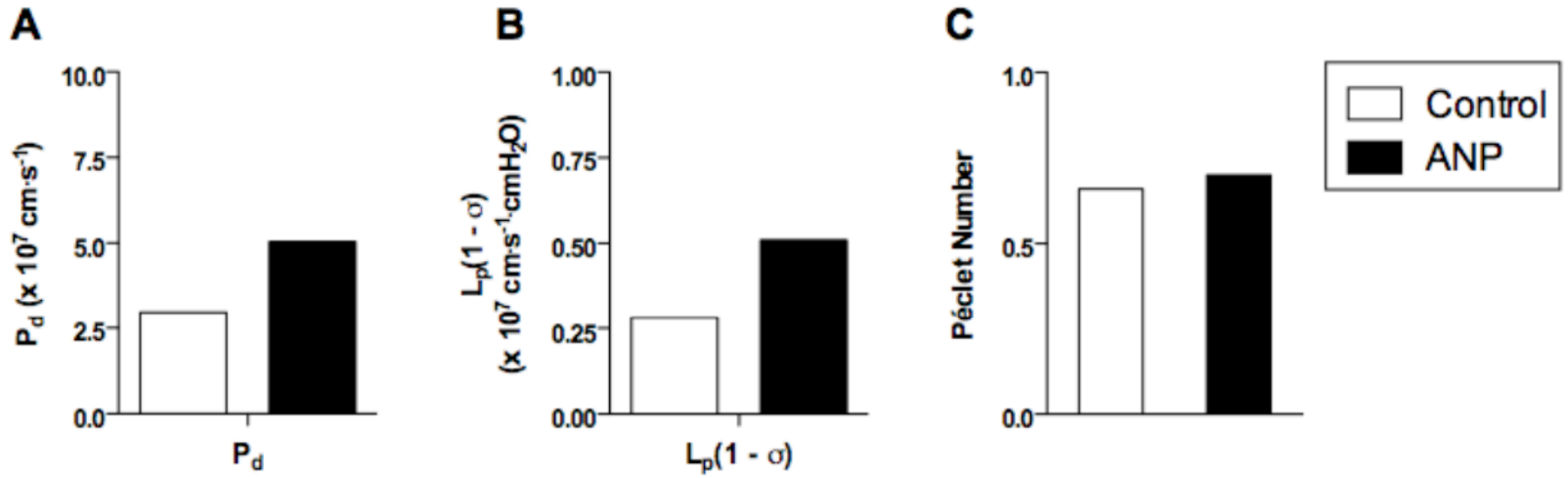

Figure 12. Values derived from the Fig. 10 graph are shown and include estimates of the diffusive permeability to albumin (P_d), $L_p(1 - \sigma)$, and the Péclet number (Pé) at the average *in vivo* collecting lymphatic hydrostatic pressure (7 cmH_2O, (110)). Open bars are values calculated from control data and solid bars are values calculated from data obtained during perfusion of the same vessels with ANP.

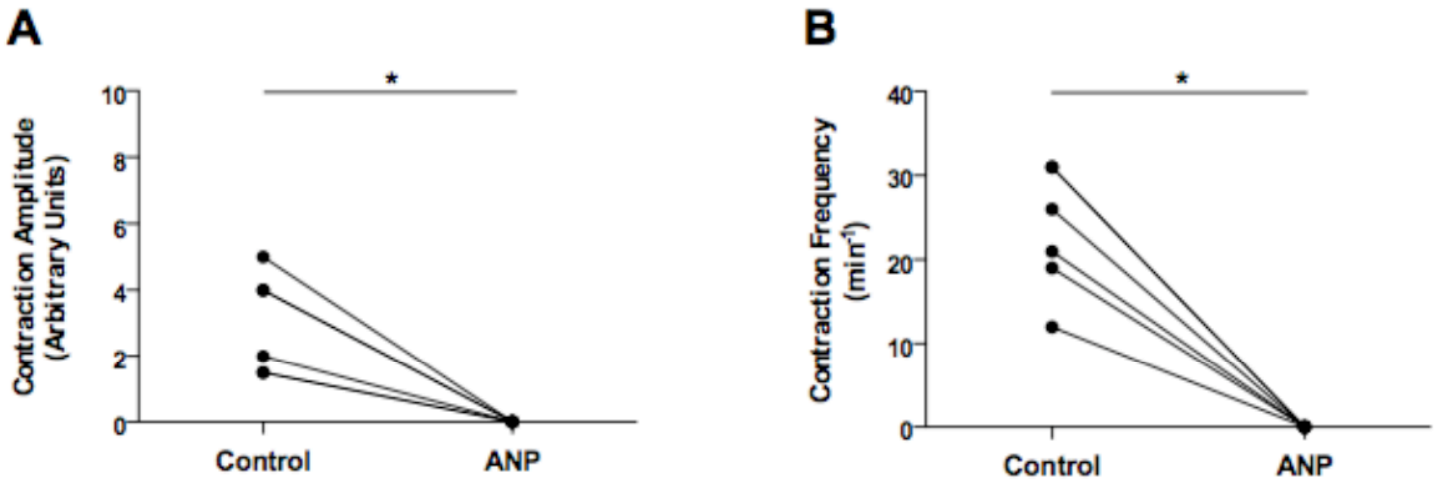

Figure 13. Perfusion of 100 nM ANP (N=6) abolishes spontaneous contraction amplitude (**A**) and frequency (**B**) generated by collecting lymphatic vessels. Amplitude and frequency were measured from the fluorescence intensity data tracing obtained prior to or during solute flux measurements. All measures were paired, meaning that the same vessel was perfused with a control solution followed by an identical one containing ANP. Each pair was measured at one hydrostatic pressure and at the same vessel segment. No significant changes in diameter were observed. *, $p < 0.05$.

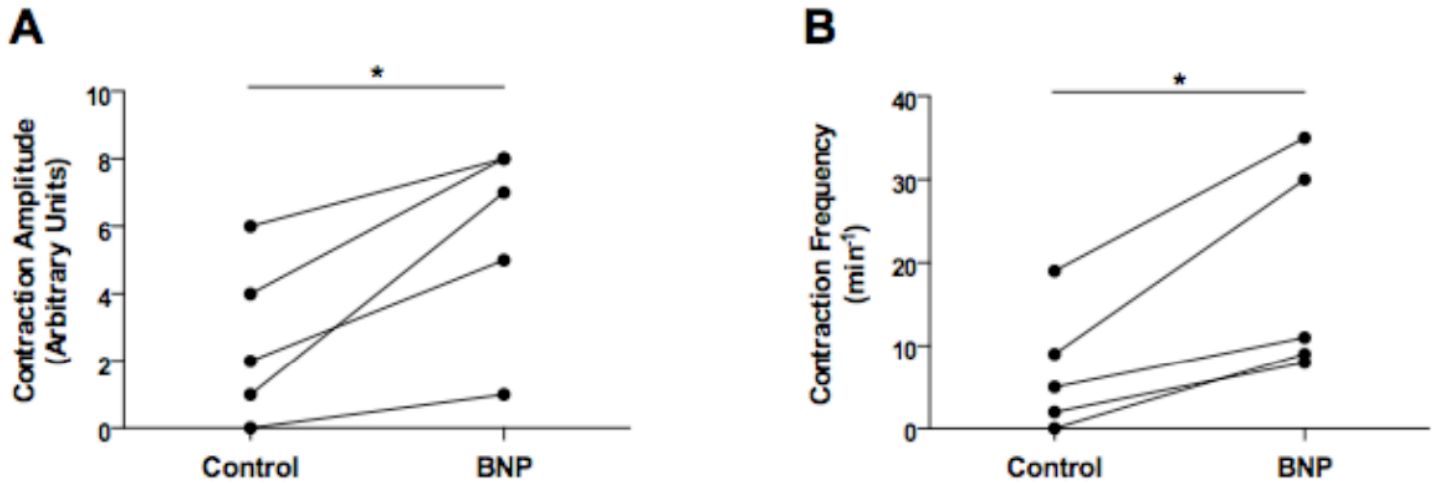

Figure 14. Perfusion of 100 nM BNP (N=5) increases both collecting lymphatic spontaneous contraction amplitude (**A**) and frequency (**B**) by approximately 2-fold. Contractile function was measured from the fluorescence intensity data tracing obtained prior to or during solute flux measurements. All measures were paired, meaning that the same vessel was perfused with a control solution followed by an identical one containing BNP. Each pair was measured at one hydrostatic pressure and at the same vessel segment. No significant changes in diameter were observed. *, $p < 0.05$.

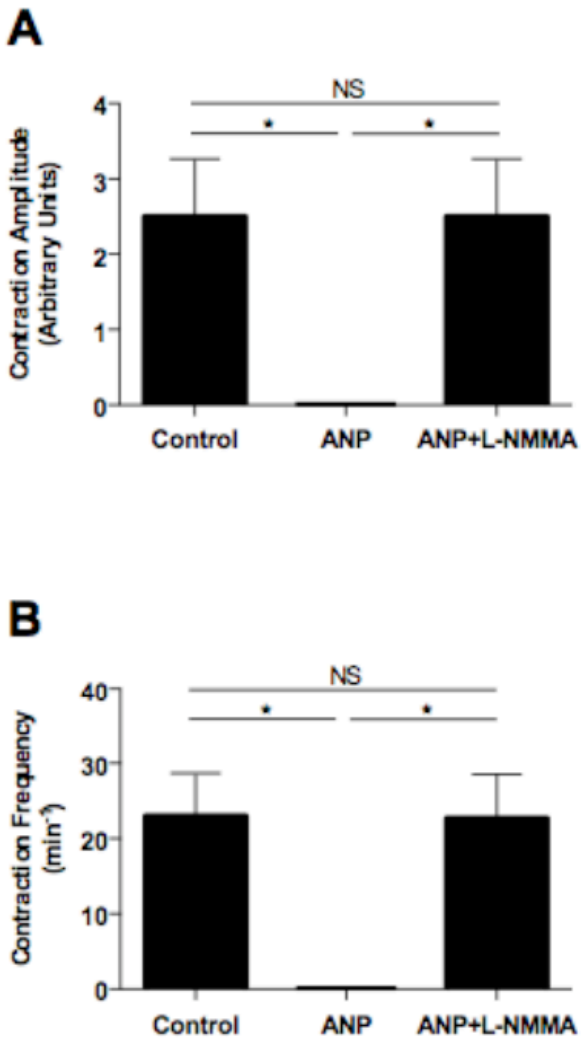

Figure 15. The mechanism by which ANP inhibits collecting lymphatic spontaneous contractions is mediated by nitric oxide (NO). Contraction amplitude (**A**) and frequency (**B**) were measured as in Fig. 12. The same lymphatic vessels (N=3) were perfused with a control solution, followed by 100 nM ANP, and finally 10 μM L-NMMA in addition to the ANP (all drugs were delivered via the perfusate). Amplitude and frequency were again inhibited by ANP. Upon treatment with L-NMMA in addition to ANP, spontaneous contractions reappeared at control levels. *, $p < 0.05$; NS, not significantly different.

Discussion

The lymphatic vasculature is well documented to absorb protein-containing fluid from the interstitium (8, 113). More recent reports, however, are showing that lymphatic vessels are capable of both absorption and extravasation of protein and fluid (19, 110) likely as a mechanism to control the fluid distribution between the tissue and vascular spaces. Therefore, the present study aimed to clarify whether, and to what extent, NPs, which are released into the circulation on volume expansion, modulate collecting lymphatic vessel permeability. We accepted our hypothesis that *in vivo* collecting lymphatics respond to ANP and BNP through an increase in permeability to albumin (P_s) and that the response does not differ between peptides. Further, when the coupling of albumin flux to water flux was examined with respect to ANP treatment, pathways carrying albumin and water were affected similarly. Overall, our data supported that lymphatic vessels are capable of regulating their P_s in response to changes in circulating natriuretic peptides and the theory that lymphatic extravasation of protein and water is a compensatory response to volume overload.

Collecting Lymphatic Vessel Permeability to Albumin: Responses to ANP and BNP

The lymphatic P_s responses to ANP and BNP were a 2-fold elevation above control and compare well with the 2-3-fold response reported previously for venular capillaries (80). That collecting lymphatic vessels appear to mirror the venules with respect to regulation of microvascular permeability supports further the rationale that these two vessel types likely possess similar function as a result of their common embryological origin (114). In addition, the responses to ANP and BNP do not differ

statistically, although there is a tendency for a stronger mean P_s response to BNP (2.0±0.4 versus 2.7±0.8 fold). When sensitivity of the lymphatic P_s response is viewed graphically (i.e. when the response is plotted against control P_s in Fig. 10), it becomes evident that on exposure to ANP, a lymphatic vessel with a lower basal P_s will respond more strongly than a vessel with a higher basal P_s, confirming the relationship of the venular hydraulic conductivity response to ANP (80). Interestingly, when the P_s response to BNP is plotted on the same graph the fitted curve is shifted to the right of the ANP data. From this relationship we conclude that although the mean lymphatic P_s responses to ANP and BNP do not differ, a single vessel with a low basal P_s ($< 4.0 \times 10^{-7}$ cm·s^{-1}) will likely produce a stronger response to BNP than ANP (compare Fig. 9B with Fig. 9A).

If changes in lymphatic diameter occurred with either peptide, they were beyond the resolution of the ocular ruler, especially during lymphatic contractions. According to Brookes and Kaufman (18), we should have expected a <5% increase in diameter, which would equate to <5 μm, much less than one eyepiece unit of 12 μm. A previous study (57) also failed to observe any changes in diameter upon perfusion of rat skeletal muscle arterioles with 1 nM ANP ($p = 0.3$), under conditions where changes on the order of 5 μm could be resolved, suggesting that the lack of vasodilatation is not limited to collecting lymphatics.

The present study could be criticized for comparing P_s responses from rat mesentery to those obtained from frog mesentery (80, 81). Yet data from preceding studies demonstrated that 1 nM ANP elicited increases in P_s of rat skeletal muscle arterioles on the order of 1.6±0.2-fold (N=12, $p < 0.01$) (57) and of porcine coronary

arterioles, 2.0±0.6-fold (N=7, $p < 0.05$) (55). Therefore, the microvascular permeability responses to ANP appear to be of similar magnitude among these three species.

The data thus far illustrate that lymphatic permeability to the protein, albumin, is elevated significantly in response to atrial and brain natriuretic peptides. However, during volume expansion a shift of fluid – in addition to protein – from the vascular space to the tissues would be necessary to relieve volume overload and stress on the heart. To address how water transport might be affected, we graphed the control and ANP treatment P_s measures as a function of net driving pressure (hydrostatic minus oncotic pressures) across the lymphatic vessel wall (Fig. 11). While the two curves do not differ statistically, likely reflecting the distribution in P_s data that have been described as non-normal and left skewed (110), the two curves can still provide physiologically relevant data, namely, estimates of the diffusive permeability (P_d) and $L_p(1 - \sigma)$. Apparent from Fig. 12 are that both $L_p(1 - \sigma)$ (a measure of volume flux through the pathways conducting both fluid and protein) and P_d (a measure of diffusive protein permeability) are nearly doubled upon treatment of collecting lymphatics with ANP. Because Pé is the ratio that describes water-driven ($L_p(1 - \sigma)$) to diffusion-mediated (P_d) solute flux, it does not change with ANP perfusion consistent with a study of venules (80). The Pé value (Fig. 12C) also suggests that if lymphatic L_p (i.e. hydraulic conductivity) undergoes an increase similar in magnitude to P_d during perfusion with ANP, then the reflection coefficient, σ, would not change. The latter scenario likely describes the effect of ANP on lymphatic L_p as the basal lymphatic P_s and its response mirrored that of the venules, for which σ has been demonstrated not to change during ANP infusion (80, 81) or to provide another example,

during hyperglycemia (95). Additionally, changes in pore size (σ) result in large, exponential increases in L_p (to the fourth power if the transendothelial pathways are cylindrical or the second power if they are described by slits (27)). Instead for changes to occur in L_p and P_d comparable to those measured here, either the number of 'pores' doubled or the thickness of the transendothelial channels was halved. While it is possible that a fraction of the permeability to albumin reflects a vesicular transport mechanism, the changes in P_d and $L_p(1 - \sigma)$ are not consistent with changes occurring solely in this pressure-independent component (i.e. increases in vesicular turnover would not change $L_p(1 - \sigma)$). These data point to the need for a follow-up study of lymphatic hydraulic conductivity to measure not only whole vessel lymphatic L_p and its response to NPs, but also to determine whether the lymphatic σ is altered by NPs.

Collecting Lymphatic Vessel Contractile Function is Altered Differentially by ANP and BNP

While we were recording albumin flux of collecting lymphatics, we observed that the contraction amplitude and frequency were affected by ANP and BNP. Strikingly, every lymphatic vessel exposed to ANP lost spontaneous contractions altogether (Fig. 13A and 13B), a finding that is supported by the literature (90). In contrast to the ANP response, BNP increased both contraction amplitude and frequency by approximately twofold (Fig. 14A and 14B). Upon reviewing the literature, we formulated and tested the hypothesis that ANP stimulates nitric oxide (NO) production, a known inhibitor of lymphatic spontaneous contractions (132, 139). To our surprise L-NMMA, an inhibitor of

NO production, perfused in the same solution with ANP (Fig. 15) restored lymphatic contraction amplitude and frequency to control levels for every vessel.

Mounting evidence supports the theory that ANP upon binding to the NPR-C 'clearance' receptor can stimulate NO production (5, 25, 47, 83, 137). The current hypothesis (depicted in Fig. 16) is that NPR-C is a G_i-protein coupled receptor that not only inhibits adenylyl cyclase, but also activates endothelial nitric oxide synthase to produce NO, which binds to the soluble guanylyl cyclase receptor to produce cGMP (5). Our lymphatic contractile data fit well with this theory because the inhibition of NO synthesis reversed completely the effects of ANP, suggesting, consistent with others (132), that cGMP inhibits collecting lymphatic spontaneous contractions. Importantly, one must not neglect that we chose to use 100 nM ANP and BNP to elicit maximal responses and that others reported a dose-dependent effect of ANP on lymphatic contractile function (90), unlike our experience with solute permeability or hydraulic conductivity (81). Therefore, with lower doses of ANP and BNP we would expect attenuation, not inhibition, of spontaneous contractions.

In a single collecting lymphatic vessel measures of P_s to albumin were made under control, ANP, and ANP+L-NMMA treatments. ANP treatment doubled P_s as before, but adding L-NMMA to ANP failed to abolish the P_s response. Instead, L-NMMA caused a further doubling in P_s beyond ANP treatment alone. To account for this unexpected result, we surmise that treatment with L-NMMA eliminated NO production and therefore halted the conversion of GTP to cGMP by the soluble guanylyl cyclase receptor, leaving additional substrate in the form of GTP for the NPR-A receptor (Fig.

16, dashed lines). Notably, NPR-A would convert this excess GTP to cGMP, which serves to increase endothelial permeability and at the same time the NPR-C receptor would inhibit the formation of cAMP that serves to otherwise attenuate endothelial permeability (135).

That the permeability responses to ANP and BNP did not differ, while the contractile responses were polarized, illustrates clearly that contraction, *per se*, is not a mechanism regulating the barrier properties of the collecting lymphatics. Net volume flux, though, might be expected to differ depending on how attenuation or potentiation of spontaneous contractions affect hydrostatic pressure. With respect to BNP, the increased contractile activity is expected to cause greater excursions in pressure, thereby increasing net volume flux (Figure 7) and reducing the efficiency of lymph flow (38, 130). Because ANP would attenuate the contractile activity, lymph flow is still expected to be lessened, but a more constant pressure might produce a smaller volume flux than that of BNP (Fig. 7).

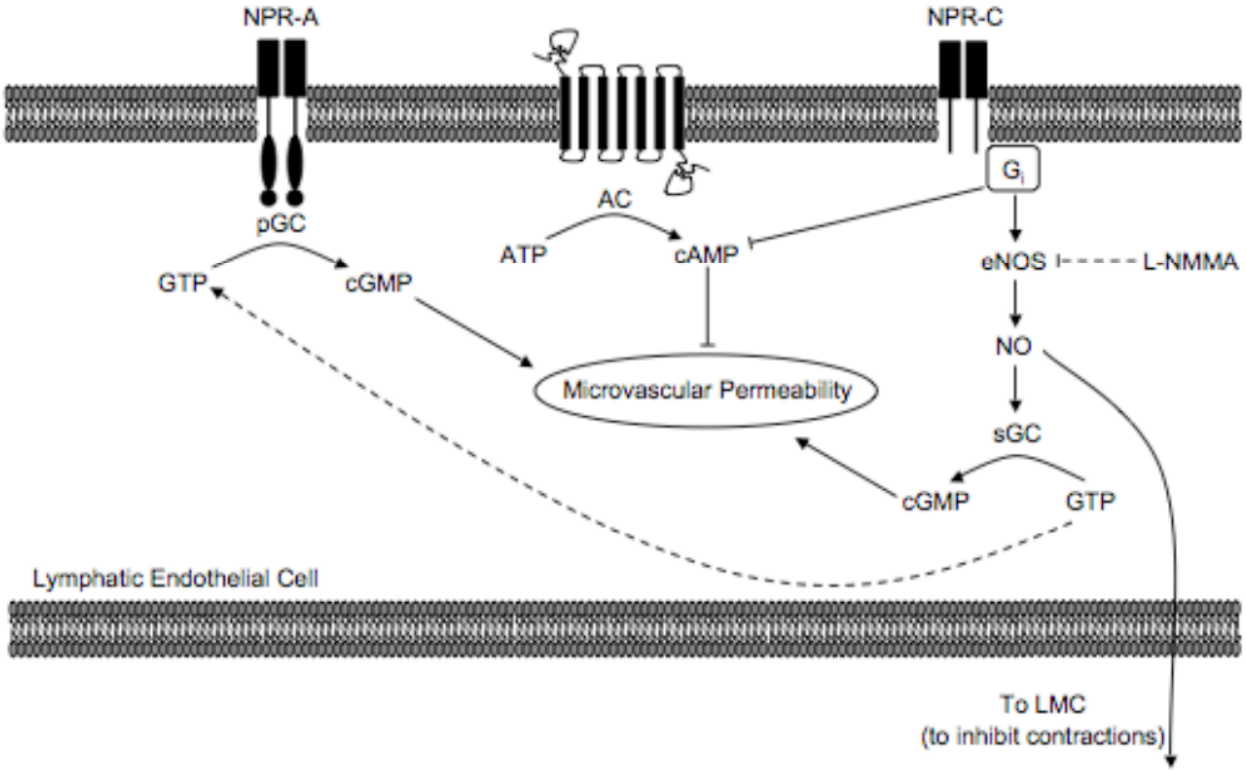

Figure 16. Proposed mechanism that accounts for increases in lymphatic permeability along with inhibition of lymphatic contractions with the layered L-NMMA and ANP treatment. Briefly, ANP binds to both the NPR-A and NPR-C receptors with the effects of increasing permeability and eliminating contractions, respectively. When L-NMMA is perfused along with ANP, NO synthesis is blocked so that an excess of GTP forms, leading to elevated permeability. Solid lines represent known cellular signaling pathways that occur upon ANP binding to the NPR-A or NPR-C receptor. Dashed lines represent the anticipated result from L-NMMA treatment in this study. AC, adenylyl cyclase; eNOS, endothelial nitric oxide; LMC, lymphatic muscle cell; NO, nitric oxide; pGC, particulate guanylate cyclase; sGC, soluble guanylate cyclase.

Physiological Significance of the Lymphatic Responses to Natriuretic Peptides

The data obtained from this study revealed that rat mesenteric collecting lymphatic vessels respond to ANP and BNP by doubling their permeability to albumin. Further, collecting lymphatic spontaneous contractions were abolished completely by ANP, but became stronger and faster with perfusion of BNP. Importantly, one must realize that increases in solute permeability, and likely hydraulic conductivity, serve to augment the rate of protein and fluid extravasation from the microvasculature into the interstitium as demonstrated by others (19, 110, 125, 127). An extravasation of fluid and protein of this magnitude reduces the vascular volume by preventing the capillary filtrate from being absorbed and returned to the bloodstream by the lymphatic vasculature. We propose that the modest dilation of lymphatic vessels caused by ANP (18) would act to slow lymph flow and increase lymph volume to enable a greater loss of fluid and protein into the tissue spaces, suggesting that modulation of permeability is a primary function of NPs in the lymphatic vasculature. Moreover, we expect that attenuation of lymphatic contractions by ANP, and potentiation by BNP, will further reduce the efficiency of lymph flow (38, 130). Finally, it remains to be determined which of these peptides dictates contractile activity under the *in vivo* condition where the collecting lymphatics are presented with a mixture of ANP and BNP of varying ratios, such as is encountered during congestive heart failure.

CHAPTER 4: GENERAL DISCUSSION

Armed with a more complete understanding of lymphatic vessel permeability developed over the last two chapters, we now return to the questions posed originally in the Specific Aims section of this dissertation: 1) are lymphatic vessels absorptive, leaky, or are they impermeable; 2) would increases in collecting lymphatic permeability be expected to resolve or create edema; and, 3) do collecting lymphatics really concentrate solute along their length? More importantly, we can now conclude that **Hypotheses 1** and **2** were accepted; i.e. that collecting lymphatic permeability to albumin does not differ from that of the venules, and that vasoactive peptides would elevate this permeability from control. The next few sections will examine these raised questions and the implications of the answers obtained in the context of the data presented here.

Lymphatic Barrier Properties

Before discussing the permeability properties of collecting lymphatic vessels, a brief outline of what is known about their barrier will be presented, as this influences the ability of solute and water to traverse the vessel wall. The lymphatic barrier (going from the lumen to the tissue) is comprised of an endothelial layer, followed by a basement membrane and pericytes, and ends with lymphatic muscle cells at the vessel-tissue interface. Whether lymphatic muscle, or even vascular smooth muscle on venules, poses a significant barrier to solute or volume flux is unknown.

Interestingly, initial lymphatic vessels lack pericytes, whereas collecting lymphatic vessels do not (96). This pattern opposes that seen in the blood microvasculature where smaller capillaries are vested with pericytes, but the larger vessel pericytes are relatively lacking. Initial lymphatics (a.k.a. lymphatic capillaries) have a much larger diameter than traditional blood-filled capillaries, but so do blood endothelial cell tubes cultured in the absence of pericytes, reflecting the role for pericytes in stabilizing endothelial tubes by inducing basement membrane accretion (117). Still remaining to be tested is whether pericytes are able to modulate endothelial permeability, be they of a blood or lymphatic origin.

Collecting lymphatic vessels possess intraluminal valves, resembling those identified in the larger veins. When the vessel wall is stained for smooth muscle actin and imaged, a lack of lymphatic muscle around the valves can be visualized. In addition, we have observed in some vessels focal leaks of fluorescently labeled albumin from around the valve regions (unpublished observations). A role for lymphatic muscle in comprising part of the barrier to solute and water should be thoroughly investigated.

For blood microvessels, a glycocalyx has been described as an endothelial secretion of glycoproteins that contain sialic and hyaluronic acid (54). Germane to the interpretation of this work, the glycocalyx hinders solute movement due to its web like structure and its highly negative charge. Since albumin is also negatively charged its transport is restricted by this structure. If a glycocalyx were present on the lymphatic endothelium, one would expect that it is similar in composition to that of the blood microvessels, since the permeability to albumin of these two vessel types does not differ.

However, a protein that bears resemblance to those of the blood microvessel glycocalyx has been identified, and may comprise part of the putative lymphatic glycocalyx. Podoplanin, also known as glycoprotein-38, is a negatively charged protein (due to O-glycosylation and that it contains sialic acid, constituents of the microvessel glycocalyx (108)) present on the luminal side of lymphatic endothelium, and is absent completely from blood microvessel endothelium (112). When this protein is lost from podocytes in the kidney, proteinuria ensues suggesting a role for this protein in maintaining a patent barrier against solute (65). If the glycocalyx of lymphatic vessels differs from blood vessels in the face of similar permeability properties, then other proteins may be involved. Another related protein, podocalyxin, is not expressed on lymphatic endothelium but is abundant on blood microvessel endothelium (123). Further research is necessary to tease out the presence, components, and significance of a lymphatic glycocalyx.

Albumin and Volume Flux Within the Lymphatic Vasculature

In Chapter 2 the assessment of collecting lymphatic vessel (CLV) permeability to albumin leads to the conclusion that, indeed, CLV are permeable to protein. When the question arises as to whether this solute flux is significant physiologically, we can conclude that it is because we show that the permeability between CLV and venules does not differ. Further, albumin transport was found to be dependent upon hydrostatic pressure, which would only occur if some of the albumin was crossing the endothelium through pathways conducting albumin and water. Therefore, these vessels likely conduct

water across the endothelial barrier in a manner analogous to the venules. Finally, if one models solute and fluid flux across the barrier, assuming that the reflection coefficients do not differ between the two vessel types, then the hydraulic conductivities between CLV and venules do not differ. These findings are striking given the differences between CLV and venules – their *in vivo* hydrostatic pressures, surface areas, and flow velocities all differ, not to mention that CLV generate spontaneous contractions at a regular frequency giving rise to a pulsatile pressure and flow, while venules possess a steady state pressure and flow. This last point argues for a mechanism by which CLV regulate their permeability properties at a basal set point near that of the venules. Future experiments will be needed to determine whether the permeability responses (e.g. to inflammatory mediators, exercise, signaling molecules, etc.) differ between these two vessel types.

To answer whether CLV are absorptive or leaky (i.e. whether solute is transported *from* or *into* the vessel lumen) simultaneous measures of lymph, interstitial fluid, and plasma protein concentrations indicated that for CLV, at least in rat mesentery, a protein gradient existed favoring the net expulsion of protein and fluid. The result is further supported by experiments performed in the rat splenic microvasculature, where FITC-labeled BSA leaked from the lymphatic vessels into the interstitium upon endotoxemia or infusion of ANP (18, 19). Macromolecule extravasation cannot occur if the concentration gradient across the lymphatic vessel wall is not such that the protein concentration inside the vessel is higher than in the interstitium. It is also highly unlikely that the ANP infusion or endotoxemia caused the concentration gradient to reverse spontaneously

within a short time period. Therefore, one can deduce that the rat spleen is another organ containing lymphatic vessels from which macromolecules diffuse into the interstitium under basal conditions.

Concerning the movement of water across the lymphatic wall, estimates were made of lymphatic hydraulic conductivity (L_p) from the measures of albumin flux. In addition, collecting lymphatic hydrostatic pressures were measured prior to assessing lymphatic solute permeability (P_s). From these two pieces of information, a convincing argument was made for the filtration of water from collecting lymphatics into the interstitium as a consequence of the oscillating pressures in the lymphatic vasculature. The spontaneous contractions of collecting lymphatics generate a pulsatile pressure and flow, which places the volume flux on the transient state line (Eqn. 2.5), rather than the steady state relationship (Eqn. 2.6a; Figure 7B). Significantly, vessels undergoing transient changes in pressure, thus volume flux, are capable of transient fluid absorption. In contrast, vessels at a steady state pressure cannot reabsorb fluid (Fig. 6B) and constantly filter a finite amount of water (e.g. venules). For collecting lymphatics the estimated hydrostatic pressure below which fluid reabsorption occurs is 1.5 cmH_2O. For individual vessels the threshold pressure below which fluid reabsorption occurs will vary, but to ascertain the real L_p and σ of albumin, which determine this threshold value, experiments must be designed carefully to measure these parameters in contracting lymphatic vessels.

Implications of Collecting Lymphatic Permeability Properties

The data discussed thus far have profound consequences for overall fluid balance. The permeability properties of CLV are regulated such that a finite, significant extravasation of protein and water occurs. Any process, inflammatory or not, that increases the permeability of CLV to water and protein will promote edema via two mechanisms: 1) an increase in the rate of water and protein leak into the interstitium promotes edema directly; and 2) if the water loss from CLV is substantial, then the overall lymph flow will be compromised to cause a backup of the capillary filtrate into the interstitium, facilitating edema indirectly. Lymph flow can be expected to affect the efficiency of this process because a bolus of lymph flowing quickly through the CLV has less time to exchange its contents with the tissue compared to a bolus of lymph moving slower. Therefore, CLV permeability to water and solute must be considered an edema safety factor because its maintenance promotes fluid balance through direct and indirect means.

That CLV are capable of continuous fluid reabsorption, while blood vessels (of any type) are not, carries its own significant implications. One is that CLV may be able to absorb fluid from the interstitium to alleviate the accumulation of interstitial fluid. If this is a normal process, then when the interstitial volume expands and increases interstitial pressure (and decreases interstitial oncotic pressure), the Starling forces would be shifted to favor absorption of excess fluid via this pathway. Secondly, if spontaneous contractions were to cease, then fluid transport would be shifted to the steady state relationship (Figure 7B) where fluid reabsorption would not be possible.

Another implication from this work is that the composition of lymph cannot be assumed to be identical to interstitial fluid. Several groups have proposed that CLV are able to concentrate their luminal contents (17, 56, 119), which would cause great error if one measured the oncotic pressure of lymph to assess that of interstitial fluid or if the lymph volume/protein concentration was used to assess capillary permeability. The potential of CLV to concentrate lymph is discussed below, as an extravasation of water from lymph is a mechanism that explains this effect. That macromolecules are retained in the CLV lumen relative to water argues that the lymphatic vasculature may be designed primarily for macromolecule and solute return to the blood, with the secondary consequence of returning some fluid.

Is the Lymphatic Circulation Absorptive or Leaky?

Taken together, the albumin flux data and volume flux models support our proposed theory of macromolecule handling by the lymphatic vasculature: that while the initial lymphatics absorb interstitial fluid, the concentration and pressure gradients of the microlymphatic and collecting lymphatic vessels (downstream) favor extravasation of a portion of this protein and water into the interstitium (Figs. 5 & 7). Furthermore, at a hydrostatic pressure of 5 cmH_2O (close to the average CLV pressure), the P_s to albumin was less than 3×10^{-7} $cm \cdot s^{-1}$ whereas volume flux per unit surface area (J_v/S) at the same pressure was greater than 7×10^{-7} $cm \cdot s^{-1}$ (Fig. 7). The effect is augmented at a higher, yet still physiological, pressure of 10 cmH_2O with a P_s to albumin of $\sim 3 \times 10^{-7}$ $cm \cdot s^{-1}$ versus a J_v/S of $\sim 18 \times 10^{-7}$ $cm \cdot s^{-1}$. Thus, water traverses the CLV barrier approximately 3-6

times faster than does albumin, depending on the pressure of the vessel. When these units of permeability ($cm \cdot s^{-1}$) are used to determine absolute amounts (i.e. flux; J_s ($mol \cdot s^{-1}$) or J_v ($L \cdot s^{-1}$)) transported in one second per unit area (Fig. 17), a CLV segment loses only femtomoles of albumin compared to picoliters of water (10^{-15} mol versus 10^{-12} liters) – a thousand-fold difference! A result of this astonishing property is that over the length of the CLV, more water than solute travels into the interstitium thereby concentrating the luminal protein. These data explain the physiology underlying recurring claims that CLV are capable of concentrating their contents (17, 56, 119). For this reason one cannot assume that lymph is representative of interstitial fluid with regard to oncotic pressure, overall volume, or protein concentrations.

Calculating the ratio of albumin flux to water flux (J_s/J_v, mol/L) yields an approximate value of the vessel filtrate molarity. The CLV filtrate is 1.7 mM, while that of venules is twice as concentrated at 3.4 mM (at each vessel's average hydrostatic pressure). So while the diffusional permeabilities of the two vessels to albumin do not differ, nor the hydraulic conductivities nor even the fluid fluxes, the luminal concentration of albumin in CLV is about half that of the venules (26.2 versus 13.2 mg/mL RSA, Table 2) leading to a diminished filtrate concentration of the CLV relative to the venules. While more information is required regarding the protein concentration difference for microlymphatic vessels, which possess a 10-fold greater permeability to albumin than that of CLV, it would be interesting to determine the molarity of their filtrate as these vessels appear to possess a much greater cumulative area than the CLV.

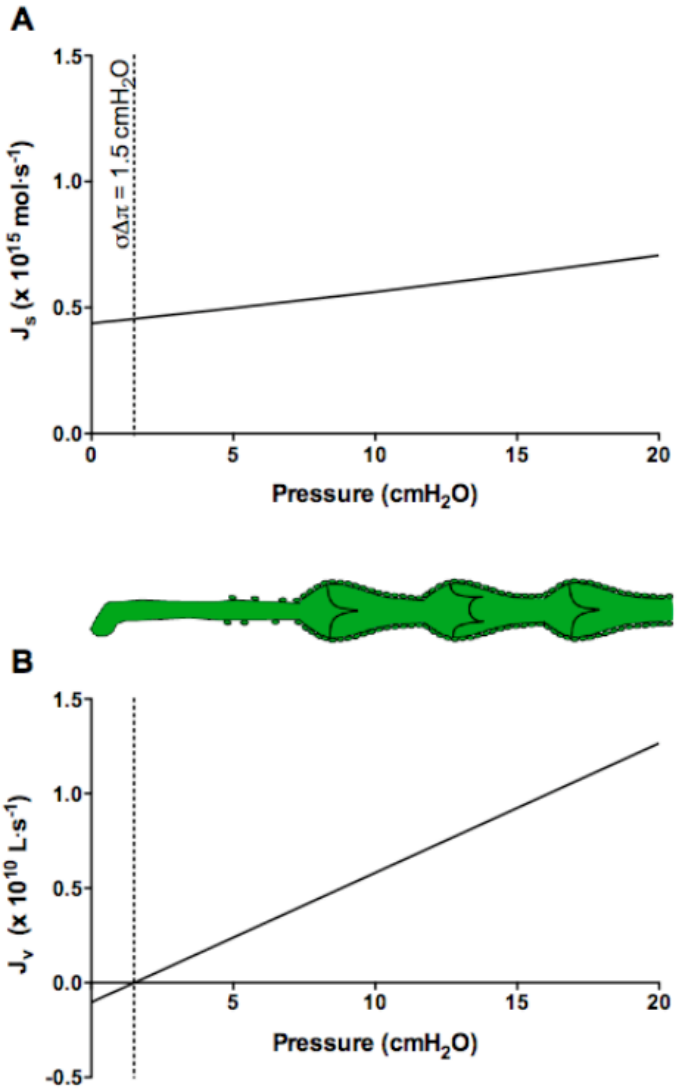

Figure 17. A, Solute flux (J_s) determined from the diffusive permeability to albumin and **B**, volume flux (J_v) determined from Eqn. 2.5 and the concentration gradients measured directly (Table 2). Both graphs are for flux across a lymphatic segment with a length of 1 cm. The cartoon of an initial lymphatic transitioning into a collecting lymphatic vessel in the middle is to depict how a rising hydrostatic pressure through the lymphatic network influences albumin and water transport (see Discussion for details).

A global conclusion, then, is that the lymphatic circulation is both an absorptive sump and a leaky pump. While the majority of functional research has focused on the lymphatic muscle pump, the regulation of lymphatic vessel permeability is an equally important, novel mechanism for the maintenance of fluid homeostasis. Factors regulating CLV permeability, as well as the consequences of an elevated permeability, are discussed next.

Modification of Lymphatic Solute Permeability

To address the question of whether the lymphatic vasculature is able to modulate its permeability to solute, or whether it is simply a fixed value, the albumin permeability of CLV was determined in the absence and presence of two natriuretic peptides (Chapter 3). Collecting lymphatics exhibited a rapid and sustained twofold elevation in permeability upon exposure to either 100 nM ANP or BNP, leading to the conclusion that CLV permeability is regulated actively in a manner similar to the rest of the blood microvasculature. In detail, this study demonstrated that natriuretic peptides, likely through the actions of cGMP, modulate CLV permeability and, through a nitric oxide-dependent mechanism, they can either attenuate or potentiate lymphatic spontaneous contractions. The same signaling scheme has been elucidated in the context of mammalian venular permeability, in that cGMP elevates permeability and, conversely, cAMP leads to enhanced barrier function (135). In one study using lymphatic endothelial cells grown in a collagen tube, cAMP was found to enhance lymphatic barrier integrity through an increased expression of VE-cadherin (98). Together these data suggest that

natriuretic peptide signaling is conserved between lymphatic and blood microvessels. However, it remains to be determined if the same phosphodiesterase isoforms are present in the same amounts in lymphatic and blood endothelia and, if different, could lead to the interesting situation where lymphatic and microvessel permeability are differentially regulated.

Paradoxically, ANP and BNP through binding the NPR-C receptor exert opposite effects on lymphatic muscle spontaneous contraction amplitude and frequency (Chapter 3). A possible hypothesis that resolves this dilemma is that NPR-C signaling is constitutive and therefore regulates lymphatic muscle contractile activity not only during diseases where natriuretic peptides are released but also during conditions of health. Having a greater concentration of circulating BNP than ANP, then, would lead to the observed effects only if BNP inhibited the nitric oxide cascade after binding to NPR-C. The ratio of BNP to ANP would either increase or decrease lymphatic contractile activity, and would agree with BNP as a predictor of patient mortality in CHF. To test this hypothesis, experiments from Chapter 3 could be repeated with control, BNP, and BNP+sodium nitroprusside treatments (in the same vessel) to determine whether nitric oxide replacement mitigates or eliminates the potentiation of lymphatic contractions by BNP.

Before continuing it is worth mentioning that all the data discussed thus far have demonstrated that collecting lymphatic permeability and its responses to natriuretic peptides mirror that of the venules. Because the embryologic origin of the lymphatic endothelium is the cardinal vein (114), and expression of Prox-1 alone is sufficient to

coerce a blood endothelial cell to become a lymphatic endothelial cell (60), we reasoned that lymphatic vessels share many genes, therefore function, with the blood microvasculature. However, it must be recognized that many genes differ between these two cell types and that Prox-1 is a transcription factor that likely controls the expression of numerous downstream proteins. One set of proteins that would be interesting to discover under the control of Prox-1 would be junctional adhesion proteins. Whether or not Prox-1 controls the lymphatic barrier is currently unknown.

The novel data presented in this dissertation are anticipated to influence several pathological states, especially pathologies associated with edema. The next few sections examine the possible interplay between lymphatic permeability and disease.

Lymphatic Permeability in Pathology

Edema, or the unchecked accumulation of protein and fluid in the tissue spaces, is a hallmark of inflammation that, by itself, is a component of several illnesses, some of which include allergic reactions, asthma, cancer, diabetes, ischemia/reperfusion injury, malnutrition, and obesity. Indeed, one of the earliest events in inflammation is a compromised endothelial barrier leading to an increase in protein and fluid extravasation that serves several functions (111). To date, this has only been studied with respect to *microvascular* permeability, since lymphatic vessels have been assumed to be impermeable or solely absorptive. Mentioned earlier, a possible consequence of elevated microvessel permeability in the absence of a corresponding increase in lymphatic permeability is that the capillary filtrate could be reabsorbed by the lymphatic

vasculature. To maintain an edematous state, microvessels and lymphatic vessels are expected to undergo permeability increases together, again supporting parallel signaling pathways between the two vessel types.

An intriguing hypothesis is that changes in microvessel and lymphatic permeability can become uncoupled, leading to differential regulation of their barriers. The literature has already hinted at this phenomenon, as a sufficient increase in lymphatic permeability unaccompanied by a corresponding change in microvessel permeability would be expected to give rise to lymphedema, any edema occurring solely from lymphatic dysfunction. Much attention has been placed on the importance of defective lymphatic pumping, not only because it is an obvious defining feature, but also because pumping is needed to transport lymph *against* a hydrostatic pressure gradient. However, some peculiar cases of lymphedema cannot be explained by reduced lymphatic pumping even after enhanced capillary filtration is taken into account. One example is breast cancer-related lymphedema, which is associated with lymph node removal and/or axillary radiation and obesity (87). Several hypotheses for the cause of this ailment have been tested, but do not wholly account for the fluid retention, delayed onset, or that a low-protein edema is formed instead of the expected high-protein edema (11). A mechanism that has not been tested is whether surgery and/or radiation cause damage to the lymphatic circulation precipitating an increase in lymphatic permeability. A 'lymphatic permeability edema' would be expected to produce a low-protein edema, since water is lost across the lymphatic vessel wall more readily than solute.

Another important example comes from experimental models characterized by 'leaky' lymphatic vessels but intact blood microvessel barriers. Specifically, mice heterozygous for the *Prox-1* gene possess malformed, 'leaky' lymphatic vessels and develop adult-onset obesity (46). Therefore, it would be interesting to determine whether increases in lymphatic permeability lead to obesity, or whether the obesity in this mouse model is caused by signaling defects downstream of *Prox-1*, or both. The former case is an apt culprit, as collecting lymphatics in the mesentery drain the intestinal lacteals and are the only route for the absorption of dietary fats; an enhanced leakage of these fats into the tissue spaces may stimulate adipogenesis and obesity. Such a mechanism is not limited to the intestinal vasculature because lymphatic vessels throughout the body contain fatty acids, lipids, and cholesterol (74). Finally, this animal model implies that junctional protein expression may be under the control of Prox-1, a hypothesis that remains to be tested.

Recently, lymphatic vessel growth was assessed in a rat model of salt-sensitive hypertension where a compensatory lymphangiogenic response to high salt treatment occurred (73). Upon macrophage depletion the lymphangiogenic response was inhibited and blood pressure increased. While the results were interpreted as subsequent to macrophage expression of a tonicity responsive protein that controlled vascular endothelial growth factor-C signaling, it remains unknown whether the lymphatic endothelium itself could serve as a primary sensor of interstitial tonicity by expressing this protein (tonicity-responsive enhancer binding protein). Alternatively, another sensor (i.e. the heart) could target the lymphatic circulation. In many animal models of

hypertension, atrial natriuretic peptide plasma concentrations are elevated (105) and knockout of the NPR-A receptor results in hypertension and a volume expansion of 30% (59, 97). ANP and BNP, therefore, are expected to play a profound role in the maintenance of vascular volume not only during hypertension, but also during basal conditions. Combined with the data from this dissertation providing evidence for natriuretic peptide signaling in the lymphatic vasculature, it seems reasonable to propose that the lymphatic vasculature acts as a regulator of vascular volume by modulating its permeability. As a result systemic blood pressure might be affected indirectly.

Natriuretic peptides were originally thought to play a large role in congestive heart failure (CHF). However, natriuretic peptide receptor desensitization is believed to occur over time through receptor phosphorylation (97), limiting their usefulness as a treatment. In acute CHF, before receptor desensitization has a chance to occur, these peptides would be a major way to reduce volume load by elevating both lymphatic and microvessel permeability (short-term reduction), while at the same time eliciting diuresis to reduce vascular volume in the long-term. A novel mechanism was discovered during this dissertation work, that natriuretic peptides can additionally target the contractile activity of collecting lymphatics to reduce lymph flow, enabling a longer time for lymph-tissue fluid and solute exchange (Chapter 3).

Although it is not a pathological state, *per se*, the arrangement of a venule draining a tissue bed adjacent to an arteriole feeding the same bed, named an ‘arteriovenous pair’, has been proposed to allay pathogenesis. The significance of this countercurrent, parallel vessel arrangement is that inflammatory mediators drained by the

venules are able to diffuse to the arterioles, or cause a secondary diffusible signal to be released from the venule, with the end effect of modulating arteriolar tone, thus blood flow, capillary pressure, and capillary filtration (45). One important component of the vasculature, collecting lymphatic vessels, has been overlooked in this context because the permeability of these vessels had not been determined until now. A result of this thesis work is that collecting lymphatics are permeable and are capable of signaling nearby feeding arterioles. Here a new term should be presented to describe this 'new' threefold arrangement – 'arteriovenolymphatic (AVL) triads' – whose physiological relevance remains to be elucidated.

In conclusion, the regulation of lymphatic permeability is likely an unidentified feature of several disease conditions, in particular those that possess edema and/or inflammation components. Some implications of increasing lymphatic vessel permeability are that: 1) solute and protein will be lost to the tissue spaces to facilitate edema formation, 2) as a result lymph flow will be diminished to a proportional degree, and 3) inflammatory signals may diffuse from lymphatic vessels more readily to signal nearby tissues or vessels. Whether elevation of lymphatic permeability precedes leukocyte adhesion or rolling in collecting lymphatics must be examined. Finally, the permeability and contractile activity of the lymphatic vasculature may be an additional target for the regulation of vascular volume by natriuretic peptides and a causative factor in adult-onset obesity.

CHAPTER 5: CONCLUSION

The work presented within this dissertation was a direct test of 2 hypotheses: 1) that collecting lymphatic vessels are permeable to albumin to an extent that mimics that of the venules, and 2) that natriuretic peptides elicit twofold increases in collecting lymphatic permeability to albumin. Both hypotheses were accepted, suggesting that collecting lymphatic vessel permeability is regulated during conditions of health and illness. In addition, collecting lymphatic permeability resembles the permeability of venular microvessels not only under basal conditions, but also in its response to natriuretic peptide signaling. Functional distinctions between the two vessel types (including hydrostatic pressure, surface area, and lymphatic spontaneous contractions) are compensated for because their net fluid and protein transport are similar.

In addition, several unexpected discoveries were made during the course of this project. One is that collecting lymphatics, at least in the rat mesentery, possess a greater concentration of total protein and albumin than is present in the interstitium leading to protein and fluid extravasation into the tissue spaces. A second was that collecting lymphatic fluid flux models predict, as a consequence of lymphatic phasic contractions, that both filtration and reabsorption of fluid by the lymphatic vasculature are possible. Lastly, ANP and BNP were found to exert opposing effects on the spontaneous contraction amplitude and frequency of lymphatic muscle, somehow by binding the same receptor. Overall, this dissertation establishes the lymphatic vasculature as both an absorptive sump and a leaky pump with profound implications in many diseases, as

changes in permeability properties are involved in the precipitation of edema and inflammation. In particular, lymphatic permeability dysregulation was proposed to be the missing cause of adult-onset obesity and discussed in the context of several pathologies.

APPENDIX 1: LIST OF ABBREVIATIONS

AC, adenylyl cyclase

ANP, atrial natriuretic peptide

BNP, brain natriuretic peptide

BSA, bovine serum albumin

ΔC, transmural concentration difference (mM)

CHF, congestive heart failure

CLV, collecting lymphatic vessel(s)

CNP, C-type natriuretic peptide

D, vessel diameter (cm)

dI_f/dt, rate of interstitial fluorescence accumulation

FITC, fluorescein isothiocyanate dye

I_f, fluorescence intensity

I_o, initial fluorescence intensity

J_s, solute flux ($mmol \cdot s^{-1}$)

J_v, volume, or fluid, flux ($mL \cdot s^{-1}$ or $cm^3 \cdot s^{-1}$)

J_v/S, volume flux per unit surface area ($cm \cdot s^{-1}$)

L-NAME, L-N^G-nitroarginine methyl ester

L-NMMA, N^G-monomethyl-L-arginine

L_p, hydraulic conductivity ($cm \cdot s^{-1} \cdot cmH_2O^{-1}$)

NO, nitric oxide

NPs, natriuretic peptides

NPR, natriuretic peptide receptor (-A, -B, or -C)

ΔP, transmural hydrostatic pressure difference (cmH_2O)

P_c, microvessel hydrostatic pressure (cmH_2O)

P_d, diffusive permeability to solute ($cm \cdot s^{-1}$)

pGC, particulate guanylate cyclase receptor

P_i, interstitial hydrostatic pressure (cmH_2O)

P_{lumen}, native vessel pressure (cmH_2O), measured prior to solute flux in Chapter 2

P_s or P_s^{RSA}, apparent solute permeability to rat serum albumin ($cm \cdot s^{-1}$)

Pé, Péclet number (no units)

RSA, rat serum albumin

S, surface area (cm^2)

sGC, soluble guanylate cyclase receptor

STD, spontaneous transient depolarizations

$\Delta\pi$, transmural oncotic pressure difference (cmH_2O)

π_c or π_L, microvessel or lymphatic vessel oncotic pressure (cmH_2O)

π_i, interstitial oncotic pressure (cmH_2O)

σ, reflection coefficient (no units)

APPENDIX 2: RAW DATA TABLES

Table 1. Basal permeability (P_s) values for rat serum albumin.

Date	*Vessel Type*	*Diameter (μm)*	*P_{Lumen} (cmH_2O)*	*P_s^{RSA} ($x10^{-7}$ cm/s)*
02/01/08	CL1	113	1	3.6
06/03/08	CL2	76	10	4.0
08/06/08	CL3	101	~0	8.8
08/11/08	CL4	88	2.5	16.7
08/12/08	CL5	113	~0	1.5
08/27/08	CL6	101	5	4.8
09/01/08	CL7	139	10	2.7
09/05/08	CL8	139	16	1.0
09/09/08	CL9	101	6	1.5
09/24/08	CL10	139	11	2.7
09/25/08	CL11	126	9	7.0
10/20/08	CL12	139	12	2.7
12/05/08	CL13	88	5	3.2
12/17/08	CL14	88	9	6.4
01/21/09	CL15	101	2	15.2
01/23/09	CL16	88	~0	4.0
2/05/09	CL17	50	5	3.3
02/06/09	CL18	126	10	9.9
03/02/09	CL19	113	10	0.2
03/05/09	CL20	63	5	3.1
03/10/09	CL21	88.2	8.5	4.3
03/11/09	CL22	88.2	8.5	3.2
08/26/08	V1	63	20	6.1
09/03/08	V2	38	23	6.2
09/26/08	V3	50	17	3.3
04/17/09	V4	25	17	3.9
09/23/09	V5	38	21	4.1
09/23/09	V6	38	17	9.1
09/23/09	V7	38	20	3.4
09/23/09	V8	25	21	0.5
Mean ± S.E.M.	*CL*	*103 ± 5**	*7 ± 1**	*5.0 ± 0.9*
	V	*39 ± 4*	*20 ± 1*	*4.6 ± 0.9*
Median ± MAD	*CL*			*3.5 ± 1*
	V			*4.0 ± 1*

P_s values are x 10^{-7} cm·s^{-1}; CL, collecting lymphatic; V, venule; P_{Lumen}, native vessel pressure (measured during relaxation phase for lymphatics); MAD, median absolute deviation; *, $p<0.01$ versus venules.

Table 2. Measured Total Protein and Albumin Concentration of Lymph, Peritoneal Fluid, and Plasma.

	Plasma	*Peritoneal Fluid*	*Lymph*
Total Protein (mg/mL)	41.6 ± 2.4	31.3 ± 0.9	32.4 ± 1.1
Albumin (mg/mL)	26.2 ± 0.8	9.5 ± 1.5$^{\#}$	13.2 ± 1.5$^{\#}$
Albumin/Total Protein Ratio (%)	63.4 ± 3.7	30.3 ± 4.5$^{\#}$	40.9 ± 5.1$^{\#}$
Total Protein Oncotic Pressure* (cmH_2O)	23.9 ± 1.7	7.2 ± 1.4†	9.4 ± 1.0†
Albumin Oncotic Pressure* (cmH_2O)	11.9 ± 0.4	3.9 ± 0.6$^{\#}$	5.5 ± 0.7$^{\#}$

*Oncotic pressure is calculated from the Landis-Pappenheimer equation for total protein or albumin, respectively. $^{\dagger, \#}$ Paired t-tests between peritoneal fluid and lymph; † $p < 0.05$, $^{\#}$ $p < 0.1$. Values are reported as means ± SE from 4 animals.

Table 3. Permeability (P_s) to rat serum albumin during control and natriuretic peptide solution perfusion.

Date	*Diameter (μm)*	*P_s^{RSA} ($x10^{-7}$ cm/s)*	*P_s^{ANP} ($x10^{-7}$ cm/s)*	*P_s^{BNP} ($x10^{-7}$ cm/s)*	*Response (fold)*	*Perfusion P (cmH_2O)*
02/06/09	126	9.9	18.9		1.9	25
03/10/09	88	1.1	4.6		4.2	23
03/10/09	88	7.5	6.4		0.86	29
03/11/09	88	2.6	8.0		2.5	19
11/03/09	164	8.5	13.3		1.6	25
11/04/09	101	7.7	10.6		1.4	15
03/10/10	113	8.3	12.0		1.5	15
12/03/09	88	7.2		3.1	0.43	15
01/19/10	126	2.0		2.9	1.5	15
01/29/10	113	4.9		8.2	1.7	15
02/09/10	113	9.5		13.1	1.4	15
02/11/10	82	6.3		17.8	2.8	25
02/17/10	101	5.5		29.3	5.3	15
02/18/10	88	4.5		27.2	6.0	15
Mean ± S.E.M.	*106 ± 6*	*6.1 ± 0.7*	*10.5 ± 2*	*14.5 ± 4*	*2.4 ± 0.4*	*19 ± 1*

P_s values are x 10^{-7} cm·s^{-1}; P_s^{RSA}, control permeability; P_s^{ANP}, permeability to RSA during ANP perfusion; P_s^{BNP}, permeability to RSA during BNP perfusion.

REFERENCES

1. Albertine KH and O'Morchoe CC. Renal lymphatic ultrastructure and translymphatic transport. *Microvasc Res* 19: 338-351, 1980.

2. Alitalo K, Tammela T, and Petrova TV. Lymphangiogenesis in development and human disease. *Nature* 438: 946-953, 2005.

3. Almeida FA, Suzuki M, and Maack T. Atrial natriuretic factor increases hematocrit and decreases plasma volume in nephrectomized rats. *Life Sci* 39: 1193-1199, 1986.

4. Amerini S, Ziche M, Greiner ST, and Zawieja DC. Effects of substance P on mesenteric lymphatic contractility in the rat. *Lymphat Res Biol* 2: 2-10, 2004.

5. Anand-Srivastava MB. Natriuretic peptide receptor-C signaling and regulation. *Peptides* 26: 1044-1059, 2005.

6. Asellius G. De lactibus, sive lacteis venis, quarto vasorum mesarai coruum genere, novo invento. Milan: J. B. Bidellium, 1627.

7. Aukland K, Kramer GC, and Renkin EM. Protein concentration of lymph and interstitial fluid in the rat tail. *Am J Physiol* 247: H74-79, 1984.

8. Aukland K and Reed RK. Interstitial-lymphatic mechanisms in the control of extracellular fluid volume. *Physiol Rev* 73: 1-78, 1993.

9. Baluk P, Fuxe J, Hashizume H, Romano T, Lashnits E, Butz S, Vestweber D, Corada M, Molendini C, Dejana E, and McDonald DM. Functionally specialized junctions between endothelial cells of lymphatic vessels. *J Exp Med* 204: 2349-2362, 2007.

10. Barber BJ, Schultz TJ, and Randlett DL. Comparative analysis of protein content in rat mesenteric tissue, peritoneal fluid, and plasma. *Am J Physiol* 258: G714-718, 1990.

11. Bates DO, Levick JR, and Mortimer PS. Change in macromolecular composition of interstitial fluid from swollen arms after breast cancer treatment, and its implications. *Clin Sci (Lond)* 85: 737-746, 1993.

12. Benoit JN, Zawieja DC, Goodman AH, and Granger HJ. Characterization of intact mesenteric lymphatic pump and its responsiveness to acute edemagenic stress. *Am J Physiol* 257: H2059-2069, 1989.

13. Berne RM and Levy MN, *The Microcirculation and Lymphatics.*, in *Physiology*, Berne RM and Levy MN, Editors. 1983, C.V. Mosby: St. Louis, MO. p. 517-530.

14. Bingaman S, Huxley VH, and Rumbaut RE. Fluorescent dyes modify properties of proteins used in microvascular research. *Microcirculation* 10: 221-231, 2003.

15. Blankfield RP. Fluid matters in choosing antihypertensive therapy: a hypothesis that the data speak volumes. *J Am Board Fam Pract* 18: 113-124, 2005.

16. Boron WF and Boulpaep EL. *Medical Physiology: A Cellular and Molecular Approach*. Philadelphia: Elsevier Saunders, 2005.

17. Brace RA, Taylor AE, and Guyton AC. Time course of lymph protein concentration in the dog. *Microvasc Res* 14: 243-249, 1977.

18. Brookes ZL and Kaufman S. Effects of atrial natriuretic peptide on the extrasplenic microvasculature and lymphatics in the rat in vivo. *J Physiol* 565: 269-277, 2005.

19. Brookes ZL, Mansart A, McGown CC, Ross JJ, Reilly CS, and Brown NJ. Macromolecular leak from extrasplenic lymphatics during endotoxemia. *Lymphat Res Biol* 7: 131-137, 2009.

20. Casley-Smith JR. A theoretical support for the transport of macromolecules by osmotic flow across a leaky membrane against a concentration gradient. *Microvasc Res* 9: 43-48, 1975.

21. Casley-Smith JR. The fine structure and functioning of tissue channels and lymphatics. *Lymphology* 13: 177-183, 1980.

22. Chambers R and Zweifach BW. Topography and function of the mesenteric capillary circulation. *Am J Anat* 75: 173-205, 1944.

23. Clerico A, Del Ry S, Maffei S, Prontera C, Emdin M, and Giannessi D. The circulating levels of cardiac natriuretic hormones in healthy adults: effects of age and sex. *Clin Chem Lab Med* 40: 371-377, 2002.

24. Clough G and Smaje LH. Simultaneous measurement of pressure in the interstitium and the terminal lymphatics of the cat mesentery. *J Physiol* 283: 457-468, 1978.

25. Costa MA, Elesgaray R, Balaszczuk AM, and Arranz C. Role of NPR-C natriuretic receptor in nitric oxide system activation induced by atrial natriuretic peptide. *Regul Pept* 135: 63-68, 2006.

26. Cueni LN and Detmar M. The lymphatic system in health and disease. *Lymphat Res Biol* 6: 109-122, 2008.

27. Curry FE, *Mechanics and thermodynamics of trancapillary exchange*, in *Handbook of Physiology, section 2, The Cardiovascular System, vol IV, Microcirculation*, Renkin EM and Michel CC, Editors. 1984, American Physiological Society: Bethesda, MD. p. 309-374.

28. Curry FE, Joyner WL, and Rutledge JC. Graded modulation of frog microvessel permeability to albumin using ionophore A23187. *Am J Physiol* 258: H587-598, 1990.

29. Curry FR, Rygh CB, Karlsen T, Wiig H, Adamson RH, Clark JF, Lin YC, Gassner B, Thorsen F, Moen I, Tenstad O, Kuhn M, and Reed RK. Atrial natriuretic peptide modulation of albumin clearance and contrast agent permeability in mouse skeletal muscle and skin: role in regulation of plasma volume. *J Physiol* 588: 325-339, 2010.

30. Daniel WW. *Applied Nonparametric Statistics*. Boston: PWS-Kent, 1990.

31. Davis MJ, Lane MM, Davis AM, Durtschi D, Zawieja DC, Muthuchamy M, and Gashev AA. Modulation of lymphatic muscle contractility by the neuropeptide substance P. *Am J Physiol Heart Circ Physiol* 295: H587-597, 2008.

32. Davis MJ, Davis AM, Ku CW, and Gashev AA. Myogenic constriction and dilation of isolated lymphatic vessels. *Am J Physiol Heart Circ Physiol* 296: H293-302, 2009.

33. Davis MJ, Davis AM, Lane MM, Ku CW, and Gashev AA. Rate-sensitive contractile responses of lymphatic vessels to circumferential stretch. *J Physiol* 587: 165-182, 2009.

34. de Bold AJ, Borenstein HB, Veress AT, and Sonnenberg H. A rapid and potent natriuretic response to intravenous injection of atrial myocardial extract in rats. *Life Sci* 28: 89-94, 1981.

35. Dongaonkar RM, Stewart RH, Laine GA, Davis MJ, Zawieja DC, and Quick CM. Venomotion modulates lymphatic pumping in the bat wing. *Am J Physiol Heart Circ Physiol* 296: H2015-2021, 2009.

36. Drinker CK. The Functional Significance of the Lymphatic System: Harvey Lecture, December 16, 1937. *Bull N Y Acad Med* 14: 231-251, 1938.

37. Gashev AA, Orlov RS, and Zawieja DC. [Contractions of the lymphangion under low filling conditions and the absence of stretching stimuli. The possibility of the sucking effect]. *Ross Fiziol Zh Im I M Sechenova* 87: 97-109, 2001.

38. Gashev AA, Davis MJ, and Zawieja DC. Inhibition of the active lymph pump by flow in rat mesenteric lymphatics and thoracic duct. *J Physiol* 540: 1023-1037, 2002.

39. Gerbes AL, Dagnino L, Nguyen T, and Nemer M. Transcription of brain natriuretic peptide and atrial natriuretic peptide genes in human tissues. *J Clin Endocrinol Metab* 78: 1307-1311, 1994.

40. Gibson H and Gaar KA. Dynamics of the implanted capsule. *Fed Proc* 29: 319, 1970.
41. Gnepp DR. *Lymphatics*. New York: Raven Press, 1984.

42. Guyton AC. Interstitial Fluid Presure. Ii. Pressure-Volume Curves of Interstitial Space. *Circ Res* 16: 452-460, 1965.

43. Guyton AC. *Textbook of Medical Physiology*. Philadelphia: W.B. Saunders, 1971.

44. Guyton AC, Granger HJ, and Taylor AE. Interstitial fluid pressure. *Physiol Rev* 51: 527-563, 1971.

45. Harris NR. Arteriovenous pairing: a determinant of capillary exchange. *News Physiol Sci* 18: 83-87, 2003.

46. Harvey NL, Srinivasan RS, Dillard ME, Johnson NC, Witte MH, Boyd K, Sleeman MW, and Oliver G. Lymphatic vascular defects promoted by Prox1 haploinsufficiency cause adult-onset obesity. *Nat Genet* 37: 1072-1081, 2005.

47. Hobbs A, Foster P, Prescott C, Scotland R, and Ahluwalia A. Natriuretic peptide receptor-C regulates coronary blood flow and prevents myocardial ischemia/reperfusion injury: novel cardioprotective role for endothelium-derived C-type natriuretic peptide. *Circulation* 110: 1231-1235, 2004.

48. Hogan RD. *Lymph formation in the bat wing*. Kensington: Univ. of New South Wales, 1981.

49. Hollywood MA, Cotton KD, Thornbury KD, and McHale NG. Tetrodotoxin-sensitive sodium current in sheep lymphatic smooth muscle. *J Physiol* 503 (Pt 1): 13-20, 1997.

50. Huxley VH, Curry FE, and Adamson RH. Quantitative fluorescence microscopy on single capillaries: alpha-lactalbumin transport. *Am J Physiol* 252: H188-197, 1987.

51. Huxley VH, Tucker VL, Verburg KM, and Freeman RH. Increased capillary hydraulic conductivity induced by atrial natriuretic peptide. *Circ Res* 60: 304-307, 1987.

52. Huxley VH, Curry FE, Powers MR, and Thipakorn B. Differential action of plasma and albumin on transcapillary exchange of anionic solute. *Am J Physiol* 264: H1428-1437, 1993.

53. Huxley VH, McKay MK, Meyer DJ, Jr., Williams DA, and Zhang RS. Vasoactive hormones and autocrine activation of capillary exchange barrier function. *Blood Cells* 19: 309-320; discussion 320-304, 1993.

54. Huxley VH and Williams DA. Role of a glycocalyx on coronary arteriole permeability to proteins: evidence from enzyme treatments. *Am J Physiol Heart Circ Physiol* 278: H1177-1185, 2000.

55. Huxley VH, Wang JJ, and Sarelius IH. Adaptation of coronary microvascular exchange in arterioles and venules to exercise training and a role for sex in determining permeability responses. *Am J Physiol Heart Circ Physiol* 293: H1196-1205, 2007.

56. Jacobsson S and Kjellmer I. Flow and Protein Content of Lymph in Resting and Exercising Skeletal Muscle. *Acta Physiol Scand* 60: 278-285, 1964.

57. Ji L-P and Huxley VH. Elevation of skeletal muscle arteriole permeability to protein by atrial natriuretic peptide. *FASEB J* 14: A25, 2000.

58. Johansson B and Mellander S. Static and dynamic components in the vascular myogenic response to passive changes in length as revealed by electrical and mechanical recordings from the rat portal vein. *Circ Res* 36: 76-83, 1975.

59. John SW, Veress AT, Honrath U, Chong CK, Peng L, Smithies O, and Sonnenberg H. Blood pressure and fluid-electrolyte balance in mice with reduced or absent ANP. *Am J Physiol* 271: R109-114, 1996.

60. Johnson NC, Dillard ME, Baluk P, McDonald DM, Harvey NL, Frase SL, and Oliver G. Lymphatic endothelial cell identity is reversible and its maintenance requires Prox1 activity. *Genes Dev* 22: 3282-3291, 2008.

61. Kendall S and Michel CC. The measurement of permeability in single rat venules using the red cell microperfusion technique. *Exp Physiol* 80: 359-372, 1995.

62. Kessler MA, Meinitzer A, and Wolfbeis OS. Albumin blue 580 fluorescence assay for albumin. *Anal Biochem* 248: 180-182, 1997.

63. Kim MH, Harris NR, and Tarbell JM. Regulation of hydraulic conductivity in response to sustained changes in pressure. *Am J Physiol Heart Circ Physiol* 289: H2551-2558, 2005.

64. Kirkpatrick CT and McHale NG. Electrical and mechanical activity of isolated lymphatic vessels [proceedings]. *J Physiol* 272: 33P-34P, 1977.

65. Koop K, Eikmans M, Wehland M, Baelde H, Ijpelaar D, Kreutz R, Kawachi H, Kerjaschki D, de Heer E, and Bruijn JA. Selective loss of podoplanin protein expression accompanies proteinuria and precedes alterations in podocyte morphology in a spontaneous proteinuric rat model. *Am J Pathol* 173: 315-326, 2008.

66. Kousai A, Mizuno R, Ikomi F, and Ohhashi T. ATP inhibits pump activity of lymph vessels via adenosine A1 receptor-mediated involvement of NO- and ATP-sensitive K+ channels. *Am J Physiol Heart Circ Physiol* 287: H2585-2597, 2004.

67. Landis EM and Pappenheimer JR, *Exchange of substances through the capillary walls*, in *Handbook of Physiology*, Hamilton WF, Editor. 1963, American Physiological Society: Washington, DC. p. 961-1034.

68. Leak LV and Burke JF. Ultrastructural studies on the lymphatic anchoring filaments. *J Cell Biol* 36: 129-149, 1968.

69. Leak LV. Electron microscopic observations on lymphatic capillaries and the structural components of the connective tissue-lymph interface. *Microvasc Res* 2: 361-391, 1970.

70. Leak LV. Studies on the permeability of lymphatic capillaries. *J Cell Biol* 50: 300-323, 1971.

71. Leak LV. The transport of exogenous peroxidase across the blood-tissue-lymph interface. *J Ultrastruct Res* 39: 24-42, 1972.

72. Levick JR. Capillary filtration-absorption balance reconsidered in light of dynamic extravascular factors. *Exp Physiol* 76: 825-857, 1991.

73. Machnik A, Dahlmann A, Kopp C, Goss J, Wagner H, van Rooijen N, Eckardt KU, Muller DN, Park JK, Luft FC, Kerjaschki D, and Titze J. Mononuclear phagocyte system depletion blocks interstitial tonicity-responsive enhancer binding protein/vascular endothelial growth factor C expression and induces salt-sensitive hypertension in rats. *Hypertension* 55: 755-761, 2009.

74. Marble A FM, Drinker CE, and Smith RM. The permeability of the blood capillaries to lipoids. *American Journal of Physiology* 109: 467-474, 1934.

75. Mayerson HS. *The physiologic importance of lymph.* Baltimore, MD: Williams & Wilkins, 1963.

76. McCloskey KD, Hollywood MA, Thornbury KD, Ward SM, and McHale NG. Kit-like immunopositive cells in sheep mesenteric lymphatic vessels. *Cell Tissue Res* 310: 77-84, 2002.

77. McGrath MF, de Bold ML, and de Bold AJ. The endocrine function of the heart. *Trends Endocrinol Metab* 16: 469-477, 2005.

78. McHale NG. *Nature of lymphatic innervation*. London: Portland Press, 1995.

79. McKay MK. Studies on the Permeability of the Capillary Barrier: Effects of Perfusate Proteins and Natriuretic Factors. Columbia: University of Missouri at Columbia, 1994.

80. McKay MK and Huxley VH. ANP increases capillary permeability to protein independent of perfusate protein composition. *Am J Physiol* 268: H1139-1148, 1995.

81. Meyer DJ, Jr. and Huxley VH. Differential sensitivity of exchange vessel hydraulic conductivity to atrial natriuretic peptide. *Am J Physiol* 258: H521-528, 1990.

82. Michel CC and Phillips ME. Steady-state fluid filtration at different capillary pressures in perfused frog mesenteric capillaries. *J Physiol* 388: 421-435, 1987.

83. Murthy KS, Teng B, Jin J, and Makhlouf GM. G protein-dependent activation of smooth muscle eNOS via natriuretic peptide clearance receptor. *Am J Physiol* 275: C1409-1416, 1998.

84. Muthuchamy M, Gashev A, Boswell N, Dawson N, and Zawieja D. Molecular and functional analyses of the contractile apparatus in lymphatic muscle. *Faseb J* 17: 920-922, 2003.

85. Negrini D and Fabbro MD. Subatmospheric pressure in the rabbit pleural lymphatic network. *J Physiol* 520 Pt 3: 761-769, 1999.

86. Neter J, Wasserman W, and Kutner M. *Applied Linear Statistical Models: Regression, Analysis of Variance, and Experimental Designs*. Homewood, IL: Irwin, 1990.

87. Nielsen I, Gordon S, and Selby A. Breast cancer-related lymphoedema risk reduction advice: a challenge for health professionals. *Cancer Treat Rev* 34: 621-628, 2008.

88. O'Morchoe CC, Jones WR, 3rd, Jarosz HM, O'Morchoe PJ, and Fox LM. Temperature dependence of protein transport across lymphatic endothelium in vitro. *J Cell Biol* 98: 629-640, 1984.

89. Ohhashi T, Azuma T, and Sakaguchi M. Active and passive mechanical characteristics of bovine mesenteric lymphatics. *Am J Physiol* 239: H88-95, 1980.

90. Ohhashi T, Watanabe N, and Kawai Y. Effects of atrial natriuretic peptide on isolated bovine mesenteric lymph vessels. *Am J Physiol* 259: H42-47, 1990.

91. Ohtani O and Ohtani Y. Organization and developmental aspects of lymphatic vessels. *Arch Histol Cytol* 71: 1-22, 2008.

92. Parsons RJ and McMaster PD. The effect on the pulse upon the formation and flow of lymph. *J Exp Med* 68: 353-376, 1938.

93. Patlak CS, Goldstein DA, and Hoffman JF. The flow of solute and solvent across a two-membrane system. *J Theor Biol* 5: 426-442, 1963.

94. Patterson RM, Ballard CL, Wasserman K, and Mayerson HS. Lymphatic permeability to albumin. *Am J Physiol* 194: 120-124, 1958.

95. Perrin RM, Harper SJ, Corrall R, and Bates DO. Hyperglycemia stimulates a sustained increase in hydraulic conductivity in vivo without any change in reflection coefficient. *Microcirculation* 14: 683-696, 2007.

96. Petrova TV, Karpanen T, Norrmen C, Mellor R, Tamakoshi T, Finegold D, Ferrell R, Kerjaschki D, Mortimer P, Yla-Herttuala S, Miura N, and Alitalo K. Defective valves and abnormal mural cell recruitment underlie lymphatic vascular failure in lymphedema distichiasis. *Nat Med* 10: 974-981, 2004.

97. Potter LR, Abbey-Hosch S, and Dickey DM. Natriuretic peptides, their receptors, and cyclic guanosine monophosphate-dependent signaling functions. *Endocr Rev* 27: 47-72, 2006.

98. Price GM, Chrobak KM, and Tien J. Effect of cyclic AMP on barrier function of human lymphatic microvascular tubes. *Microvasc Res* 76: 46-51, 2008.

99. Reddy NP, Krouskop TA, and Newell PH, Jr. Biomechanics of a lymphatic vessel. *Blood Vessels* 12: 261-278, 1975.

100. Renkin EM. Some consequences of capillary permeability to macromolecules: Starling's hypothesis reconsidered. *Am J Physiol* 250: H706-710, 1986.

101. Rubattu S, Sciarretta S, Valenti V, Stanzione R, and Volpe M. Natriuretic peptides: an update on bioactivity, potential therapeutic use, and implication in cardiovascular diseases. *Am J Hypertens* 21: 733-741, 2008.

102. Rumbaut RE. Nitric Oxide and Microvascular Permeability (Dissertation). Columbia, MO: University of Missouri at Columbia, 1998.

103. Rumbaut RE, Wang J, and Huxley VH. Differential effects of L-NAME on rat venular hydraulic conductivity. *Am J Physiol Heart Circ Physiol* 279: H2017-2023, 2000.

104. Rumbaut RE and Huxley VH. Similar permeability responses to nitric oxide synthase inhibitors of venules from three animal species. *Microvasc Res* 64: 21-31, 2002.

105. Ruskoaho H. Atrial natriuretic peptide: synthesis, release, and metabolism. *Pharmacol Rev* 44: 479-602, 1992.

106. Sabin FR. On the origin of the lymphatic system from the veins, and the development of the lymph hearts and thoracic duct in the pig. *Am J Anat* 1: 367-389, 1902.

107. Sarelius IH, Kuebel JM, Wang J, and Huxley VH. Macromolecule permeability of in situ and excised rodent skeletal muscle arterioles and venules. *Am J Physiol Heart Circ Physiol* 290: H474-480, 2006.

108. Sawa Y, Iwasawa K, and Ishikawa H. Expression of podoplanin in the mouse tooth germ and apical bud cells. *Acta Histochem Cytochem* 41: 121-126, 2008.

109. Scallan JP and Huxley VH. Assessing rat mesenteric collecting lymphatic permeability to albumin (Abstract). *Microcirculation* 14: 511, 2007.

110. Scallan JP and Huxley VH. In vivo determination of collecting lymphatic vessel permeability to albumin: a role for lymphatics in exchange. *J Physiol* 588: 243-254, 2010.

111. Scallan JP, Huxley VH, and Korthuis RJ, *Capillary Fluid Exchange: Regulation, Functions, and Pathology*, in *Integrated Systems Physiology: From Molecules to Function eBook series*, Granger DN and Granger JP, Editors. 2010, Morgan-Claypool.

112. Schacht V, Ramirez MI, Hong YK, Hirakawa S, Feng D, Harvey N, Williams M, Dvorak AM, Dvorak HF, Oliver G, and Detmar M. T1alpha/podoplanin deficiency disrupts normal lymphatic vasculature formation and causes lymphedema. *Embo J* 22: 3546-3556, 2003.

113. Schmid-Schonbein GW. Microlymphatics and lymph flow. *Physiol Rev* 70: 987-1028, 1990.

114. Srinivasan RS, Dillard ME, Lagutin OV, Lin FJ, Tsai S, Tsai MJ, Samokhvalov IM, and Oliver G. Lineage tracing demonstrates the venous origin of the mammalian lymphatic vasculature. *Genes Dev* 21: 2422-2432, 2007.

115. Stanton AW, Modi S, Bennett Britton TM, Purushotham AD, Peters AM, Levick JR, and Mortimer PS. Lymphatic drainage in the muscle and subcutis of the arm after breast cancer treatment. *Breast Cancer Res Treat* 117: 549-557, 2009.

116. Starling EH. On the Absorption of Fluids from the Connective Tissue Spaces. *J Physiol* 19: 312-326, 1896.

117. Stratman AN, Malotte KM, Mahan RD, Davis MJ, and Davis GE. Pericyte recruitment during vasculogenic tube assembly stimulates endothelial basement membrane matrix formation. *Blood* 114: 5091-5101, 2009.

118. Suga S, Nakao K, Hosoda K, Mukoyama M, Ogawa Y, Shirakami G, Arai H, Saito Y, Kambayashi Y, Inouye K, and et al. Receptor selectivity of natriuretic peptide family, atrial natriuretic peptide, brain natriuretic peptide, and C-type natriuretic peptide. *Endocrinology* 130: 229-239, 1992.

119. Takahashi T, Shibata M, and Kamiya A. Mechanism of macromolecule concentration in collecting lymphatics in rat mesentery. *Microvasc Res* 54: 193-205, 1997.

120. Taylor A and Gibson H. Concentrating ability of lymphatic vessels. *Lymphology* 8: 43-49, 1975.

121. Taylor AE, Gaar KA, and Gibson H. Effect of tissue pressure on lymph flow. *Biophys J* 10: 45A, 1970.

122. Taylor AE, Gibson WH, Granger HJ, and Guyton AC. The interaction between intracapillary and tissue forces in the overall regulation of interstitial fluid volume. *Lymphology* 6: 192-208, 1973.

123. Testa JE, Chrastina A, Li Y, Oh P, and Schnitzer JE. Ubiquitous yet distinct expression of podocalyxin on vascular surfaces in normal and tumor tissues in the rat. *J Vasc Res* 46: 311-324, 2009.

124. Trzewik J, Mallipattu SK, Artmann GM, Delano FA, and Schmid-Schonbein GW. Evidence for a second valve system in lymphatics: endothelial microvalves. *Faseb J* 15: 1711-1717, 2001.

125. Tucker VL, Simanonok KE, and Renkin EM. Tissue-specific effects of physiological ANP infusion on blood-tissue albumin transport. *Am J Physiol* 263: R945-953, 1992.

126. Vainionpaa N, Butzow R, Hukkanen M, Jackson DG, Pihlajaniemi T, Sakai LY, and Virtanen I. Basement membrane protein distribution in LYVE-1-immunoreactive lymphatic vessels of normal tissues and ovarian carcinomas. *Cell Tissue Res* 328: 317-328, 2007.

127. Valentin JP, Ribstein J, and Mimran A. Effect of nicardipine and atriopeptin on transcapillary shift of fluid and proteins. *Am J Physiol* 257: R174-179, 1989.

128. Van Helden DF, von der Weid PY, and Crowe MJ. *Electrophysiology of lymphatic smooth muscle*. London: Portland Press, 1995.

129. VanBavel E, Mooij T, Giezeman MJ, and Spaan JA. Cannulation and continuous cross-sectional area measurement of small blood vessels. *J Pharmacol Methods* 24: 219-227, 1990.

130. Venugopal AM, Stewart RH, Rajagopalan S, Laine GA, and Quick CM. Optimal lymphatic vessel structure. *Conf Proc IEEE Eng Med Biol Soc* 5: 3700-3703, 2004.

131. von der Weid PY. Review article: lymphatic vessel pumping and inflammation--the role of spontaneous constrictions and underlying electrical pacemaker potentials. *Aliment Pharmacol Ther* 15: 1115-1129, 2001.

132. von der Weid PY, Zhao J, and Van Helden DF. Nitric oxide decreases pacemaker activity in lymphatic vessels of guinea pig mesentery. *Am J Physiol Heart Circ Physiol* 280: H2707-2716, 2001.

133. von der Weid PY and Zawieja DC. Lymphatic smooth muscle: the motor unit of lymph drainage. *Int J Biochem Cell Biol* 36: 1147-1153, 2004.

134. von der Weid PY, Rahman M, Imtiaz MS, and van Helden DF. Spontaneous transient depolarizations in lymphatic vessels of the guinea pig mesentery: pharmacology and implication for spontaneous contractility. *Am J Physiol Heart Circ Physiol* 295: H1989-2000, 2008.

135. Wang J, Bingaman S, and Huxley VH. Intrinsic sex-specific differences in microvascular endothelial cell phosphodiesterases. *Am J Physiol Heart Circ Physiol* 298: H1146-1154, 2010.

136. Wiig H, Reed RK, and Aukland K. Measurement of interstitial fluid pressure in dogs: evaluation of methods. *Am J Physiol* 253: H283-290, 1987.

137. William M, Hamilton EJ, Garcia A, Bundgaard H, Chia KK, Figtree GA, and Rasmussen HH. Natriuretic peptides stimulate the cardiac sodium pump via NPR-C-coupled NOS activation. *Am J Physiol Cell Physiol* 294: C1067-1073, 2008.

138. Woods RL. Cardioprotective functions of atrial natriuretic peptide and B-type natriuretic peptide: a brief review. *Clin Exp Pharmacol Physiol* 31: 791-794, 2004.

139. Yokoyama S and Ohhashi T. Effects of acetylcholine on spontaneous contractions in isolated bovine mesenteric lymphatics. *Am J Physiol* 264: H1460-1464, 1993.

140. Zawieja DC and Barber BJ. Lymph protein concentration in initial and collecting lymphatics of the rat. *Am J Physiol* 252: G602-606, 1987.

141. Zawieja DC, von der Weid PY, and Gashev AA. *Microlymphatic Biology*. San Diego, CA: Elsevier Inc., 2008.

142. Zhang RZ, Gashev AA, Zawieja DC, and Davis MJ. Length-tension relationships of small arteries, veins, and lymphatics from the rat mesenteric microcirculation. *Am J Physiol Heart Circ Physiol* 292: H1943-1952, 2007.

143. Zweifach BW and Prather JW. Micromanipulation of pressure in terminal lymphatics in the mesentery. *Am J Physiol* 228: 1326-1335, 1975.

VITA

Joshua Paul Scallan was born in Bossier City, Louisiana on March 1, 1984, and was raised in Blanchard, a town in close proximity to the Shreveport-Bossier area. He graduated from C.E. Byrd High School in 2001, moving on to obtain a B.S. in Biology from Centenary College of Louisiana in 2005. During his undergraduate work, he applied for and accepted a student worker position under Dr. Ron Korthuis in the Physiology Department at Louisiana State University Health Sciences Center, where his interest in cardiovascular physiology was nurtured. In the same department, Josh met Dr. Norman Harris, who inspired him to study the lymphatic vasculature. A year later, Dr. Korthuis recruited Josh to the Medical Pharmacology and Physiology Department at the University of Missouri at Columbia where he continued researching the lymphatic vasculature under the careful guidance of Dr. Virginia Huxley. Three years after beginning this program, he married Megan Polito in The Woodlands, TX on June 28, 2008. Josh earned his doctoral degree in Physiology in May of 2010. Pursuing a career in lymphatic biology, he accepted a postdoctoral fellowship with Dr. Guillermo Oliver at St. Jude Children's Research Hospital in Memphis, TN.